LIÈGE université
Gembloux
Agro-Bio Tech

CHINESE ACADEMY OF AGRICULTURAL SCIENCES

Molecular Mechanisms of Midgut Defense Against *Bacillus thuringiensis* Insecticidal Proteins in Lepidopteran Insects

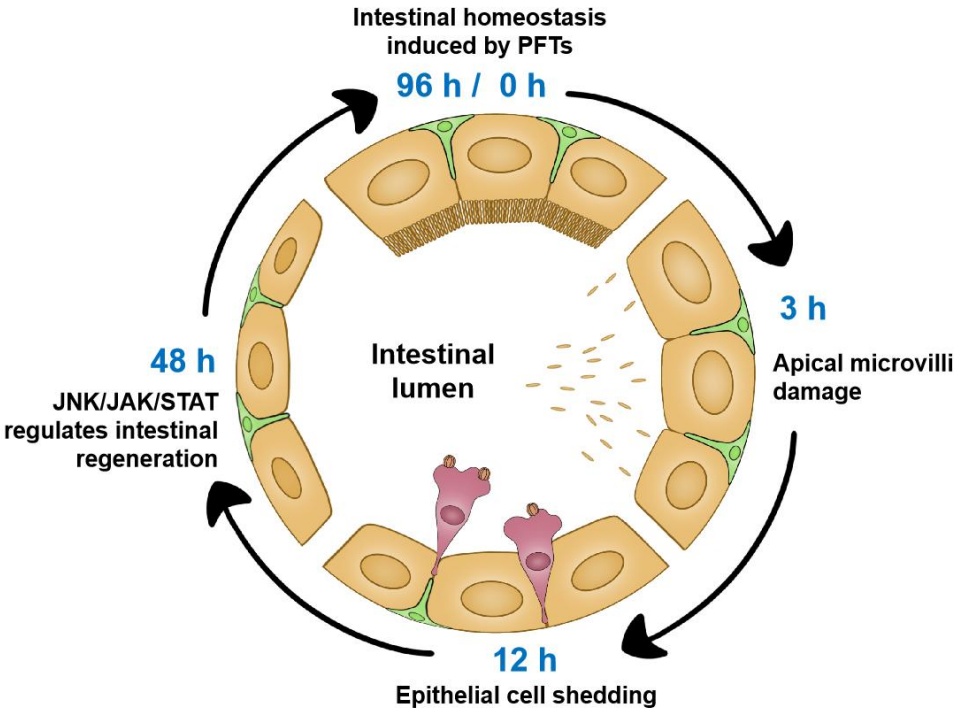

Yangchao Yang

Promoters: Prof. Frédéric Francis

Prof. Jie Zhang

2025

FRENCH COMMUNITY OF BELGIUM
UNIVERSITY OF LIÈGE – GEMBLOUX AGRO-BIO TECH
BELGIUM

Molecular Mechanisms of Midgut Defense Against *Bacillus thuringiensis* Insecticidal Proteins in Lepidopteran Insects

Yanchao Yang

Original assay for graduation as a doctor in agricultural sciences and biological engineering

Promoters : Prof. Frédéric Francis
Prof. Jie Zhang

Civil year : 2025

Abstract

Bacillus thuringiensis (Bt) is widely utilized in microbial insecticides and genetically modified crops for effective pest management. Its insecticidal proteins disrupt the midgut epithelium by forming pores, ultimately causing larval mortality. The insect midgut plays a vital role in digestion and nutrient absorption while also serving as a protective barrier against toxins and pathogens. These defense mechanisms can diminish the effectiveness of Bt-based products and potentially contribute to resistance development. This study investigated the specific midgut defense mechanisms induced by sublethal concentrations of Bt insecticidal proteins in lepidopteran insects. Additionally, a lepidopteran midgut defense gene research system based on RNA interference (RNAi) was established. Using this system, the study explored the genes and pathways involved in the midgut defense response of lepidopteran larvae against Bt insecticidal proteins.

In Chapter 3, the midgut defense mechanisms of *Chilo suppressalis* larvae against *Bacillus thuringiensis* Cry9A protein were elucidated using histopathological, molecular, and biochemical analyses. The results showed that a sublethal concentration of Cry9A (LC_{20}) induced structural remodeling of midgut tissue, including epithelial cell shedding and midgut regeneration. Rapid Cry9A-induced midgut damage was observed, characterized by 20-30% reductions in epithelial thickness and cell loss within 48 hours, followed by full recovery by 96 hours. Cell shedding was quantified via aminopeptidase N (APN) release, showing an increase in luminal activity at 24 hours. Regeneration involved intestinal stem cell (ISC) proliferation, evidenced by phospho-histone H3 (PH3) upregulation, and Notch-mediated differentiation, with *Delta* expression peaking at 72 hours. These findings demonstrate a biphasic response - elimination of damaged cells and subsequent repair - orchestrated by ISC activation, providing insights into lepidopteran adaptive strategies against Bt toxins.

In Chapter 4, we focused on the homologous genes of Epidermal Growth Factor Receptor (*Egfr*) and Stathmin 4 (*Stmn4*), which have been reported to regulate stem cell proliferation and cell cycle progression in *Drosophila*, and applied them to *Spodoptera frugiperda*, a major migratory agricultural pest, to establish an efficient RNAi-based system for studying midgut defense genes in lepidopteran pests. Our results demonstrated that, compared to the *E. coli*-expressed dsRNA, *in vitro* synthesized dsRNA exhibited significantly higher gene silencing efficiency, especially when complexed with star polycation (SPc) nanoparticles. When fed at a concentration of 25 μg/g for 48 hours, the gene silencing efficiency reached over 75%. Pre-treatment with dsRNA for 48 hours increased the larval mortality rate by more than 30% following Cry1F exposure, outperforming the simultaneous feeding method of dsRNA and Cry1F protein. Furthermore, the silencing of *SfEgfr* and *SfStmn4* inhibited the proliferation of midgut stem cells after Cry1F exposure, leading to an increased mortality rate. Our findings offer a novel concept and theoretical framework for the biological management of lepidopteran pests.

In Chapter 5, Cry9A-induced intestinal regeneration is regulated by Jun N-terminal kinase (JNK) and the Janus kinase/signal transducer and activator of transcription (JAK/STAT) signaling pathway. These factors mediate gut regeneration by promoting intestinal stem cell proliferation and differentiation, offering protection against three different Bt proteins, including Cry9A, Cry1F, and Vip3A, in *Chilo suppressalis* and *Spodoptera frugiperda*. To enhance pesticide efficacy, a nano-biopesticide was developed by combining *Stat*

double-stranded RNA (dsRNA) nanoparticles with Bt strains. This formulation demonstrated superior pest control, suggesting its potential to reduce reliance on synthetic insecticides in agricultural environments.

Overall, we identified that the JNK/JAK/STAT pathway regulates midgut regeneration in lepidopteran larvae following pore formation induced by Bt pore-forming toxins (PFTs). Furthermore, we demonstrated that RNAi-mediated silencing of the JAK/STAT pathway enhances the toxicity of different PFTs in two distinct lepidopteran species. Based on these findings, we developed a novel and effective formulation combining Bt and ds*Stat* nanopesticides for controlling *Chilo suppressalis* and *Spodoptera frugiperda* larvae. This innovative strategy, which integrates Bt strains with dsRNA targeting insect defense mechanisms, offers a promising approach for managing crop pests that exhibit low susceptibility to Bt PFTs.

Keywords: *Bacillus thuringiensis*, RNA interference, midgut defense, JNK, JAK/STAT, *Chilo suppressalis*, *Spodoptera frugiperda*

Résumé

Bacillus thuringiensis (Bt) est largement utilisé dans les insecticides microbiens et les cultures génétiquement modifiées pour une gestion efficace des ravageurs. Ses protéines insecticides perturbent l'épithélium du mésentéron en formant des pores, ce qui entraîne finalement la mortalité larvaire. Le mésentéron des insectes joue un rôle essentiel dans la digestion et l'absorption des nutriments, tout en servant également de barrière protectrice contre les toxines et les agents pathogènes. Ces mécanismes de défense peuvent diminuer l'efficacité des produits à base de Bt et contribuer potentiellement au développement de résistances. Cette étude a examiné les mécanismes spécifiques de défense du mésentéron induits par des concentrations sublétales de protéines insecticides de Bt chez les insectes lépidoptères. De plus, un système de recherche sur les gènes de défense du mésentéron chez les lépidoptères basé sur l'interférence par ARN (ARNi) a été établi. En utilisant ce système, l'étude a exploré les gènes et les voies de signalisation impliqués dans la réponse de défense du mésentéron des larves de lépidoptères contre les protéines insecticides de Bt.

Dans le Chapitre 3, les mécanismes de défense du mésentéron des larves de *Chilo suppressalis* contre la protéine Cry9A de *Bacillus thuringiensis* ont été élucidés à l'aide d'analyses histopathologiques, moléculaires et biochimiques. Les résultats ont montré qu'une concentration sublétale de Cry9A (LC_{20}) induisait un remodelage structurel du tissu mésentérique, comprenant une desquamation des cellules épithéliales et une régénération du mésentéron. Des lésions rapides du mésentéron induites par Cry9A ont été observées, caractérisées par une réduction de 20 à 30 % de l'épaisseur de l'épithélium et une perte cellulaire en 48 heures, suivies d'une récupération complète en 96 heures. L'élimination des cellules a été quantifiée via la libération d'aminopeptidase N (APN), montrant une augmentation de l'activité luminale à 24 heures. La régénération impliquait la prolifération des cellules souches intestinales (ISC), attestée par une augmentation de la phospho-histone H3 (PH3), ainsi qu'une différenciation médiée par la voie Notch, avec un pic d'expression de Delta à 72 heures. Ces résultats démontrent une réponse biphasique - élimination des cellules endommagées puis réparation- -orchestrée par l'activation des cellules souches intestinales, fournissant des éclairages sur les stratégies adaptatives des lépidoptères contre les toxines de Bt.

Dans le Chapitre 4, nous nous sommes concentrés sur les gènes homologues du récepteur du facteur de croissance épidermique (*Egfr*) et de la Stathmine 4 (*Stmn4*), qui ont été rapportés comme régulant la prolifération des cellules souches et la progression du cycle cellulaire chez *Drosophila*, et nous les avons appliqués à *Spodoptera frugiperda*, un important ravageur agricole migrateur, afin d'établir un système efficace basé sur l'ARNi pour étudier les gènes de défense du mésentéron chez les lépidoptères. Nos résultats ont démontré que, comparé à l'ARN double-brin exprimé par *E. coli*, l'ARN double-brin synthétisé in vitro présentait une efficacité de silençage génique significativement plus élevée, en particulier lorsqu'il était complexé avec des nanoparticules de polycation étoilé (SPc). Administré à une concentration de 25 μg/g pendant 48 heures, le taux de silençage génétique dépassait les 75%. Une pré-exposition à l'ARN double-brin pendant 48 heures augmentait le taux de mortalité larvaire de plus de 30% après exposition à Cry1F, surpassant la méthode d'alimentation simultanée avec l'ARN double-brin et la protéine Cry1F. En outre, la suppression de *SfEgfr* et *SfStmn4* inhibait la prolifération des cellules souches du mésentéron après exposition à Cry1F,

entraînant une augmentation du taux de mortalité. Nos résultats offrent un concept novateur et un cadre théorique pour la gestion biologique des ravageurs lépidoptères.

Dans le Chapitre 5, il a été démontré que la régénération intestinale induite par Cry9A est régulée par la kinase Jun N-terminale (JNK) et la voie de signalisation Janus kinase/signal transducteur et activateur de la transcription (JAK/STAT). Ces facteurs assurent la régénération du mésentéron en favorisant la prolifération et la différenciation des cellules souches intestinales, apportant une protection contre trois protéines de Bt différentes, notamment Cry9A, Cry1F et Vip3A, chez *Chilo suppressalis* et *Spodoptera frugiperda*. Afin d'améliorer l'efficacité des pesticides, un nanobiopesticide a été développé en combinant des nanoparticules d'ARN double-brin ciblant Stat avec des souches de Bt. Cette formulation a démontré une efficacité supérieure de lutte contre les ravageurs, suggérant son potentiel à réduire la dépendance aux insecticides synthétiques dans les environnements agricoles.

Dans l'ensemble, nous avons identifié que la voie JNK/JAK/STAT régule la régénération du mésentéron chez les larves de lépidoptères suite à la formation de pores induite par les toxines de Bt formant des pores (PFTs). En outre, nous avons démontré que le silençage médié par l'ARNi de la voie JAK/STAT amplifie la toxicité de différentes PFTs chez deux espèces lépidoptères distinctes. Sur la base de ces résultats, nous avons développé une formulation nouvelle et efficace combinant des souches de Bt avec des nanobiopesticides à base de dsStat pour lutter contre les larves de *Chilo suppressalis* et *Spodoptera frugiperda*. Cette stratégie innovante, qui intègre les souches de Bt avec des ARN double-brin ciblant les mécanismes de défense des insectes, constitue une approche prometteuse pour la gestion des ravageurs des cultures peu sensibles aux PFTs de Bt..

Mots-clés: *Bacillus thuringiensis*, interférence par ARN, défense du mésentéron, JNK, JAK/STAT, *Chilo suppressalis*, *Spodoptera frugiperda*

Acknowledgements

First and foremost, I would like to express my sincere gratitude to my promoters, Professor **Frédéric Francis** (Functional & Evolutionary Entomology, University of Liege – Gembloux Agro-Bio Tech, Belgium) and Professor **Jie Zhang** (Institute of Plant Protection, Chinese Academy of Agricultural Sciences, China) for their patient guidance, erudite knowledge and valuable suggestions from the beginning to the end of this Ph.D. project.

I gratefully acknowledge the financial scholarship from the National Natural Science Foundation of China (32001970 to ZW), National Key Research and Development Program of China (2023YFE0104800), Guizhou Provincial Science and Technology Projects (2023 No. Great 004). and China Scholarship Council (202303250106), the support associated with studying and researching facilities from **University of Liege – Gembloux Agro-Bio Tech** (Belgium) and **Chinese Academy of Agricultural Sciences** (China), the assistance related to data collection, project communication, and research guidance from Associate Professor **Zeyu Wang** (Institute of Plant Protection, Chinese Academy of Agricultural Sciences, China). Thanks to Professor **Changlong Shu** and Associate Professor **Lili Geng** for their invaluable scientific guidance and unwavering support throughout my doctoral studies. Thanks to Professor **Mingjun Zhang** (Graduate School of Chinese Academy of Agricultural Sciences, China) for his invaluable assistance and unwavering support throughout the course of my doctoral studies. Sincere thanks to **all members of my thesis committee** for their meticulous guidance, which has been of great assistance to me. Undoubtably, their support has been instrumental in shaping the course of my academic journey.

I wish to acknowledge that, beyond my individual endeavors, the accomplishment of this thesis is significantly indebted to the encouragement and guidance extended by numerous individuals. I seize this moment to convey my appreciation to all those who have generously contributed their assistance and offered invaluable counsel during this undertaking, encompassing, though not confined to, **my friends and colleagues**.

Last but not least, I would like to wholeheartedly express my profound gratitude to my cherished family. Their unwavering belief in my abilities, understanding, and the immeasurable sacrifices they have made alongside me have always been my rock and inspiration.

Table of contents

List of figures

Figure 4-2. Relative expression levels of *SfEgfr* and *SfStmn4* across different developmental stages (A) and tissues (B) in *S. frugiperda*. Uppercase letters indicate significant differences in *SfEgfr* expression, and lowercase letters indicate significant differences in *SfStmn4* expression, based on one-way ANOVA followed by a least significant difference test.

Figure 4-3. Relative expression levels of *SfEgfr* and *SfStmn4* after treatment with dsRNA synthesized by different methods (A), different treatment times (B) and different concentrations of dsRNA (C). Significant differences between the treatments and control were determined by Student's t-test (***: $P < 0.001$).

Figure 4-4. Insecticidal bioassay of Cry1F against fall armyworm larvae after treatment with dsRNA for 48 h (A) or treatment with diet containing dsRNA and Cry1F (B). Three replicates were performed. *P* values were calculated by two-sided Student's t-test (**: $P<0.01$; *: $P<0.05$; ns: $P>0.05$).

Figure 4-5. The roles of *SfEgfr* and *SfStmn4* in the defense of *S. frugiperda* midgut against Cry1F protein (A) Representative images from seventy-two 4th instar larvae treated with Cry1F (LC_{20}) for 72 h with or without silencing *SfEgfr* and *SfStmn4*. (B) Quantification of length from seventy-two 4th instar larvae treated with Cry1F (LC_{20}) for 72 h after treating with or without silencing *SfEgfr* and *SfStmn*. (C) Western blot detection of PH3 in midgut tissue samples from larvae of 4th instar fall armyworm after 36 h of Cry1F (LC_{20}) intoxication with or without dsRNA treatment. *P* values were calculated by one-way ANOVA and Tukey's test (***: $P<0.001$).

Figure 5-1. JAK/STAT pathway gene expression in the intestine from 15 larvae of striped stem borer after treatment with Cry9A (LC_{20}) for different times (6 and 48 h) determined by RT-qPCR. Control (Ctrl) were larvae treated with non-toxic Cry9A-D125R. The data were normalized to control on biological triplicate samples. Three independent experiments were performed. *P* values were calculated by two-sided Student's t-test, $P<0.01$ shows statistically significant differences. $P>0.05$ shows no significant difference. The error bar represents ±SEM.

Figure 5-2. Bioassays after silencing JAK/STAT pathway genes or adding inhibitor. (A) Insecticidal toxicity assay of Cry9A against neonate larvae of striped stem borer after silencing JAK/STAT pathway genes (*Stat92E* and *Socs36E* genes) by RNAi for 48 h. Thirty-five neonates were analyzed with each treatment. Three replicates were performed. $P<0.0001$ shows statistically significant difference (two-sided Student's t-test). The error bar represents ±SEM. (B) Insecticidal toxicity assay of Cry9A against neonates of striped stem borer after treatment with JAK/STAT pathway inhibitor Nifuroxazide for 48 h. Thirty-five neonates were analyzed with each treatment. Three replicates were performed. $P<0.001$ shows statistically significant difference (two-sided Student's t-test). The error bar represents ±SEM. Control (Ctrl) were larvae treated with non-toxic Cry9A-D125R. The error bar represents ±SEM.

Figure 5-3. Changes in midgut tissue morphology after silencing JAK/STAT pathway genes or adding inhibitor. (A) Sagittal view representative images of larvae midgut tissues isolated from larvae treated with Cry9A with or without *Stat92E* dsRNA or nifuroxazide treatment observed in the LSCM. Hoechst33342 (blue color) labels nuclei. Phalloidin-647 (red color) labels F-actin. Control (Ctrl) were larvae treated with non-toxic Cry9A-D125R. (B

and C) Quantification of the fluorescent signal of intestinal thickness (B) and cell number (C). Control (Ctrl) are midguts treated with the non-toxic Cry9A-D125R mutant. Toxin-free treated intestine was measured as 100%. *n*=36 images per treatment. *P* values were calculated by two-sided Student's t-test, *P*<0.0001 shows statistically significant differences. *P*>0.05 shows no significant difference. The large bar corresponds to the mean, whereas the smaller ones represent ±SEM.

Figure 5-4. Analysis of the activation of JNK and EGFR pathway after Cry9A treatment. *Jnk*, *puc* and *Egfr* genes expression in the intestine from fifteen 3rd instar larvae of striped stem borer after treatment with Cry9Aa (LC_{20}) for different times determined by RT-qPCR. Control (Ctrl) were larvae treated with non-toxic Cry9A-D125R. The data were normalized to uninfected control and *EF-1* gene was used as reference gene. The data were from triplicate biological samples performed in three independent experiments. *P* values were calculated by two-sided Student's t-test, *P*<0.05 shows significant difference. *P*>0.05 shows no significant difference. The error bar represents ±SEM.

Figure 5-5. Bioassays after silencing JNK and EGFR pathway genes. Insecticidal toxicity assay of Cry9Aa against neonate larvae of striped stem borer after silencing JAK/STAT pathway genes (*Jnk* and *egfr*) by RNAi. Thirty-five neonates were analyzed with each treatment. Silencing *gfp* was used as negative control. Three replicates were performed. *P*<0.001 shows statistically significant difference (one-way ANOVA and Tukey's test). The error bar represents ±SEM.

Figure 5-6. Bioassays after adding JNK inhibitor. Insecticidal toxicity assay of Cry9Aa (LC_{20}) against neonates of striped stem borer after treatment with JNK pathway inhibitor SP600125. Thirty-five neonates were analyzed with each treatment. Three replicates were performed. *P*<0.001 shows statistically significant difference (two-sided Student's t-test). The error bar represents ±SEM. Control (Ctrl) were larvae treated with non-toxic Cry9A-D125R.

Figure 5-7. Changes in midgut tissue morphology after silencing *Jnk* or adding inhibitor. (A) Sagittal view representative images of midgut tissues isolated from 3rd instar alive striped stem borer larvae treated with Cry9Aa (LC_{20}) with or without *Jnk* dsRNA or SP600125 inhibitor treatment observed in the LSCM. Hoechst33342 (blue color) labels nuclei. Phalloidin-647 (red color) stains F-actin present in the brush border (upper arrows) and in the visceral muscles (lower arrows). Control (Ctrl) were larvae treated with non-toxic Cry9A-D125R. (B and C) Quantification of the fluorescent signal of intestinal thickness (B) and cell number (C) obtained after Cry9Aa (LC_{20}) with or without *Jnk* dsRNA or SP600125 inhibitor treatment. Control (Ctrl) are midguts treated with the non-toxic Cry9A-D125R mutant. Toxin-free treated intestine was measured as 100%. *n* = 36 images per treatment. *P* values were calculated by one-way ANOVA and Tukey's test, *P*<0.0001 shows statistically significant differences. *P*>0.05 shows no significant difference. The large bar corresponds to the mean, whereas the smaller ones represent ±SEM.

Figure 5-8. Analysis of the upstream and downstream relationship between JNK and JAK/STAT. (A) Quantification of gene expression determined by RT-qPCR in intestines isolated from 15 larvae treated with Cry9A (LC_{20}) for time series. The data were normalized to uninfected control on biological triplicate samples and three independent experiments were performed. The error bar represents ±SEM. (B) Quantification of gene expression determined by RT-qPCR in intestines isolated from 15 silenced larvae treated with Cry9A (LC_{20}) for 6

and 48 h. Gene expression detected in toxin-free treated intestine was measured as 100%. Fifteen larvae were analyzed after silencing for each treatment. The data were normalized to uninfected control on biological triplicate samples and three independent experiments were performed. *P* values were calculated by two-sided Student's t-test, $P<0.05$ shows statistical differences. $P>0.05$ shows no significant difference. The error bar represents ±SEM.

Figure 5-9. Role of JNK and JAK/STAT in midgut regeneration induced by Cry9A. (A) Sagittal view representative images of midgut tissues isolated from Cry9Aa (LC_{20}) treated 3rd instar alive striped stem borer larvae pretreated with or without *Jnk* or *Stat* dsRNA treatment observed in LSCM. Six midgut tissues were analyzed and phospho-histone H3 (PH3) was detected by using a specific anti-PH3 antibody followed by FITC labeled secondary antibody (green color). Hoechst33342 (blue color) labels nuclei. Phalloidin-647 (red color) labels cytoskeleton. Control (Ctrl) were larvae treated with the non-toxic Cry9Aa-D125R. (B) Western blot detection of PH3 in midgut tissue samples from fifteen 3rd instar larvae after Cry9A (LC_{20}) intoxication after pretreatment with or without *Jnk* or *Stat* dsRNA. β-actin was detected as an internal reference. Histone H3 (H3) was detected to show that the loading quantity of H3 was similar. Control (Ctrl) were larvae treated with non-toxic Cry9A-D125R.

Figure 5-10. Role of JNK and JAK/STAT in defense responses induced by Cry9A. Representative images of seventy-two larvae treated with Cry9Aa (LC_{20}) for 120 h after treating with or without silencing *Jnk* or *Stat*. Negative control (Ctrl) was treated with the non-toxic Cry9A-D125R. (F) Quantification of length of seventy-two larvae treated with Cry9Aa (LC_{20}) for 120 h after treating with or without silencing *Jnk* or *Stat*. *P* values were calculated by one-way ANOVA and Tukey's test, $P<0.0001$ shows statistically significant differences.

Figure 5-11. Insecticidal bioassays of *S. frugiperda* against Bt insecticial protein. Insecticidal bioassay of Cry1Fa and Vip3Aa against neonate fall armyworm larvae that were pretreated with dsRNA of *Stat*. Thirty-five two-day-old larvae were analyzed in each treatment. Three replicates were performed. *P* values were calculated by two-sided Student's t-test, $P<0.0001$ shows statistically significant differences. $P>0.05$ shows no significant difference. The error bar represents ±SEM.

Figure 5-12. Changes in midgut tissue morphology after silencing *Stat*. (A) Sagittal view representative images of 4th instar fall armyworm larvae midgut tissues isolated after 72h of Cry1F (LC_{20}) treatment with or without *Stat* dsRNA pretreatment observed in the LSCM. Hoechst33342 (blue color) labels nuclei. Phalloidin-647 (red color) stains F-actin present in the brush border (upper arrows) and in the visceral muscles (lower arrows). Control (Ctrl) were larvae treated with diet without Cry1F toxin. (B and C) Quantification of the fluorescent signal of intestinal thickness (B) and cell number (C) obtained after 72h of Cry1F (LC_{20}) with or without *Stat* dsRNA pretreatment. Control (Ctrl) are midguts treated with the toxin-free artificial diet. Toxin-free treated intestine was measured as 100%. n=36 images per treatment. *P* values were calculated by one-way ANOVA and Tukey's test, $P<0.0001$ shows statistically significant differences. $P>0.05$ shows no significant difference. The large bar corresponds to the mean, whereas the smaller ones represent ±SEM.

Figure 5-13. Analysis of the midgut regeneration after silencing *Stat*. (A) Sagittal view representative images of midgut tissues isolated after 36 h of Cry1F (LC_{20}) treatment from 4th instar alive fall armyworm larvae with or without *Stat* dsRNA pretreatment observed in

LSCM. Six midgut tissues were analyzed and phospho-histone H3 (PH3) was detected by using a specific anti-PH3 antibody followed by FITC labeled secondary antibody (green color). Hoechst33342 (blue color) labels nuclei. Phalloidin-647 (red color) labels cytoskeleton. Control (Ctrl) were larvae treated without toxin. (B) Western blot detection of PH3 in midgut tissue samples from fifteen larvae of 4th instar fall armyworm after 36 h of Cry1F (LC_{20}) intoxication with or without *Stat* dsRNA treatment. β-actin was detected as an internal reference. Histone H3 (H3) was detected to show that the loading quantity of H3 was similar. Control (Ctrl) were larvae treated without toxin. (C) *Delta* gene expression determined by RT-qPCR in intestines isolated from fifteen 4th instar fall armyworm larvae treated with Cry1F or Vip3A (LC_{20}) for 36 h. The error bar represents ±SEM. *P* values were calculated by two-sided Student's t-test, $P<0.05$ shows statistical difference. (D) Representative images from seventy-two 4th instar larvae treated with Cry1F (LC_{20}) for 72 h with or without silencing *Stat*. Negative control (Ctrl) was treated without toxin. (E) Quantification of length from seventy-two 4th instar larvae treated with Cry1F (LC_{20}) for 72 h after treating with or without silencing *Stat*. *P* values were calculated by one-way ANOVA and Tukey's test, $P<0.0001$ shows statistically significant differences.

Figure 5-14. Analysis of the synergistic insecticidal activity between silencing *Stat* and Bt for pesticide protecting rice seedlings from damage by striped stem borer. (A) Mortality of 2nd instar larvae of striped stem borer (six larvae per plant) on rice seedlings sprayed with the mixture of Bt *fukuokaensis* strain and *Stat*-dsRNA or *gfp*-dsRNA combined nanoparticles. Representative larvae treated with Bt strain for 3 days with or without silencing *Stat*. Negative control were plants sprayed without Bt strain. The error bar represents ±SEM. (B) Growth of rice seedlings sprayed with or without the mixture of Bt pesticide and *Stat*-dsRNA combined nanoparticles. Negative control were plants sprayed with Bt strain and *gfp*-dsRNA combined nanoparticles. Two rice seedlings at four-leaf stage per pot and two pots per treatment, with three replicates were performed. (C) Representative images of wormholes produced by the larvae that damage the rice stems, especially near the ground. The different treatments were indicated in the figure. (D) Quantification of plant height of rice seedlings sprayed with or without mixture of Bt strain and *Stat*-dsRNA combined nanoparticles and the infected with striped stem borer larvae. *P* values were calculated by one-way ANOVA and Tukey's test. $P<0.0001$ indicates statically significant difference. The large bar corresponds to the mean, whereas the smaller ones represent ±SEM.

List of tables

List of acronyms

Bt: *Bacillus thuringiensis*

RNAi: RNA interference

ISC: intestinal stem cell

EGFR: Epidermal Growth Factor Receptor

dsRNA: double-stranded RNA

JAK/STAT: Janus kinase/signal transducer and activator of transcription

Vip: vegetative insecticidal proteins

Sip: secreted insecticidal proteins

Cry: Crystal proteins

BBMVs: brush border membrane vesicles

GC: Goblet cells

PFTs: pore-forming toxins

AMPK: AMP-activated protein kinase

JNK: c-Jun N-terminal kinase

EBs: enteroblasts

VM: visceral muscles

ECs: enterocytes

Chapter 1

The complexity of insect midgut cells: types, peculiarities, and functions: a review

Abstract

Lepidoptera, the second largest order of insects, encompasses a vast diversity of species, many of which are among the most destructive agricultural pests globally. These insects, including notorious species such as *Spodoptera frugiperda*, *Helicoverpa armigera*, and *Chilo suppressalis*, are responsible for extensive damage to a wide variety of economically important crops, forests, and horticultural plants, thereby threatening food security and agricultural sustainability. To mitigate these threats, chemical insecticides have been widely employed; however, their excessive and prolonged use has led to several negative consequences, including environmental contamination, the decline of non-target organisms, bioaccumulation in ecosystems, and serious risks to human health.

Bacillus thuringiensis (Bt), a gram-positive soil-dwelling bacterium, has emerged as the most successful and environmentally friendly biological agent for pest control. Bt-based microbial insecticides and genetically modified crops expressing Bt-derived insecticidal proteins - particularly Cry and Vip toxins - have been extensively utilized in integrated pest management programs. These insecticidal proteins exert their toxic effects primarily through the formation of pores in the midgut epithelial cells of susceptible insect larvae. Upon ingestion, the Bt protoxins are solubilized and activated in the alkaline gut environment, bind to specific receptors on the brush border membrane, and subsequently oligomerize to form transmembrane pores, leading to osmotic imbalance, epithelial disruption, septicemia, and eventually larval death.

Despite their proven efficacy, the long-term effectiveness of Bt-based products has been challenged by the emergence of insect resistance and diminished toxicity in field populations. One of the key factors contributing to this phenomenon is the intrinsic defense response of the insect midgut. The midgut not only serves as the central site for nutrient digestion and absorption but also functions as a frontline immune barrier against ingested pathogens and xenobiotics, including Bt toxins. In response to pore formation and epithelial damage, insects can activate complex defense mechanisms such as epithelial cell shedding, stem cell-mediated tissue regeneration, production of antimicrobial peptides, and upregulation of detoxification enzymes. These adaptive responses help maintain midgut integrity and reduce the overall susceptibility to Bt toxins.

In this review, we examine the structure and physiological roles of the insect midgut, with a specific focus on its multifaceted defensive strategies in response to Bt-derived pore-forming toxins. We also discuss the signaling pathways implicated in midgut defense, including the JAK/STAT, JNK, and caspase-related cascades, which regulate processes such as immune activation, apoptosis, and epithelial regeneration. Understanding these molecular mechanisms is essential for developing novel strategies to counteract resistance and enhance the efficacy of Bt-based pest control.

***Keywords*:** Lepidoptera, *Bacillus thuringiensis*, midgut, defense responses, pore-forming toxins

1. Introduction

Lepidoptera is the second largest order within the class Insecta, encompassing more than 180,000 described species, with estimates suggesting that the actual number may be significantly higher due to ongoing discoveries and taxonomic revisions (Perveen and Khan, 2017). This diverse order is traditionally divided into two major subgroups: Rhopalocera and Heterocera, which exhibit distinct morphological, behavioral, and ecological characteristics. Lepidopteran insects are distributed worldwide, occupying a wide range of habitats from temperate to tropical ecosystems, with the greatest species richness occurring in tropical and subtropical regions where climatic conditions and plant diversity support high levels of lepidopteran biodiversity.

The larval stages of Lepidoptera are predominantly phytophagous and are known for their voracious feeding behavior. These larvae include some of the most destructive and economically important agricultural pests. Species such as *Chilo suppressalis*, *Helicoverpa armigera*, *Ostrinia nubilalis*, *Spodoptera litura*, *Plutella xylostella*, *Pieris rapae*, *Spodoptera frugiperda*, *Conogethes punctiferalis*, and *Dendrolimus punctatus* have been documented to inflict severe damage across a variety of crops including rice, maize, cotton, soybean, cruciferous vegetables, and forest trees (Powell et al., 2009; Zalucki et al., 2002).

These pests not only reduce crop yields and quality but also incur substantial economic losses due to increased control costs and trade restrictions. Their impact is further exacerbated by their high reproductive potential, migratory behavior, polyphagy, and, in some cases, resistance to conventional chemical insecticides. As a result, the management of lepidopteran pests remains a major challenge in modern agriculture, driving the need for more sustainable, environmentally friendly, and effective pest control strategies (Subedi et al., 2023).

1.1 *Chilo suppressalis*

Chilo suppressalis (Walker) (Lepidoptera: Pyralidae), commonly known as the rice stem borer, is a major lepidopteran pest that is extensively distributed across the vast agricultural regions of China. Its geographical range spans from the northeastern province of Heilongjiang to the southern island of Hainan, encompassing a wide array of climatic zones and cropping systems. This pest is regarded as one of the most destructive insects affecting rice (*Oryza sativa*) and *Zizania latifolia*, two significant crops in China. Rice, as one of China's most important staple crops, has high nutritional value and is among the most heavily promoted and widely cultivated crops in the country (Saud et al., 2022). Meanwhile, *Z. latifolia* is a perennial aquatic crop native to East Asia and uniquely cultivated in China. Traditionally grown in paddy fields south of the Huai River, it is particularly favored in the middle and lower Yangtze River regions due to its tender edible stems, which are rich in dietary fiber, vitamins, and minerals. The crop enjoys growing consumer demand and plays a key role in the diversification and modernization of regional agricultural economies (Huang et al., 2022). *C. suppressalis* has inflicted severe economic damage on both of these crops in China. The larvae bore into plant stems, damaging vascular tissues and disrupting nutrient flow, which leads to stunted growth, lodging, and in severe cases, complete crop failure. The concealed feeding behavior of the larvae within the stem tissues makes early detection and control particularly challenging. As a result, *C. suppressalis* has become a persistent threat to rice production and a growing concern in *Z. latifolia* cultivation. The pest’s widespread

prevalence and strong adaptability, combined with the difficulty of effective management, contribute to substantial annual yield losses and economic damage. This has made the development of more sustainable and targeted pest control strategies - such as biological control - an urgent priority in integrated pest management programs across China.

The number of annual generations of *Chilo suppressalis* on rice varies significantly with geographical location and climatic conditions. In regions with warmer climates and longer growing seasons, particularly in southern China, the pest can complete up to five generations per year, greatly increasing its potential to cause recurring and cumulative damage throughout the cropping season (Wu et al., 2009). Although each larva may infest and damage approximately 3 to 5 rice tillers, the exponential growth of populations under favorable conditions can result in widespread infestation and significant agricultural losses. High reproductive capacity, overlapping generations, and the pest's concealed feeding habits enable rapid population buildup, often overwhelming conventional pest control strategies (Xiang et al., 2023). During the tillering stage, *C. suppressalis* infestation results in "double drying" symptoms. At the panicle initiation stage, its damage manifests as injured stems, leading to severe yield losses. If not effectively managed, *C. suppressalis* outbreaks can reduce rice yields by up to 30%, depending on the severity of infestation, crop variety, and regional farming practices (Li et al., 2020). This pest is recognized as one of the three most destructive lepidopteran pests in rice agroecosystems. Its impact extends beyond individual farms, posing a systemic threat to food security, farmer income, and regional agricultural sustainability. According to recent estimates, economic losses attributed to *C. suppressalis* infestation in China exceed 11.5 billion RMB annually, underscoring the urgent need for more effective, environmentally sound, and sustainable pest management strategies.

Zizania latifolia also suffers severe damage from *C. suppressalis*, as the larvae bore into the plant, leading to significant reductions in both quality and yield (Yu et al., 2004). Compared to its impact on rice, *C. suppressalis* infestation in *Z. latifolia* fields is more concealed. Newly hatched larvae primarily feed within the leaf sheaths, and from the second instar onward, they burrow into the plant, making pest control in *Z. latifolia* fields considerably more challenging (Zheng et al., 2003).

1.2 *Spodoptera frugiperda*

The fall armyworm (*Spodoptera frugiperda* J. E. Smith) is a significant agricultural pest in the family Noctuidae (Lepidoptera), originally from the tropical and subtropical regions of the Americas. It is a major pest with substantial economic impacts on agricultural production (Todd et al., 1980). Known for its remarkable migratory abilities, the fall armyworm can rapidly spread over long distances through flight and can reproduce in large numbers under favorable environmental conditions (Baudron et al., 2019). One of the most alarming features of *S. frugiperda* is its extraordinary migratory behavior. Adult moths are strong fliers capable of traveling hundreds of kilometers in a single night, allowing the species to quickly colonize new areas. This high mobility, combined with favorable climatic conditions, enables the pest to expand its range rapidly, even in non-native regions (Baudron et al., 2019). Following its transatlantic invasion into Africa in 2016, the fall armyworm has subsequently spread to Asia, including China, India, and Southeast Asia, where it has adapted quickly to local environmental conditions and host plant availability. *S. frugiperda* is a highly polyphagous

insect capable of feeding on at least 353 plant species across 76 botanical families, encompassing a wide range of economically important crops (Montezano et al., 2018). These include maize, rice, sorghum, wheat, soybean, sugarcane, cotton, various legumes, and numerous vegetable crops. This broad host range not only enhances its survival prospects but also complicates management strategies, as it can persist even when rotated across different crop types. Genetic and behavioral studies have identified two host-adapted strains of the fall armyworm: the corn strain and the rice strain, which differ in their host plant preferences and geographical distributions (Nagoshi et al., 2007). The corn strain predominantly infests maize, cotton, and sorghum, whereas the rice strain tends to prefer rice, grasses, and other monocots. Although morphologically indistinguishable, these strains exhibit distinct molecular markers and feeding behaviors, which have implications for pest surveillance, resistance management, and targeted control strategies.

Since its emergence as a global invasive pest in 2015, the fall armyworm has demonstrated an alarming capacity for long-distance dispersal and rapid establishment across diverse agroecological regions. Its global spread has become one of the most serious transboundary plant pest challenges in recent decades. In early 2016, the pest was first reported in West and Central Africa, specifically in Nigeria, Benin, São Tomé and Príncipe, and Togo (Goergen et al., 2016). Within a remarkably short time frame of less than three years, it had invaded 44 African countries, causing devastating damage to staple crops such as maize, which is a critical source of food and income for smallholder farmers (FAO, 2018). Following its establishment in Africa, *S. frugiperda* continued its eastward migration, reaching the Indian subcontinent by mid-2018. Initial detections in India were quickly followed by outbreaks across Southeast and East Asia, with confirmed invasions in countries such as Thailand, Myanmar, Vietnam, South Korea, and Japan (Guo et al., 2018; Shylesha et al., 2018). In December 2018, the fall armyworm was first reported in Yunnan Province, China (Yang et al., 2019), marking its entry into one of the world's largest and most densely cultivated agricultural regions. Due to its strong flight ability, broad host range, and favorable climatic conditions, *S. frugiperda* spread rapidly across the country. Within just one year, infestations were recorded in 26 provinces, affecting key crops such as maize, sugarcane, and sorghum, and posing a major threat to national food security and agricultural sustainability (Zhang et al., 2019; Jiang et al., 2019). The global spread of *S. frugiperda* has continued unabated. As of 2021, it had been reported in over 70 countries spanning Africa, Asia, Oceania, and the Americas, and for the first time, the pest was detected in Europe - specifically in the Canary Islands of Spain (FAO, 2021; CABI, 2021). Its invasion into Europe raises serious concerns for continental agriculture, given the EU's extensive maize cultivation and the limited availability of approved emergency pest control measures. The ongoing expansion of *S. frugiperda* highlights its status as a truly global pest, requiring international collaboration and long-term integrated pest management strategies.

The fall armyworm poses a critical threat to global agricultural production, particularly due to its voracious feeding habits, wide host range, and rapid population growth. In the absence of effective control measures, the potential impact on crop yields - especially maize - is devastating. According to estimates by Day et al. (2017), maize yield losses attributable to *S. frugiperda* infestations could range from 4.1 to 17.7 million tons annually across 12 major maize-producing countries in Africa. These losses translate into significant economic damage,

with projected financial losses ranging from 1.088 billion to 4.661 billion USD per year. In a broader context, total crop losses due to fall armyworm infestations in Sub-Saharan Africa are estimated to reach up to 13 billion USD, underscoring the scale of this agricultural crisis (Mendesil et al., 2023). China has also experienced serious economic repercussions following the invasion of the fall armyworm. Since its first detection in Yunnan Province in 2018, the pest has rapidly established itself in key maize-growing regions. In 2019 alone, the direct economic losses attributed to *S. frugiperda* infestations in Dehong, Yunnan, amounted to approximately 3.6651 million RMB. Meanwhile, Qujing, another major maize-producing area in Yunnan, reported direct losses reaching 29.6227 million RMB (Wan et al., 2022; Zhang et al., 2020). These figures reflect only the initial wave of damage, and do not account for long-term productivity decline or broader economic ripple effects. Beyond yield reduction and crop destruction, the presence of *S. frugiperda* has significantly increased the financial burden on farmers. The need for emergency pest control has led to higher expenditures on pesticides, seeds (including those bred for pest resistance), and labor.

Currently, the predominant strategies for managing major agricultural pests such as the fall armyworm (*Spodoptera frugiperda*) heavily rely on the use of synthetic chemical pesticides. Among these, pyrethroids, carbamates, and organophosphates are commonly applied due to their relatively low cost, high availability, and immediate insecticidal effects (Kumela et al., 2019). However, the widespread and often indiscriminate use of these chemical agents has led to several unintended consequences. This has raised serious concerns regarding environmental pollution, food safety, and human health risks. Prolonged exposure of pest populations to the same chemical agents exerts strong selective pressure, accelerating the development of pesticide resistance. This resistance not only diminishes the efficacy of pest control but also necessitates higher dosages or the application of more toxic alternatives, further escalating control costs and environmental risks. In addition, chemical pesticides can have deleterious non-target effects, harming beneficial insects such as pollinators and natural enemies, and disrupting ecological balance in agroecosystems. In contrast, biological control represents a more sustainable and environmentally friendly alternative to chemical pest management. It involves the use of living organisms - such as natural predators, parasitoids, and microbial agents - to suppress pest populations. Biological control strategies offer several advantages: they are generally safer for humans and animals, have minimal environmental impact, and reduce the likelihood of resistance development due to their often complex modes of action. During the larval stages of pests like *S. frugiperda*, the application of microbial biopesticides such as *Bacillus thuringiensis* (Bt) and *Beauveria bassiana* has proven to be an effective strategy. Bt, a Gram-positive soil bacterium, produces insecticidal crystal (Cry) proteins that specifically target the midgut epithelial cells of susceptible insects, leading to pore formation, osmotic imbalance, and ultimately larval death. Due to its host specificity, safety profile, and lack of toxicity to humans, animals, and most non-target organisms, Bt has become the most widely used and successful microbial agent in integrated pest management (IPM) programs worldwide. Similarly, *Beauveria bassiana*, an entomopathogenic fungus, infects a wide range of insect hosts through direct penetration of the cuticle, making it another valuable tool in the biocontrol arsenal.

In summary, while chemical control remains an important component of pest management, the integration of biological control methods - particularly those involving Bt and other

entomopathogenic microbes - offers a promising path toward reducing reliance on synthetic pesticides, mitigating resistance development, and fostering a more resilient and sustainable agricultural system.

2. *Bacillus thuringiensis*

Bacillus thuringiensis (Bt) is a Gram-positive, rod-shaped, spore-forming bacterium belonging to the family *Bacillaceae*. It is recognized as one of the most important microbial agents in the biological control of insect pests due to its potent insecticidal properties. Bt is ubiquitous in nature and has been isolated from diverse ecological niches, including soil, freshwater and marine environments, the phyllosphere of various coniferous and deciduous plant species, and even from necrotic human tissues and insect cadavers (Vilas et al., 2007; Raymond et al., 2010; Rubio et al., 2016; Jisha et al., 2013). This widespread distribution highlights its ecological versatility and adaptive capacity to survive under various environmental conditions.

The discovery of *B. thuringiensis* dates back to the early 20th century. In 1901, Japanese biologist Shigetane Ishiwata first isolated the bacterium from diseased silkworm (*Bombyx mori*) larvae exhibiting symptoms of flaccid paralysis. He initially named the bacterium *Bacillus sotto* and noted its potential pathogenicity to insects (Ishiwata et al., 1901). Independently, in 1915, German scientist Ernst Berliner isolated a similar bacterium from larvae of the Mediterranean flour moth (*Ephestia kuehniella*) in the Thuringia region of Germany. He named it *Bacillus thuringiensis* in reference to its geographic origin (Berliner et al., 1915). It was later recognized that both isolates belonged to the same species, now universally known as *Bacillus thuringiensis*.

Based on flagellar (H) -antigens, *Bacillus thuringiensis* (Bt) is primarily classified into 63 serotypes, each typically exhibiting specific insecticidal activity against particular insect orders (Thiery and Frachon, 1997; Zeigler, 2000). For instance, most strains of the Bt *israelensis* subspecies are toxic to Dipteran pests such as mosquito larvae and flies (Fillinger et al., 2003; Goldberg and Margalit, 1977). The Bt *aizawai* and Bt *kurstaki* subspecies exhibit insecticidal activity against Lepidopteran larvae (Dulmage, 1970; Ohba and Aizawa, 1986), while the Bt *tenebrionis* and Bt *japonensis* subspecies are effective against certain Coleopteran larvae (Ohba et al., 1992; Krieg et al., 1983). Furthermore, novel Bt strains with unique insecticidal spectra have been identified. For example, strain Bt185 demonstrates toxicity toward larvae of the superfamily Scarabaeoidea (Coleoptera) (Yu et al., 2006). Strains Bt1012 and C9F11, discovered in 2018, have shown insecticidal activity against planthopper pests such as *Laodelphax striatellus* and *Nilaparvata lugens*, which belong to the family Delphacidae (order Homoptera) (Cao et al., 2020; Liu et al., 2018). In addition, certain Bt strains have demonstrated toxicity against nematodes (Aschelminthes) (Luo et al., 2013). To date, most studies indicate that Bt is safe for humans, mice, rabbits, and other vertebrates (McClintock et al., 1995; Siegel, 2001; Ignoffo, 1973; Lemos et al., 2013), and growing evidence supports the safety of commercially applied Bt strains for pollinators such as honeybees (Mommaerts et al., 2010).

The main distinguishing feature of *Bacillus thuringiensis* (Bt) from other species in the *Bacillus* genus is its ability to produce insecticidal crystal proteins (ICPs), which include the Cry and Cyt proteins. These proteins are produced during the later stages of growth, coinciding with the formation of spores. The Cry and Cyt proteins exist in an inactive

crystalline form within the bacterial cells and are released into the environment upon the breakdown of the bacterial spores. When ingested by insect larvae, these proteins undergo activation in the insect's alkaline gut environment, where they bind to specific receptors in the gut cells, causing cell disruption, gut paralysis, and ultimately, insect death. The toxicity of these proteins is highly specific to certain insect pests, particularly those from the orders Lepidoptera and Hymenoptera. Because of their selective toxicity, these proteins are often referred to as insecticidal crystal proteins (ICPs). Interestingly, some Bt strains produce additional insecticidal proteins that exhibit activity against other types of pests. In particular, certain Cry proteins are also capable of targeting nematodes, mites, and even some protozoa, expanding the potential application of Bt as a biopesticide across different pest groups (Mohanty et al., 2025; Tan et al., 2025).

In addition to the crystalline proteins, Bt also produces a variety of insecticidal proteins during its vegetative phase. These include vegetative insecticidal proteins (Vip) and secreted insecticidal proteins (Sip), which are released into the growth medium as the bacterium grows. Vip proteins, for instance, are produced in the actively growing vegetative cells and can target a range of insects. Sip proteins are secreted extracellularly and have similar insecticidal properties, further enhancing the bacterium's pest control capabilities (Palma et al., 2014; Gupta et al., 2021; Mendoza-Almanza et al., 2020; Cao et al., 2022).

One of the major advantages of Bt insecticidal proteins is their specificity. These proteins are highly selective, typically affecting only the target pests and having no harmful effects on humans, vertebrates, plants, or beneficial insects such as pollinators. This selectivity makes Bt an environmentally friendly alternative to traditional chemical pesticides, which can have broader ecological consequences. Because of its safety profile and effectiveness, Bt is widely used in the production of biological insecticides that serve as alternatives to chemical pesticides for the control of agricultural pests, as well as pests in public health management, such as mosquitoes. These biopesticides are seen as crucial tools for integrated pest management systems, promoting sustainable agriculture while minimizing environmental and health risks (Rubio et al., 2016; Jisha et al., 2013; Herrero et al., 2016).

Overall, Bt’s unique ability to produce a diverse array of insecticidal proteins, coupled with its environmental safety, has established it as one of the most important and effective biocontrol agents available for pest management worldwide.

2.1 Crystal proteins (Cry)

The largest class of insecticidal proteins produced by *Bacillus thuringiensis* (Bt) are the Cry proteins, which play a central role in the bacterium’s effectiveness as a biopesticide. These proteins are highly effective against a broad spectrum of insect pests, including species from the orders Coleoptera, Lepidoptera, Diptera, and Hymenoptera. Due to their potency and specificity, Cry proteins have been widely utilized in both agricultural pest management and in controlling pests that affect public health. In addition to their well-known insecticidal properties, Cry proteins have demonstrated a range of beneficial effects beyond insect control. These proteins have been shown to exhibit activity against nematodes, mites, and snails, which further extends their utility in pest management. More surprisingly, some Cry proteins have also been found to have potential therapeutic effects, including the ability to treat human

cancer cells, making them of interest in medical research (Sanahuja et al., 2011; Moazamian et al., 2018; Ohba et al., 2009; Mizuki et al., 2000).

Bt Cry proteins can be classified into several distinct groups based on their molecular structure and homology. The most well-known and studied group is the three-domain Cry proteins, which are characterized by their tripartite structure. These proteins are composed of three distinct structural domains, each playing a crucial role in the protein's insecticidal activity. The three-domain Cry proteins represent the largest and most extensively researched group of Cry proteins, with numerous variants and subtypes identified, each with varying levels of specificity for different insect species. In addition to the three-domain Cry proteins, there are other groups of Cry proteins, including Mtx-like proteins and Bin-like proteins. Mtx-like proteins share structural similarities with the three-domain proteins but differ in certain aspects of their molecular architecture. These proteins have been found to exhibit insecticidal activity as well, though they are less studied compared to the well-established three-domain Cry proteins. Similarly, Bin-like proteins are another class of Cry proteins, which are named after their structural features that resemble binuclear complexes. These proteins have been shown to have insecticidal properties, though their molecular mechanisms and specificities are still under investigation. As research into Bt Cry proteins continues to expand, there is growing interest in understanding the "non-three-domain" Cry proteins, which do not fit neatly into the established three-domain classification. These proteins, while less understood, are becoming increasingly recognized for their unique properties and their potential in pest control. New insights into their structure, function, and insecticidal mechanisms are emerging, providing a broader understanding of the diversity of Cry proteins and their applications in biocontrol (Domínguez et al., 2020).

As shown in Figure 1-1, the Cry protein family from Bt displays significant variation in their amino acid sequences. However, despite these differences, all Cry proteins share a highly similar and conserved three-dimensional structural arrangement. These proteins are globular in shape and consist of three distinct structural domains that possess similar topological structures, which are critical to their insecticidal function (Bravo et al., 2010; Li et al., 1991; Grochulski et al., 1995; Morse et al., 2001; Siegfried et al., 2005; Boonserm et al., 2005; Boonserm et al., 2006). The conserved structural organization of Cry proteins is central to their ability to target and kill specific insect pests.

Domain I of the Cry protein consists of seven α-helices. Among these, six helices form a double-channel structure that surrounds a central hydrophobic α-helix (referred to as α-helix-5). This helical region is crucial for the protein's ability to insert into the cell membranes of target organisms, where it facilitates pore formation. The membrane insertion and pore formation abilities are key to the toxic effects of the Cry proteins. Upon ingestion by an insect, the Cry protein is activated in the insect's gut, and the membrane-insertion activity of Domain I leads to the formation of pores in the gut epithelial cells. This disruption of gut cells leads to paralysis and eventual death of the insect (Ibrahim et al., 2010; Rahman et al., 2011; De Maagd et al., 2003; Pigott et al., 2007; Zhang et al., 2008; Meng et al., 2024).

Domain II is the most variable of the three domains in Bt toxins and plays a critical role in determining the host specificity of the toxin. The variability in this domain influences which insect species the Cry protein will target, making it a key factor in the protein's selectivity. Specifically, Domain II contains a loop structure formed by an anti-parallel β-sheet. This loop

is the least conserved region of the toxin and is involved in the interaction between the three domains of the protein. Additionally, it is responsible for the binding of the Cry protein to homologous receptors on the insect gut cells. Variations in Domain II's structure, particularly in the loop, influence how the protein binds to specific receptors and, consequently, the range of insect pests that the protein can effectively target (Thammasittirong et al., 2023; Ibrahim et al., 2010; Rahman et al., 2011; De Maagd et al., 2003; Pigott et al., 2007; Zhang et al., 2008; Adegawa et al., 2022; Shen et al., 2024).

Domain III, consisting of two anti-parallel β-sheets, plays a comprehensive role in the overall function of the Cry protein. This domain is involved in the binding of the Cry protein to receptors on the insect gut cells, as well as in the formation of ion channels in the cell membrane. The interaction between Domain III and the receptors is a critical step in the activation of the Cry protein, as it determines how well the protein can bind and initiate the toxic effects. The ability of Domain III to facilitate receptor binding and pore formation is directly related to the overall toxicity of the Cry protein. Additionally, this domain contributes to the protein's stability and its ability to maintain its insecticidal activity in the insect gut (Ibrahim et al., 2010; Rahman et al., 2011; De Maagd et al., 2003; Pigott et al., 2007; Zhang et al., 2008; Sena da Silva et al., 2021; Gómez et al., 2020; Cong et al., 2024).

Together, these three domains collaborate to form a functional, insecticidal protein with the ability to specifically target and kill certain insect species. The conserved structural features across the Cry protein family, despite sequence variations, ensure that the proteins retain their potent activity, while also allowing for the diversity of Cry proteins that can target a wide variety of pests.

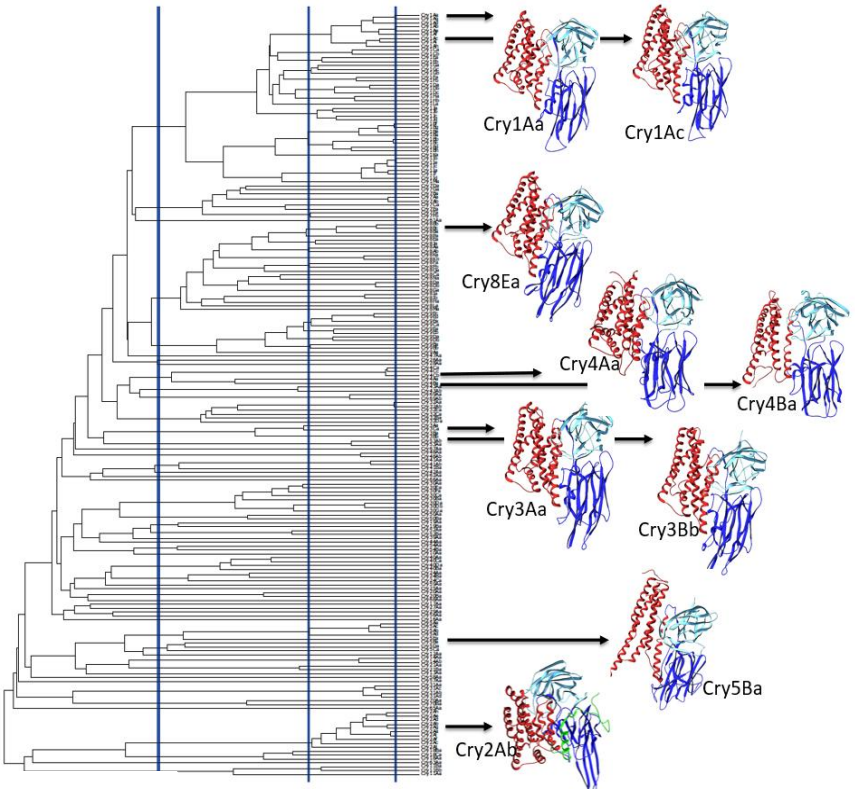

Figure 1-1. Cry toxin phylogenetic tree and protein structure (Bravo et al., 2010)

The primary mechanism of action of Cry proteins, as illustrated in Figure 1-2 (Pardo-López et al., 2013), involves a multi-step process through which the proteins form lytic pores in the apical membrane of target insect midgut epithelial cells, leading to cell rupture and insect death. The process begins immediately after the insect ingests the insecticidal crystal proteins (ICPs) and unfolds in the following sequential steps:

Ingestion and Activation: Once ingested by susceptible larvae, the Cry protein undergoes dissolution in the alkaline environment of the insect's midgut. This dissolution releases a large number of protoxin molecules, which are the precursor forms of the Cry proteins. The protoxins are then partially digested by the insect's digestive proteases, which cleave the protoxins into smaller fragments, resulting in the activation of the proteins. For example, the Cry1A protoxin, which initially has a molecular weight of approximately 130 kDa, is cleaved into a smaller, active toxin of approximately 60 kDa. This step is crucial because the activated toxin is the form that exhibits insecticidal properties;

Binding to Receptors: Once activated, the toxins then bind to specific receptors on the microvilli of midgut epithelial cells, such as the CAD (cadherin-like) receptors. This binding promotes further cleavage of the toxin and triggers oligomerization, where individual toxin molecules come together to form larger, multimeric complexes. The oligomerized toxin then binds to secondary receptors, which are membrane-bound proteins that typically anchor the toxins to the cell membrane. These secondary receptors include glycosylphosphatidylinositol (GPI)-anchored proteins such as aminopeptidase N (APN) in *Manduca sexta* or alkaline phosphatase (ALP) in *Heliothis virescens*. This secondary binding step is critical for the toxin's specific interaction with midgut cells and for its subsequent activity (Bravo et al., 2007; Jurat-Fuentes et al., 2006);

Pore Formation and Cell Disruption: Following oligomerization and receptor binding, the activated Cry toxin oligomers insert into the lipid raft membranes of the midgut epithelial cells. These membrane regions are enriched with cholesterol and other lipids, which facilitate the insertion of the toxin into the membrane. The toxin forms pores with a diameter of approximately 0.5-1.0 nm, disrupting the osmotic balance within the cells. The formation of these pores compromises the integrity of the cell membrane, leading to leakage of intracellular contents and loss of essential cellular functions. This damage to the cell membrane results in the rupture of the midgut epithelial cells, causing severe cellular dysfunction. If the insect is unable to regenerate new epithelial cells quickly enough to replace those that have been damaged or destroyed, this leads to systemic infection and septicemia. Ultimately, the insect succumbs to the damage, resulting in its death (Pardo-López et al., 2006; Zhuang et al., 2002).

In cases where the damage to the midgut cells is not immediately fatal, the insect may still experience significant negative effects. Minor damage, while it may be tolerated by the insect in the short term, can lead to a slowdown in larval growth, delayed development, and impaired feeding. This can significantly reduce the insect's overall fitness, impairing its ability to survive to adulthood or reproduce, even if it does not die immediately from the toxin (Pardo-López et al., 2006; Zhuang et al., 2002).

Thus, the Cry protein's insecticidal action is both highly specific and effective, resulting in the death of the insect after a series of carefully orchestrated molecular interactions. The combination of receptor binding, oligomerization, and pore formation makes Cry proteins

powerful tools in pest control, especially in agricultural settings, where they are employed to target specific pest species without harming beneficial insects or the environment.

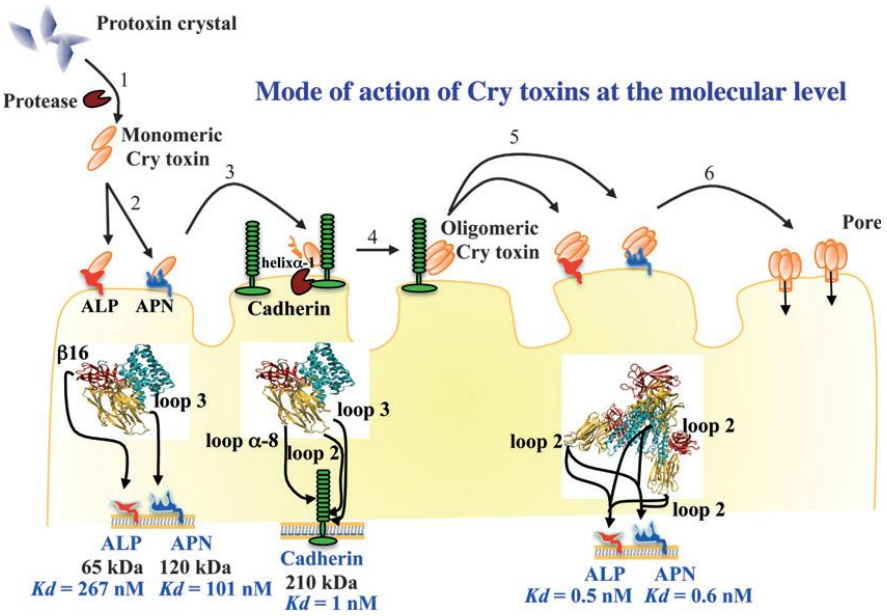

Figure. 1-2. Mode of action of Cry toxins (Pardo-López et al., 2013)

2.2 Vegetative insecticidal proteins (Vip)

In 1996, Estruch and colleagues made an important discovery by identifying a non-crystalline protein secreted by *Bacillus thuringiensis* (Bt) strains into the culture medium. This protein was named Vegetative Insecticidal Protein (Vip) (Estruch et al., 1996). Unlike the crystalline proteins, such as Cry proteins, which are produced during the later stages of bacterial growth and are stored in crystal form, Vip proteins are secreted during the vegetative phase of the bacterium's growth. This unique characteristic of Vip proteins opened up new possibilities for Bt's use in pest control.

Vip proteins are classified into four primary families: Vpb1, Vpa2, Vip3, and Vpb4. Among these, the Vip3 family is the most extensively studied and is composed of 14 different subtypes, with over 120 distinct proteins identified. These proteins have demonstrated highly efficient insecticidal activity, particularly against Lepidoptera pests, which include a wide range of economically significant agricultural pests. Notable targets include *Spodoptera exigua*, *Spodoptera frugiperda*, and *Helicoverpa armigera*, all of which are major pests in various crops (Gupta et al., 2021).

One of the standout features of Vip3 proteins, particularly Vip3A, is their ability to act effectively against Cry-insensitive pests, such as *Agrotis ypsilon*. This makes Vip3A a particularly valuable tool in pest management, as it can target pests that have developed resistance to the more commonly used Cry proteins. Vip3A's insecticidal action is also remarkable because it does not share significant homology with Cry proteins in terms of amino acid sequences, meaning it is structurally distinct from the Cry proteins. As a result, Vip3A interacts with a different receptor-binding site on the insect midgut, further enhancing its ability to target pests that are resistant to Cry proteins. Due to its unique mode of action and broad spectrum of activity, Vip3A is often used in combination with Cry proteins in

transgenic Bt crops. This combination broadens the insecticidal spectrum of the crops, allowing them to target a wider range of pest species more effectively. Furthermore, this combination strategy is crucial for managing resistance to Cry proteins. By utilizing both Cry and Vip proteins, the likelihood of pests developing resistance to the biopesticide is reduced, as the two proteins target different receptors and operate through distinct mechanisms, making it more difficult for pests to simultaneously evolve resistance to both.

The effectiveness of Vip3A, especially in the context of Cry-resistant pests, has been well-documented in several studies. For instance, Vip3A has been shown to be effective against a variety of Lepidoptera species, including those that are resistant to Cry proteins, ensuring that Bt-based biopesticides maintain their efficacy over time. The use of Vip3A in Bt crops has contributed significantly to the management of pest resistance, offering a sustainable solution to the challenge of pest control in agriculture (Sena et al., 2009; Wang et al., 2018; Kurtz et al., 2007; Jackson et al., 2007; Tabashnik et al., 2017; Xiao et al., 2019).

Overall, the discovery of Vip proteins, particularly Vip3A, has expanded the potential of *Bacillus thuringiensis* in integrated pest management. These proteins, in combination with Cry proteins, provide a powerful tool in the fight against insect pests, offering enhanced protection for crops while reducing the environmental impact compared to traditional chemical pesticides. As research continues, further understanding of Vip proteins and their applications is likely to improve pest management strategies, particularly in the face of evolving resistance in pest populations.

The high-resolution three-dimensional structure of the Vip3Aa protoxin and its activated protein was elucidated through cryo-electron microscopy, revealing that the Vip3Aa protoxin is composed of five domains (Figure 1-3). Domain I (1-198 aa) consists of four highly curved helices (α1-α4), forming a pyramid-like shape and is confirmed to be the proteinase cleavage site. Domain II (199-325 aa) forms a tetrameric core with five α-helices, and two extended loop regions (221-226 aa; 239-247 aa) move toward adjacent subunits to maintain the stability of the Vip3 oligomer. Domain III (328-536 aa) consists of three anti-parallel β-strands forming a β-prism fold, which interacts with the N-terminal fragment (14-23 aa). Domains IV and V are linked by long linkers and belong to the carbohydrate-binding module (CBM); due to their higher flexibility, they can freely interact with Domain III. Therefore, this structure suggests that the Vip3 protoxin tetramer is composed of a pyramid shape formed by the N-terminal core and an exposed C-terminal region in the solvent (Figure 1-4). Upon activation, Vip3Aa retains the same domain organization as the protoxin, with Domains II-V maintaining a similar overall conformation. However, Domain I undergoes significant conformational changes, causing the pyramid tip to transform into a needle-like structure. Specifically, the three anti-parallel helices (α2-α4) at the N-terminal undergo a folding process resembling a twisting vine, reorganizing into a continuous long helix, which then assembles into parallel four-helix bundle coils in the digested Vip3Aa tetramer.

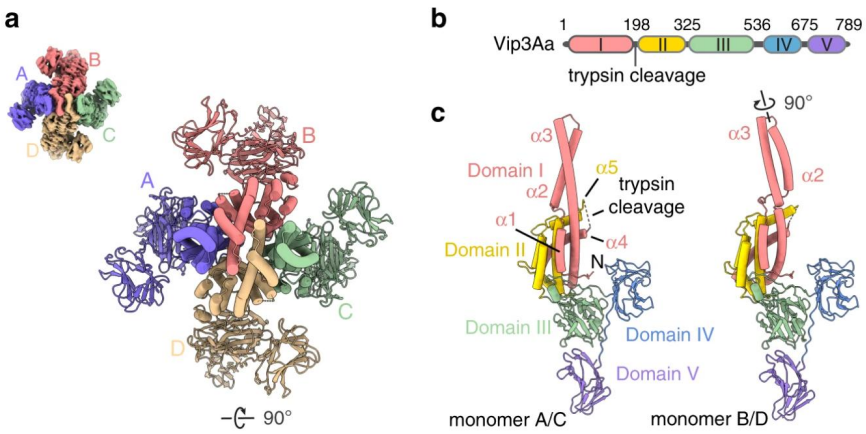

Figure 1-3. The structure of the Vip3A protoxin (Núñez-Ramírez et al., 2020)

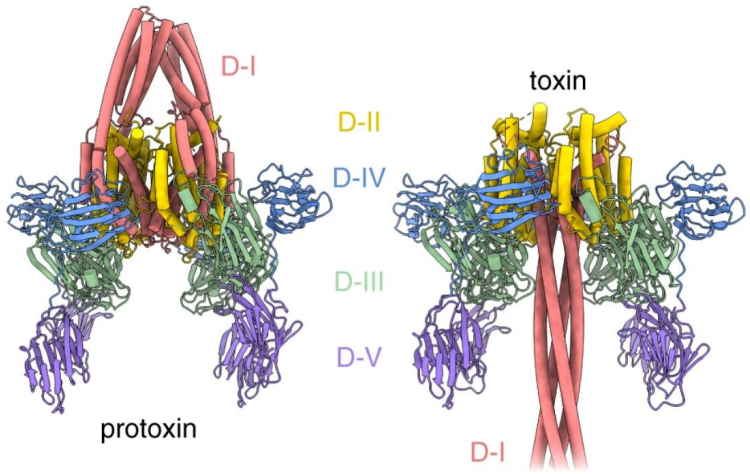

Figure 1-4. The structure of the activated Vip3A toxin (Núñez-Ramírez et al., 2020)

After being ingested by susceptible insects, Vip3Aa protein is activated by insect midgut proteases, forming several different fragments (62-66 kDa, 45 kDa, 33 kDa, and 19-22 kDa). The major cleavage product from the C-terminal region is the 62-66 kDa core peptide, which is typically considered to be the main part of the activated protein (Gayen, et al., 2012; Banyuls, et al., 2018). The differences in insecticidal activity of Vip3Aa protein across various insect species are attributed to the varying hydrolysis rates of the protein in different insects. Once activated, the N-terminal region (19-22 kDa) and the C-terminal region (62-66 kDa) of Vip3Aa combine to form a tetramer of approximately 360 kDa, which then binds to receptors on the brush border membrane vesicles (BBMVs) of the midgut cells of susceptible insects (Shao, et al., 2020). Identified receptors include fibroblast growth factor receptor-like protein (FGFR) (Jiang, et al., 2018a) and scavenger receptor class C-like protein (SR-C) (Jiang, et al., 2018b). Subsequently, conformational changes in the protein allow it to insert into the phospholipid bilayer, leading to the formation of pores on the cell surface and causing ion leakage, which ultimately results in insect death. Alternatively, some apoptosis-related signaling pathways may be activated, leading to cell apoptosis (Syed, et al., 2020).

3. Insect midgut

The digestive system of insects is composed of three distinct sections, each with specialized functions: the foregut, midgut, and hindgut (Caccia et al., 2019). The foregut includes the

pharynx, esophagus, and the specialized crop, and its main physiological functions are food transport, temporary storage, and preliminary digestion. As the central part of the digestive system, the midgut plays a critical role in the breakdown and absorption of nutrients. The hindgut primarily handles the excretion of undigested residues and metabolic waste, while also being involved in the reabsorption of some nutrients (Lemaitre & Miguel-Aliaga, 2013). In terms of embryonic development, the foregut and hindgut both arise from the ectoderm, and therefore undergo regeneration during insect molting; in contrast, the midgut originates from the endoderm and remains a functionally complex segment of the digestive tract throughout the insect's life (Terra and Ferreira, 2012). This structural division and functional specialization enable insects to efficiently complete the entire physiological process, from ingestion to excretion.

The midgut system of Lepidoptera insects is one of the most vital and specialized regions of the insect body, holding significant importance due to its complex tissue structure and its central role in physiological processes. In fact, the midgut occupies a volume second only to the integument, the outer protective layer of the insect body (Lehane, 1997). As the core component of the digestive system, the midgut is involved in a variety of essential functions that are crucial for the insect's survival and development:

Food Breakdown and Metabolism: The midgut serves as the primary site for the breakdown and digestion of food. It is equipped with a wide array of hydrolytic enzymes, such as proteases, lipases, and amylases, which are secreted by the epithelial cells lining the midgut. These enzymes are responsible for breaking down complex food molecules into simpler nutrients that can be absorbed by the insect. The digestion of proteins, fats, carbohydrates, and other essential compounds occurs in the midgut, ensuring that the insect can obtain the necessary nutrients for growth, energy production, and reproduction.

Nutrient Absorption and Ion Homeostasis: The midgut epithelium is also heavily involved in nutrient absorption, where specialized transport mechanisms help move digested nutrients across the epithelial cells into the insect's bloodstream. This process is crucial for maintaining the insect's nutritional balance and overall health. The midgut is also responsible for regulating ion homeostasis, which is essential for maintaining osmotic balance within the insect's body. The efficient uptake of nutrients and the regulation of ions such as sodium, potassium, and calcium are necessary for proper cellular function and metabolic processes (Qin et al., 2014).

Pathogen Defense: In addition to its digestive and metabolic roles, the midgut epithelium acts as a critical defense barrier against pathogens. As the first line of contact between the internal environment of the insect and the external world, the midgut forms an interface where the exchange of substances, including food and microorganisms, takes place. The epithelial cells of the midgut are equipped with protective mechanisms that help prevent the entry of harmful pathogens, such as viruses, bacteria, and fungi, from reaching deeper tissues. However, this epithelial layer can also become a vulnerable point when pathogens manage to breach the physical barrier, leading to infections (Chen et al., 2015).

When pathogenic microorganisms breach the midgut's epithelial integrity, a cascade of pathological changes occurs. The disruption of the epithelial barrier allows pathogens to spread into the insect's hemocoel, the body cavity, where they can proliferate rapidly. This often leads to systemic infections that affect vital organs and can result in the insect's death.

This process is particularly evident in the infection dynamics of viral pathogens, which commonly first colonize the midgut epithelial cells. Once inside the cells, the virus can spread to other parts of the insect's body through intercellular transmission, infecting the visceral organs and circulating through the hemolymph, the insect's circulatory system (Whitfield et al., 2015). These viral infections can cause severe damage, leading to widespread tissue degeneration and ultimately, the death of the host insect.

The midgut system's critical role in both digestion and defense mechanisms has made it a central focus of research, particularly in insect physiology and pest control. Due to the constant exposure to various microorganisms, toxins, and other potentially harmful substances during feeding, the midgut has evolved complex defense mechanisms to safeguard the insect. These mechanisms include the secretion of antimicrobial peptides, the formation of physical barriers, and immune responses that work to neutralize or eliminate pathogens. The midgut's ability to regulate the balance between nutrient absorption and pathogen defense is a key factor in the insect's overall survival.

As a result of these vital functions and its susceptibility to infection, the midgut has become a major target organ in research aimed at controlling insect pests. Understanding how the midgut operates and how it can be manipulated or protected from pathogens is crucial for developing more effective strategies in pest management. This makes the midgut not only an essential part of insect biology but also a key point of interest in biopesticide development, where interventions can be designed to disrupt midgut function and control pest populations.

3.1 Columnar cells

The midgut epithelial tissue of Lepidoptera is composed of four distinct, functionally specialized cell types: columnar cells, goblet cells, stem cells, and endocrine cells (Lehane, 1997). Each of these cell types plays an essential role in maintaining the digestive functions, immune defense mechanisms, and overall homeostasis of the insect. Among these cell types, columnar cells are the most abundant and versatile, serving dual functions in both digestive absorption and immune defense.

In terms of cellular structure, columnar cells exhibit typical characteristics of epithelial cells and can be divided into three primary regions: the basal, middle, and apical regions. The basal region of columnar cells is adjacent to the basal membrane and is characterized by its irregular columnar or conical shape. This region is divided into numerous small compartments and is rich in mitochondria and rough endoplasmic reticulum, which are crucial for energy metabolism and protein synthesis. These cellular components support the energy demands of digestion and help synthesize the various enzymes required for the breakdown of nutrients.

The middle section contains an oval-shaped nucleus with evenly distributed chromatin, indicating that gene transcription is actively occurring. This area also houses a well-developed Golgi apparatus and numerous transport vesicles, which are involved in the modification, packaging, and transport of proteins and enzymes within the cell. Additionally, the middle region contains abundant lysosomes and multivesicular bodies, which play key roles in intracellular digestion and the recycling of cellular materials. These structures help maintain the integrity and functionality of the cell by processing and recycling nutrients and waste products.

The apical region of columnar cells is covered with dense microvilli, which form a "brush border" that significantly increases the surface area for nutrient absorption. This increase in surface area facilitates the efficient uptake of nutrients from the digested food within the midgut lumen. Additionally, the apical region is responsible for the secretion of digestive enzymes via exocytosis. These enzymes are essential for breaking down complex food molecules into simpler forms that can be absorbed by the insect's body.

The primary function of columnar cells is the secretion of various digestive enzymes, including exopeptidases, maltase, endopeptidases, amylase, lipase, and lysozyme. These enzymes play a crucial role in the digestion of nutrients such as proteins, carbohydrates, and lipids, and their efficient production and activity are tightly regulated to ensure the proper breakdown of food and the insect's growth and development (Liu et al., 2017; Lee et al., 2018). Without these enzymes, the insect would be unable to extract the nutrients necessary for energy production, growth, and reproduction.

Beyond their digestive role, the microvilli and basal regions of columnar cells also perform endocrine functions. Columnar cells release differentiation factors, such as MDF-2 and MDF-3, into the midgut lumen. These factors play a crucial role in regulating the apoptosis (programmed cell death) of mature midgut cells and promoting the proliferation and differentiation of regenerative cells in the midgut (Loeb et al., 2004). This process ensures that the epithelial lining of the midgut is continually renewed and maintained, allowing the insect to adapt to environmental changes and physiological demands over time.

Additionally, columnar cells are involved in the formation of the peritrophic membrane, a chitinous structure that lines the midgut lumen and serves as a protective barrier, shielding the midgut from physical damage and preventing the invasion of pathogens (Hopkins and Harper, 2010). This membrane is vital for maintaining the integrity of the digestive system.

In addition to their digestive and regenerative roles, columnar cells also contribute to the insect's immune defense. In the midgut of the silkworm (*Bombyx mori*), a specific protease with a molecular weight of approximately 35 kDa, named Bm-SP142, has been identified with significant antiviral activity. This protease is highly expressed in the midgut region and has been shown to inhibit the replication of BmNPV (*Bombyx mori* nucleopolyhedrovirus) and reduce the spread of BmBDV (*Bombyx mori* bidens virus) in the host. These findings provide direct evidence that columnar cells secrete proteins with antiviral functions that help the insect defend against viral infections (Li et al., 2017).

Moreover, another important serine protease, BmTA (alkaline trypsin A), was found to be more highly expressed in resistant silkworm strains compared to susceptible ones. Comparative proteomic analysis revealed that the expression of BmTA was significantly higher in resistant individuals, and in vitro experiments showed that recombinant BmTA treatment led to a significant downregulation of the viral marker gene *Vp39*. These results suggest that BmTA may exert antiviral effects by interfering with the expression of viral genes, thereby limiting the ability of the virus to replicate and spread within the insect (Cao et al., 2021).

The columnar cells in the midgut of Lepidoptera play a critical role in digestion, nutrient absorption, immune defense, and tissue regeneration. Their ability to secrete digestive enzymes, support the renewal of the midgut epithelium, and provide antiviral protection makes them central to the insect's survival and health. As a result, these cells are not only

integral to the insect's digestion and metabolism but also serve as important targets in research aimed at developing new methods of pest control, including the development of biopesticides and immune-based strategies.

3.2 Goblet cells

Goblet cells in Lepidoptera are a distinct and specialized type of epithelial cell found in the midgut, which are evenly distributed between the more abundant columnar cells. These cells form a highly organized and functional morphology, contributing to the efficient digestive system of these insects. Goblet cells are pivotal for regulating the intestinal ion cycling, especially in the transport of potassium ions from the hemolymph into the midgut lumen. Their specialized function and morphology make them essential for maintaining the proper physiological conditions in the midgut, which are necessary for digestion and absorption processes.

Goblet cells exhibit a high degree of differentiation and vary significantly in their morphology and properties across different species of insects. In *Helicoverpa armigera*, a model species of Lepidoptera, goblet cells have a distinct structure. The nucleus of these cells is located at the base, and they contain an internal cavity that opens directly to the midgut lumen through a narrow neck. The apical end of the goblet cells has specialized cytoplasmic projections, which are divided into numerous smaller, villous-like protrusions. These microvilli are longer at the base than at the apex, increasing the surface area and facilitating nutrient absorption and ion transport. The villous-like structures significantly enhance the efficiency of ion exchange and contribute to the cell's overall ability to regulate the internal conditions of the midgut (Jean et al., 2007).

One of the most crucial functions of goblet cells is to maintain the alkaline environment of the midgut, which is essential for proper digestion in Lepidoptera. The Vacuolar-type H^+-ATPase (V-H^+ ATPase) system plays a central role in this process (Gomes et al., 2013; Levy et al., 2004; Azuma et al., 1995). This enzyme system uses ATP hydrolysis to generate energy, which is utilized to pump protons (H^+) against their concentration gradient from the cytoplasm of goblet cells into the goblet cell lumen. The activity of this system is crucial for maintaining the acidic environment within the cells while promoting the alkaline pH (ranging from 10 to 11) in the midgut lumen, which is required for efficient digestive enzyme activity. The mitochondria within the goblet cells, densely distributed in the microvilli, support the V-H^+ ATPase system by generating a transmembrane potential difference of approximately 150 mV (Dow et al., 1992). This mitochondrial activity ensures that the energy required for the proton pumping process is available.

The carbonic anhydrase enzyme also plays a critical role in this ion transport system. It catalyzes the production of bicarbonate ions (HCO_3^-), which further assist in the active transport of K^+ into the midgut lumen through specialized structures in the goblet cells, resembling valve-like mechanisms (Moffett et al., 1992). This synergistic action of the V-H^+ ATPase, mitochondria, and carbonic anhydrase underpins the ability of goblet cells to regulate the high alkaline pH of the midgut, providing an essential microenvironment for the efficient digestion and absorption of nutrients in Lepidoptera insects.

The alkaline conditions maintained by the goblet cells in the midgut are crucial for the digestion of food. These insects rely on the high pH environment to activate specific digestive

enzymes, which break down complex macromolecules into simpler absorbable components. In addition, the goblet cells' function in regulating ion cycling and maintaining pH stability plays an important role in the overall homeostasis of the insect's digestive system.

Given their vital role in nutrient absorption and digestion, goblet cells are also considered important targets in pest control strategies. Manipulating or interfering with the function of goblet cells, such as inhibiting the V-H^+ ATPase system or other key components of the ion transport process, could potentially disrupt the insect's ability to properly digest food and maintain pH homeostasis, thereby affecting its survival. These strategies can complement the development of biopesticides and genetically modified crops aimed at controlling pest populations.

3.3 Endocrine cells

Endocrine cells in the midgut of Lepidoptera insects, including species like the silkworm (*Bombyx mori*), play a crucial role in regulating the physiological processes that maintain gut homeostasis and contribute to the overall regulation of digestion, feeding, growth, and molting. These cells secrete a wide variety of bioactive peptides that interact with multiple physiological systems within the organism, influencing various biochemical pathways and enabling the insect to adapt to changes in its environment. These peptides regulate critical functions such as gut motility, feeding behavior, hormonal regulation, and immune responses (Abou et al., 2020; Khalid et al., 2021).

Among the many bioactive peptides secreted by endocrine cells, several are pivotal in regulating digestive functions and homeostasis within the midgut. Some of the most notable peptides include:

Allatostatins: These peptides regulate the secretion of juvenile hormone (JH), which controls various developmental processes, including molting and metamorphosis. They also influence the production of antimicrobial peptides (AMPs), which are important for immune defense (Felix et al., 2015). Diuretic Hormone 31: This peptide plays a significant role in controlling the contraction of visceral muscles in the gut, helping to regulate digestive motility and the excretion of waste (Holmes et al., 2023). Tachykinin: Involved in food sensing and digestion, tachykinin helps the insect detect and respond to food intake, regulating the overall digestive process (Reiher et al., 2011). Orcokinin: This peptide is crucial for regulating the process of ecdysis (molting), ensuring the insect sheds its exoskeleton and grows properly (Benguettat et al., 2018). Ryamide: Modulates feeding and digestion by influencing the gut's ability to process and break down food (Toyam et al., 2023). Neuropeptide F: Plays a central role in regulating feeding behavior and digestive processes, ensuring the insect's nutritional needs are met while also coordinating other physiological responses (Song et al., 2014). Myosupression: Involved in modulating gut contractions, Myosupression is important for regulating the movement of food through the digestive tract (Yamanaka et al., 2011). CCHamide: Regulates the contraction of gut muscles, facilitating the coordinated movement of food through the digestive system (Huang et al., 2011).

In the silkworm, the midgut endocrine cells are categorized into four distinct subtypes based on their spatial distribution and the specific peptides they produce. These subtypes are:

Type I Cells: These cells are found throughout all three regions of the midgut, suggesting their widespread involvement in various physiological processes across the entire digestive

tract. Type II, III, and IV Cells: These cells are localized to specific regions within the midgut, with Type II cells present in the anterior region, Type III cells in the middle, and Type IV cells in the posterior regions of the midgut. This regional specialization reflects the different functional roles that endocrine cells play in regulating digestion, absorption, and other processes across the anterior-posterior axis of the gut.

The spatial organization of these cells and the peptides they secrete ensure that the midgut can adapt to and process different types of food and nutrients at different stages of digestion. The diverse peptide profiles and their specific regional expression suggest that these cells have evolved to support the varied physiological demands of the insect's digestive system.

An interesting feature of midgut endocrine cells is their functional plasticity. In both the silkworm and the fruit fly (*Drosophila melanogaster*), individual endocrine cells are capable of expressing multiple peptides. For instance, in *Drosophila*, it has been observed that no more than three different peptides are expressed within a single cell, while in the silkworm, some endocrine cells can express as many as four different peptide genes simultaneously. This combinatorial expression of peptides likely underpins the functional diversity of endocrine cells, allowing them to participate in multiple aspects of gut regulation, from digestion and absorption to immune defense and growth regulation.

The plasticity in the expression of different peptides, as well as their combinations, suggests that endocrine cells are highly adaptable and capable of responding to the changing physiological needs of the insect. In the silkworm, around 30 different peptide combinations have been detected, classified into 17 types, each characterized by unique distributions, morphologies, and peptide profiles. This extensive variability in peptide expression highlights the complexity of the endocrine regulation of gut function and suggests that these cells can modulate a wide range of digestive, metabolic, and developmental processes in response to environmental and physiological cues (Roller et al., 2022).

In summary, the endocrine cells in the midgut of Lepidoptera species, including the silkworm, are integral to the regulation of gut homeostasis and play a vital role in digestive, immune, and developmental processes. Through the secretion of bioactive peptides, these cells control key functions such as food sensing, digestion, feeding behavior, gut motility, and immune responses. Their spatial distribution within the midgut and the combinatorial expression of different peptides provide a high degree of functional flexibility, enabling the insect to adapt its physiological processes to changing environmental conditions. As such, these cells and their bioactive peptides are important targets for understanding insect physiology and could provide new insights into pest control strategies.

3.4 Intestinal stem cells (ISCs)

In Lepidoptera species, the midgut stem cells (also referred to as regenerative cells) are located at the base of the gut epithelium, where they play a fundamental role in the continuous formation and regeneration of the midgut epithelium. These stem cells are sparsely distributed in the basal region of the midgut epithelium, often in close proximity to the basement membrane (Baldwin and Hakim, 1991; Zavascki et al., 2006). They are characterized by their undifferentiated state, exhibiting typical features of stem cells, including a low number of organelles and relatively low cytoplasmic electron density (Billingsley et al., 1996). Despite their undifferentiated status, recent studies have provided new insights into the energy storage

mechanisms in these cells. Notably, stem cells in the midgut are found to harbor significant energy reserves in the form of lipid droplets and glycogen particles, which may be crucial for supporting the rapid cellular activities associated with regeneration (Tettamanti et al., 2007; Franzetti et al., 2015).

Midgut stem cells in Lepidoptera exhibit two distinct patterns of cell division: asymmetric and symmetric division. In asymmetric division, one daughter cell maintains the stem cell properties and remains undifferentiated, while the other daughter cell differentiates into a functional, mature cell, such as a columnar or goblet cell. This type of division is essential for the maintenance of the stem cell pool over time, ensuring a continuous source of regenerative cells. In contrast, symmetric division results in the production of two identical stem cells, thereby expanding the stem cell population. This process occurs primarily under conditions where an increased number of stem cells is needed, such as during periods of rapid tissue growth or damage. The balance between asymmetric and symmetric division is tightly regulated by physiological demands, ensuring the appropriate response to different environmental or developmental cues.

In Lepidoptera, midgut stem cells respond to specific growth factors that guide them either to proliferate or differentiate into mature cell types. One example of these regulatory factors are MDF peptides (Midgut Differentiation Factors). Four distinct types of MDF peptides have been isolated and characterized, and these peptides play a key role in stimulating the differentiation of stem cells into mature columnar and goblet cells. MDF peptides have been shown to induce this process in various lepidopteran species, such as the (*Helicoverpa virescens*) and the *Manduca sexta* (Loeb and Jaffe, 2002). These peptides are essential for ensuring that the midgut epithelium maintains its functional integrity by promoting the regular turnover of epithelial cells.

Under normal physiological conditions, midgut stem cells are actively involved in the periodic renewal of the gut epithelium. This renewal process is especially pronounced during molting, the physiological process by which the insect sheds its exoskeleton to grow. During molting, midgut stem cells undergo a proliferation peak, during which the majority of stem cells differentiate into mature epithelial cells. This ensures the complete regeneration of the midgut lining, which is critical for maintaining proper digestive function. After molting, a small pool of progenitor stem cells remains to sustain the regenerative capacity of the midgut epithelium and prepare it for future rounds of epithelial turnover.

The ability of midgut stem cells to respond to pathogen invasion or toxin damage is another essential feature of their regenerative function. When the midgut is compromised due to exposure to pathogens or environmental toxins, the stem cells in the basal region of the gut quickly proliferate and differentiate to restore the damaged tissue. This regenerative response is vital for the insect's survival, as it ensures that the midgut retains its ability to perform essential digestive and immune functions.

The repair of midgut tissue following injury or infection involves complex signaling networks that coordinate the proliferative and differentiating activities of stem cells. Several critical signaling pathways play a role in regulating this process, including: JAK-STAT, EGFR, Wnt/Wg, BMP, Hippo, JNK and p38 MAPK pathways. Together, these signaling pathways help ensure the coordinated response of midgut stem cells, allowing the tissue to repair itself

rapidly and restore its function after injury or infection (Gervais et al., 2017; Boumard et al., 2021; Tian et al., 2016; Tracy et al., 2019; Ren et al., 2010; Biteau et al., 2008).

In summary, midgut stem cells (or regenerative cells) in Lepidoptera are crucial for maintaining the integrity and functionality of the midgut epithelium. These stem cells undergo both asymmetric and symmetric division to ensure the continuous generation of new cells required for tissue renewal and repair. The response of these cells to specific growth factors, such as MDF peptides, facilitates the differentiation of stem cells into specialized cell types, including columnar and goblet cells, which are essential for digestion and nutrient absorption. Additionally, the regenerative capacity of these stem cells is particularly evident during molting and in response to pathogen invasion or toxin damage, highlighting their central role in maintaining midgut health and function. The complex signaling networks that regulate the behavior of midgut stem cells underscore the intricate control mechanisms required to balance stem cell proliferation, differentiation, and tissue homeostasis in the insect gut.

4. Response of insect midgut to pore-forming toxin infection

For insects, the midgut is the primary site for nutrient digestion and absorption. When pore-forming toxins cause damage to the midgut, an imbalance of ions, metabolites, and proteins triggers various defense responses, such as autophagy, apoptosis, and cell shedding, to eliminate damaged cells and maintain midgut homeostasis by inducing midgut cell regeneration (Dal Peraro et al., 2016).

4.1 Apoptosis

In 1842, Vogt first observed dying nerve cells during the development of toads. In 1965, Lockshin and Williams introduced the term "programmed cell death" (PCD) to describe the cell death activated by genetic programs during the metamorphosis of tadpoles and insects. In 1972, Kerr et al. first used the term "apoptosis," which refers to an active, programmed, and intrinsic biological process of cell death (Degterev et al., 2003).

During the process of apoptosis, morphological features undergo staged changes. In the early stages of apoptosis, the cell volume shrinks, and cell-cell junctions gradually disappear, though the cell membrane remains intact. Subsequently, phosphatidylserine translocates to the outer leaflet of the membrane, facilitating recognition by phagocytic cells. This is followed by the loss of mitochondrial membrane potential, changes in permeability, and the release of cytochrome c from the mitochondria into the cytoplasm. Chromatin condensation appears in the nucleus, which becomes distributed along the nuclear membrane, leading to the rupture of the nucleolus and nuclear membrane, and DNA fragmentation. Finally, the cell gradually divides into apoptotic bodies, which are engulfed by other cells. During this process, the nuclear DNA is cleaved by nucleases into 180-200 bp fragments, indicating that the nuclease cleavage sites are located between nucleosomes. Consequently, apoptotic DNA shows a characteristic "ladder" pattern when subjected to nucleic acid electrophoresis (DNA Ladders) (Kerr et al., 1994; McHugh et al., 2006; Sedlakova et al., 1999).

The signaling pathways that trigger apoptosis can be classified into the extrinsic death receptor pathway, the intrinsic mitochondrial pathway, and the endoplasmic reticulum pathway. In these pathways, apoptosis is generally mediated by the caspases family of proteases. Caspases are characterized by cysteine proteases with specific cleavage sites at

aspartic acid residues, which is why they are named caspases. The death receptor pathway and the mitochondrial pathway process and relay external death signals or apoptotic stimuli, ultimately determining whether apoptosis is initiated. These pathways primarily begin with the activation of caspases, followed by the cleavage of proteins and the degradation of the cell, which leads to the execution of apoptosis.

The study of caspases originated from the nematode *Caenorhabditis elegans*, where 131 cells undergo programmed cell death during development. The genes *ced3* and *ced4* are essential for regulating apoptosis in these cells (Yuan et al., 1993). ICE (Interleukin-1β converting enzyme) is one of the earliest identified members of the caspase family. Caspases are cysteine proteases with specific aspartic acid cleavage sites and possess the following characteristics: (1) Homology with ICE; (2) Cysteine acts as the nucleophilic group for substrate cleavage; (3) Specific catalytic substrate at the aspartic acid residue, which results in cleavage at the aspartic acid-containing peptide bond; (4) Highly conserved QACXG pentapeptide sequence; (5) Present in an inactive zymogen form, which must be activated by hydrolysis of a segment of the amino terminus; typically, it binds to its inhibitor to prevent accidental activation of the zymogen, which could otherwise damage the cell; (6) Activated Caspases can hydrolyze substrates and amplify the apoptotic signal through a cascade effect.

The study of apoptosis in *Drosophila melanogaster* is the most extensive (Lockshin et al., 1965). The fruit fly has seven caspases: three initiator caspases (DRONC, DREDD, and STRICA) and four effector caspases (DRICE, DCP-1, DECAY, and DCP2/DAMM) (Hay et al., 2006). The RHG family in *Drosophila*, including Reaper, Hid, Grim, Sickle, and Jafrac2, is located upstream of the apoptosis regulation. These proteins contain a short N-terminal peptide motif (IBM: IAP-Binding-Motif), which can bind to the apoptosis inhibitor protein (*Drosophila* Inhibitor of Apoptosis Protein, DIAP) and initiate cell death (Ryoo et al., 2002; Wilson et al., 2002). The ectopic expression of Reaper, Hid, and Grim genes leads to apoptosis. These genes are activated at the transcriptional level in response to stress hormones, various developmental signals, cellular damage, and other apoptotic stimuli, thus upregulating their expression. As pro-apoptotic proteins, Reaper, Hid, and Grim, once activated, can rapidly relieve the inhibitory effect of IAPs on caspase family members, indirectly triggering the caspase-dependent apoptotic pathway in *Drosophila* (Christich et al., 2002; Nordstrom et al., 1996).

In addition to their apoptotic function, caspase family members also participate in non-apoptotic functions. The cleavage of specific substrate proteins by caspases can mediate or regulate different types of cell death processes: Activation of the Caspase-1 subfamily, including Caspase-1 and Caspase-11 in mice, and their human counterparts, Caspase-1, Caspase-4, and Caspase-5, can cleave Gasdermin D (GSDMD), removing its C-terminal domain. The N-terminal fragment of GSDMD oligomerizes and forms pores in the membrane, leading to cell lysis and triggering pyroptosis (Shi et al., 2015). Additionally, Caspase-8 can cleave receptor-interacting protein kinase 1 (RIPK1), promoting its dimerization and kinase activation. When Caspase-8 is inhibited, RIPK1 activation promotes the formation of necrosome complexes, which recruit and activate the downstream effector protein MLKL. Upon translocation of MLKL to the plasma membrane, cell lysis occurs, mediating necroptosis (Chen et al., 2022).

In the process of insect defense against pathogenic microorganisms, apoptosis plays a key role in defending the organism by clearing damaged cells and promoting the renewal of midgut epithelial cells. Apoptosis has been described as a cellular response mechanism triggered after exposing cultured cells to different pore-forming toxins (PFTs). For instance, in *in vitro* experiments with primary cultures of midgut cells from *Heliothis virescens*, apoptosis of epithelial cells induced by Cry toxins was demonstrated using TUNEL (TdT-mediated dUTP Nick-End Labeling) staining and Annexin methods (Loeb et al., 2017). Additionally, Cry1Ab and Cry1Ac proteins were shown to induce apoptosis in CF1 cells (Portugal et al., 2000). Similar results were observed when Sf9 cells were exposed to Vip3Aa protein. Flow cytometry analysis, TUNEL staining, and DNA fragmentation assays confirmed that Vip3Aa induces apoptosis in Sf9 cells, leading to cell arrest in the G2/M phase. Moreover, Vip3Aa was found to disrupt mitochondrial membrane potential ($\Delta\Psi m$) and activate Sf-caspase-1, indicating that the mitochondrial-mediated caspase-dependent pathway may be involved in Vip3Aa-induced apoptosis of Sf9 cells (Jiang et al., 2016).

In vivo experiments have demonstrated that when exposed to pore-forming toxins (PFTs), including Bt toxins, apoptosis pathways are activated in susceptible larvae. For example, after exposure to transgenic Bt Cry3Bb1 and Gpp34/Tpp35Ab1 maize roots for 10 days, the caspases, pro-apoptotic factors, and anti-apoptotic factors of *Diabrotica virgifera* larvae were activated (Coates et al., 2021). Comprehensive transcriptomic and proteomic analyses revealed that genes and proteins upregulated in *Spodoptera frugiperda* larvae following Vip3Aa exposure are primarily involved in the caspase-mediated apoptosis pathway (Jin et al., 2022). After treatment with low doses of Cry1A protein, typical apoptotic characteristics were observed in midgut epithelial cells of *Bombyx mori* larvae. TUNEL staining revealed positively stained cells, and apoptotic bodies were clearly visible under the microscope. These apoptotic cells gradually detached from the gut wall and were replaced by newly differentiated columnar cells, resulting in tissue repair (Tanaka et al., 2012). Similarly, after infection with the BtAA1-9 strain in *Spodoptera exigua* larvae, apoptosis was induced in the midgut columnar cells. As the infection progressed, the integrity of the cell membrane gradually deteriorated, and intestinal stem cells proliferated and differentiated to repair the damaged tissue (Loeb et al., 2012). Moreover, members of the Vip protein family, such as Vip3A and Vip3C, also induced midgut cell apoptosis in *Spodoptera exigua* at sub-lethal concentrations. TUNEL-positive cells were observed detaching from the basement membrane and being expelled into the gut lumen (Hernandez-Martinez et al., 2017). These findings suggest that the apoptosis process plays a critical role in the defensive response of insects to various Bt toxins.

4.2 Autophagy

Autophagy is a self-degradation process through which damaged cellular organelles, protein aggregates, and other cellular components are cleared and recycled for nutrient recovery via lysosomal degradation. In this process, cells respond to certain environmental conditions, such as nutrient deprivation. Once autophagy is induced, phagophores (the initial stage of autophagic vesicles) are formed, which then elongate and curve to form autophagosomes. These autophagosomes engulf cellular cargo and fuse with endosomes, ultimately maturing by fusing with lysosomes (He et al., 2016). Autophagy is a highly conserved cellular

degradation and recycling process across all eukaryotes. There are three major types of autophagy, based on the pathway through which substrates enter the lysosome or vacuole: microautophagy, macroautophagy, and chaperone-mediated autophagy (CMA). While these types differ morphologically, they all ultimately transport materials to the lysosome for degradation and recycling.

The process of autophagy includes several key steps. First, autophagy is induced, with the most typical trigger being nutrient deprivation. The first step in the formation of the autophagosome is the isolation of cytoplasmic components (including organelles) by a unique membrane known as the phagophore or isolation membrane, which is a very flat organelle. The autophagosome is a characteristic double-membrane organelle that forms through the coalescence of elongated phagophores. Next, the autophagosome fuses with the lysosome. The inner membrane of the autophagosome and the cytoplasmic contents within it are degraded by lysosomal hydrolases. Once the macromolecules are degraded within the lysosome, the monomeric units (such as amino acids) are released into the cytoplasm for reuse (Mizushima et al., 2007).

In vitro experiments have shown that the autophagic process in insect midgut cells is widely activated in response to pore-forming toxins. The conversion of Atg8 to lipidated Atg8 (Atg8-PE) is commonly used as a marker to evaluate autophagic activity, as the increase in Atg8-PE correlates with autophagic activation (Klionsky et al., 2016). By analyzing the changes in the ratio of Atg8-PE to Atg8, it was found that Cry1Ca toxin can induce autophagy in susceptible cell lines (Hi5, Sl-HP, Sf9). This process is dependent on the AMPK (AMP-activated protein kinase) and JNK (c-Jun N-terminal kinase) pathways (Yang et al., 2021). The increase in GFP-Atg8 puncta, appearance of autophagic vacuoles, and elevated Atg8-II protein levels confirmed that Vip3Aa can induce autophagy in Sf9 cells, and the process is regulated by the AMPK-mTOR-ULK1 pathway. Knockdown of the *ATG5* gene or the use of the autophagy inhibitor 3-MA further increased the sensitivity of Sf9 cells to Vip3Aa. Overexpression of *ATG5* reduced the cell death rate of Vip3Aa-treated cells. These results suggest that autophagy induced by Vip3Aa has a pro-survival role, which may be related to the development of insect resistance (Hou et al., 2021).

Additionally, *in vivo* experiments have demonstrated that Cry5B protein significantly affects the autophagy regulatory system in *Caenorhabditis elegans*. When nematodes were exposed to Cry5B, their autophagy-related gene expression profile was significantly altered, with a marked increase in the expression levels of key autophagy genes, such as *lgg-1* (Atg8 homolog) and *atg-18*. Researchers also observed the accumulation of the LGG-1 protein and its lipidated form LGG-1-PE (a molecular marker of autophagic activation), confirming the activation of the autophagic pathway (Chen et al., 2017). Notably, when the expression of these *atg* genes was inhibited, the nematodes' ability to repair Cry5B-induced membrane damage was significantly reduced, leading to increased sensitivity to the toxin. Moreover, the conserved transcription factor HLH-30 plays a core regulatory role in the nematode's defense mechanism against bacterial toxins. Specifically, the autophagic process induced by Cry5B depends on the transcriptional regulatory function of HLH-30. Experimental evidence showed that, compared to wild-type nematodes, hlh-30 mutants had significantly lower tolerance to Cry5B, suggesting that HLH-30-mediated autophagic activation is an important protective mechanism in nematode resistance to Cry5B toxicity (Visvikis et al., 2014).

4.3 Cell shedding

In addition to apoptosis and autophagy-mediated clearance of damaged cells, cell shedding also plays a similar role in removing damaged cells. During insect development, columnar cells that are damaged by pathogens may extrude in order to eliminate the damaged cells.

For instance, in the case of *Spodoptera litura* larvae, which were infected with sublethal doses of *Bacillus thuringiensis* (Bt) crystal endotoxins, both goblet cells and columnar cells exhibited significant swelling as a result of the toxin's effects. The columnar cells, after being subjected to pressure, eventually ruptured and were expelled into the gut lumen. This shedding process allowed for the regeneration of new cells from stem cells at the base of the epithelium, filling the gaps left by the damaged cells and leading to midgut tissue repair. This process underscores the midgut's ability to recover from the damaging effects of toxins through rapid cell turnover and regeneration (Spies et al., 1985). Similarly, when *Corcyra cephalonica* larvae were exposed to the Bt HD-1 strain, histological analyses revealed that the arrangement of midgut epithelial cells became looser, and some of the columnar cells appeared swollen. As in the case of *S. litura*, the swollen columnar cells were gradually pushed out and extruded into the gut lumen as new cells developed at the base of the epithelial layer. These new cells eventually matured and replaced the damaged cells, contributing to the recovery of midgut tissue and restoring normal digestive function (Chiang et al., 1986).

In addition to these toxin-induced responses, other pathogens, such as *Erwinia carotovora carotovora 15* (*Ecc15*), have been shown to also trigger cell turnover in insect midguts. For example, in *Drosophila melanogaster*, infection with *Ecc15*, a Gram-negative bacterium, resulted in an increased turnover rate of gut epithelial cells. Epithelial cell shedding was observed as early as 30 minutes after ingestion of the pathogen, with the total number of gut cells reaching a minimum after approximately 8 hours, where about half of the cells were lost. This shedding process was orchestrated through the Imd pathway and JNK signaling, which worked together to induce epithelial cell extrusion during bacterial infections. Additionally, the reduction of the transcription factor GATAe was required for this process, highlighting the complex regulatory networks involved in epithelial turnover during immune responses. Interestingly, these processes of cell shedding and regeneration occurred independently of ROS-related apoptosis, suggesting an alternative pathway to tissue repair and immune defense (Buchon et al., 2010; Zhai et al., 2018).

Beyond the shedding of entire damaged cells, insect midgut cells can also expel parts of damaged cells, such as damaged organelles, to mitigate the effects of pathogen attack. For instance, when exposed to hemolysin, a pore-forming toxin secreted by *Serratia marcescens*, gut epithelial cells undergo a process of thinning and recovery. Rather than completely rupturing, these cells expel apical cytoplasm, which includes damaged organelles like mitochondria, effectively removing the damaged material while avoiding full cell rupture. This type of partial extrusion helps preserve the integrity of the cell and prevents more extensive damage to the gut lining, allowing for rapid recovery and maintenance of midgut function (Lee et al., 2016).

Together, the process - cell shedding - play integral roles in maintaining midgut homeostasis and defending the insect against the harmful effects of pathogens and toxins. The ability to

rapidly expel damaged cells and replace them with new ones is essential for the insect's survival, as it ensures that the digestive system remains functional even after encountering a range of environmental challenges.

4.4 Midgut regeneration

After the midgut clears damaged cells through apoptosis, autophagy, and cell shedding, intestinal stem cells (ISCs) exhibit a rapid response, with basal stem cells quickly proliferating and differentiating to restore midgut tissue to a healthy state. This repair process is regulated by a complex signaling network, including classical pathways such as JAK-STAT and EGFR, as well as, Hippo, JNK, and p38, which play crucial roles in coordinating ISC proliferation.

4.4.1 JAK/STAT

The JAK-STAT signaling pathway is a highly conserved and evolutionarily ancient pathway found across a wide range of animal taxa, playing a central role in translating extracellular signals into precise intracellular responses. Its name originates from its two principal components: Janus kinase (JAK) and Signal Transducer and Activator of Transcription (STAT). These two proteins work together in a tightly regulated signaling cascade that is crucial for mediating responses to cytokines, growth factors, and hormones.

In *Drosophila melanogaster*, the JAK-STAT signaling pathway is a simplified yet functionally robust system that mirrors the core components of its mammalian counterpart while adapting to the unique physiological needs of insects. The pathway is composed of three cytokine ligands - Unpaired (Upd), Upd2, and Upd3 - which are homologous to mammalian interleukins. These secreted signaling molecules initiate the pathway in response to developmental cues, stress, or immune challenges. The sole receptor for these ligands is Domeless (Dome), a transmembrane protein that functions as the cytokine receptor. Dome is structurally characterized by extracellular domains that bind ligands and intracellular regions that interact with downstream signaling components. Upon ligand binding, Dome undergoes conformational changes that activate the associated JAK kinase, Hopscotch (Hop). Hop is the only JAK family member in *Drosophila*, making it essential for the pathway's activity.Activation of Hop triggers a trans-phosphorylation event - Hop molecules phosphorylate each other and also phosphorylate tyrosine residues on the cytoplasmic tail of the Dome receptor. These phosphorylated tyrosines then serve as recruitment sites for STAT92E, the only STAT transcription factor in *Drosophila*. STAT92E binds to these phosphotyrosine motifs via its SH2 (Src homology 2) domain, anchoring it to the receptor complex. Once docked, STAT92E itself is phosphorylated by Hop on a conserved tyrosine residue. This post-translational modification induces dimerization of STAT92E, a critical activation step. The resulting dimers undergo nuclear translocation, where they bind to specific DNA sequences in the promoters of target genes to modulate transcription (Arbouzova et al., 2006).

Buchon et al. (2009a) were the first to provide compelling evidence that the JAK/STAT signaling pathway plays a critical role in mediating the regenerative response of intestinal stem cells (ISCs) in *Drosophila melanogaster*. By genetically disrupting key components of the pathway, such as the transcription factor Stat92E or the cytokine receptor Domeless, they observed that ISCs failed to proliferate following infection with the Gram-negative bacterium

Erwinia carotovora carotovora 15 (*Ecc15*). This significant finding demonstrated that intact JAK/STAT signaling is indispensable for initiating ISC-driven epithelial renewal in response to bacterial-induced midgut damage (Buchon et al., 2009a).

Building on this discovery, Jiang et al. (2009) conducted further investigations into the regulatory framework of the JAK/STAT cascade. Their work extended the role of the pathway beyond bacterial infection, showing that it is equally essential under conditions of epithelial apoptosis, oxidative and stress responses triggered by the JNK pathway, and during infections caused by other pathogens such as *Pseudomonas entomophila* (Pe). These researchers also clarified the functional contributions of the cytokine ligands Upd1, Upd2, and Upd3, identifying them as primary mediators that initiate JAK/STAT signaling following epithelial damage (Jiang et al., 2009).

Subsequent studies, including those by Osman et al. (2012), have further refined this model by revealing that the source and intensity of Upd cytokine expression can vary depending on the nature and severity of the damage. For instance, Upd3 is strongly upregulated in enterocytes during infection or oxidative stress, serving as the primary damage signal, while Upd1 and Upd2 contribute more to baseline signaling and developmental regulation (Osman et al., 2012).

Overall, this body of research has firmly established the JAK/STAT pathway as a central component of the insect midgut's regenerative machinery, illustrating how immune signaling pathways are integrated with stem cell biology to ensure both defense and tissue renewal in a coordinated manner.

4.4.2 Epidermal growth factor receptor (EGFR)

The epidermal growth factor receptor (EGFR) is a pivotal member of the receptor tyrosine kinase (RTK) family, well-known for mediating a wide array of cellular processes, including proliferation, differentiation, survival, and tissue development. In *Drosophila melanogaster*, the EGFR pathway plays an especially crucial role in maintaining intestinal stem cell (ISC) dynamics and gut homeostasis, particularly in response to stress or epithelial injury.

Within the *Drosophila* midgut, three principal EGFR ligands- - Vein (Vn), Spitz (Spi), and Keren (Krn)- - are differentially expressed and function in both baseline ISC maintenance and damage-induced regeneration. The activation of these ligands is tightly regulated by a family of intramembrane serine proteases known as Rhomboids, which cleave the membrane-bound precursors of Spi and Krn, allowing their release and subsequent activation of the EGFR receptor (Suzuki et al., 2010).

In the context of epithelial stress or infection, such as exposure to the entomopathogenic bacterium *Pseudomonas entomophila*, there is a marked upregulation of both EGFR ligands and rhomboids. This triggers robust EGFR activation in ISCs, initiating downstream signaling cascades, most notably the Ras/MAPK (ERK) pathway, which leads to cell cycle entry, mitosis, and ultimately ISC proliferation. Disruption of EGFR signaling - either genetically or via pharmacological inhibition- - has been shown to abolish ISC division, thereby impairing midgut regeneration and compromising barrier integrity following injury or infection (Jiang et al., 2011).

Importantly, studies have revealed a synergistic interaction between the EGFR and JAK/STAT pathways in the regulation of ISC activity. While the JAK/STAT pathway (activated by Upd cytokines) initiates the regenerative response by inducing transcription of

proliferative genes, EGFR signaling provides the essential mitogenic drive, ensuring that ISCs not only receive the cue to divide but are also capable of executing cell division. This cross-talk highlights the multi-layered regulatory networks coordinating tissue repair and underscores how redundant and overlapping signals safeguard epithelial integrity (Buchon et al., 2010).

In addition to epithelial sources, surrounding visceral muscles (VMs) serve as a key niche component, producing constitutive levels of EGFR ligands - particularly Vein - which maintain basal levels of ERK activity in ISCs under homeostatic conditions (Biteau et al., 2011). This continuous signaling ensures that ISCs retain a "primed" state, ready to proliferate upon additional stimulation, such as oxidative stress or pathogen exposure.

Furthermore, Tian et al. (2022) demonstrated that during pathogenic infections, not only are ISCs activated, but enteroblasts (EBs) - normally post-mitotic progenitor cells - can also re-enter the mitotic cycle in response to heightened EGFR-Ras signaling, further contributing to tissue regeneration. This plasticity suggests that EGFR signaling has a broader impact across multiple cell types within the midgut epithelium, extending beyond ISCs to influence cell fate decisions and lineage flexibility (Tian et al., 2022).

Overall, EGFR signaling in the *Drosophila* midgut acts as a central hub that integrates signals from epithelial cells, visceral muscles, and immune stimuli to coordinate ISC behavior. Its essential role in promoting proliferation, maintaining a regenerative pool of stem cells, and interacting with other pathways like JAK/STAT makes it a cornerstone of gut homeostasis and repair mechanisms in insects.

4.4.3 JNK（Jun N-terminal kinase）

The Jun N-terminal kinase (JNK) pathway, originally identified for its ability to phosphorylate the transcription factor c-Jun at Ser-63 and Ser-73, thereby modulating its transcriptional activation potential (Hibi et al., 1993), represents a crucial signaling axis within the broader mitogen-activated protein kinase (MAPK) network. As a highly conserved cascade across metazoans, the JNK pathway governs a diverse array of cellular processes, including growth, differentiation, apoptosis, stress response, and importantly, tissue regeneration. In the context of insect intestinal physiology, JNK signaling emerges as a key player in orchestrating damage-induced compensatory stem cell proliferation, thereby contributing to epithelial homeostasis and regeneration.

In *Drosophila melanogaster*, the core JNK signaling module comprises a sequential kinase cascade. The upstream JNK kinase Hemipterous (Hep) phosphorylates and activates Basket (Bsk), the *Drosophila* homolog of JNK (Herrera et al., 2021). Upon intestinal injury, including oxidative stress, pathogen invasion, or chemical damage, this pathway is rapidly activated in enterocytes and progenitor cells. One of the primary outcomes of JNK activation is the induction of Ets21c, a transcription factor that triggers apoptosis in damaged or senescent cells, a necessary process to remove compromised epithelial components and prepare the tissue for repair (Mundorf et al., 2019).

Concurrently, JNK signaling in the midgut stimulates intestinal stem cell (ISC) proliferation through both cell-autonomous and non-cell-autonomous mechanisms. Notably, JNK promotes the production and secretion of growth factors, such as epidermal growth factor (EGF) ligands, and cytokines, including the Unpaired (Upd) family proteins. These secreted signals act on neighboring ISCs, activating the EGFR and JAK/STAT pathways, respectively, to

drive cell cycle entry and proliferation (Biteau et al., 2011; Jiang et al., 2009). This coordination underscores the central role of JNK as an upstream regenerative signal integrator, capable of modulating multiple downstream repair pathways.

Moreover, JNK signaling is intertwined with the Hedgehog (Hh) pathway to regulate ISC activity. Specifically, it modulates the expression of Upd2 through Hh signaling components, reinforcing the amplification of JAK/STAT signaling and further boosting ISC proliferation under stress or injury conditions (Tian et al., 2015). This inter-pathway communication exemplifies how JNK functions not in isolation but as part of a complex regenerative signaling network.

In addition to external signaling cues, JNK also affects the intrinsic transcriptional landscape of ISCs. It upregulates key transcription factors such as Sox21a, which work synergistically with the Ras/ERK (MAPK) self-renewal pathway to ensure robust ISC proliferation and lineage commitment during epithelial renewal (Meng et al., 2015). This highlights a dual regulatory role for JNK- - promoting both clearance of damaged cells via apoptosis and activation of regenerative responses through ISC proliferation and differentiation.

Collectively, these findings position the JNK pathway as a central mediator of intestinal regeneration in insects, linking damage recognition, pro-apoptotic signaling, growth factor induction, and stem cell activation into a coherent regenerative response. The intricate interplay between JNK and other pathways such as EGFR, JAK/STAT, Hh, and Ras/ERK ensures that tissue repair is finely tuned, both spatially and temporally, to maintain midgut integrity and functionality.

4.4.4 Hippo

The Hippo signaling pathway is a highly conserved regulatory cascade that spans across evolutionary lineages from *Drosophila melanogaster* to mammals, underscoring its fundamental role in controlling organ size, regulating stem cell proliferation, apoptosis, and maintaining tissue homeostasis (Ikmi et al., 2014; Sebé-Pedrós et al., 2012). At its core, the Hippo pathway functions as a molecular brake on unchecked cell division, thereby preventing abnormal tissue overgrowth and tumorigenesis.

In *Drosophila*, the canonical Hippo pathway consists of a hierarchical kinase cascade. The upstream Hippo kinase (Hpo), in complex with scaffolding proteins such as Salvador (Sav), phosphorylates and activates the downstream kinase Warts (Wts). Activated Wts, in turn, phosphorylates the transcriptional coactivator Yorkie (Yki) at multiple serine residues. This phosphorylation event inhibits Yki by promoting its cytoplasmic retention, thereby preventing it from entering the nucleus and activating growth-promoting genes (Misra and Irvine, 2018; Oh and Irvine, 2009).

However, when the Hippo pathway is inactivated, such as under stress conditions or during tissue injury, Yki becomes dephosphorylated, allowing it to translocate into the nucleus. In the nucleus, Yki partners with the DNA-binding transcription factor Scalloped (Sd) to activate a suite of target genes involved in cell survival, growth, and proliferation (Wu et al., 2008; Zhang et al., 2008; Zhao et al., 2008).

Within the intestinal epithelium of *Drosophila*, the Hippo pathway plays a context-dependent regulatory role, particularly during tissue damage and regeneration. Upon intestinal injury, differentiated enterocytes (ECs) downregulate Hippo pathway activity, enabling Yki activation and nuclear localization. This activation leads to a transcriptional upregulation of

cytokines such as Unpaired 1 (Upd1), Upd2, and Upd3, which serve as potent ligands for the JAK/STAT pathway (Ren et al., 2010; Shaw et al., 2010). These cytokines create a paracrine signaling loop, stimulating the surrounding intestinal stem cells (ISCs) to proliferate and replace damaged cells, thereby promoting epithelial renewal.

Moreover, the activation of Yki also intersects with the JNK signaling pathway, either directly or through feedback loops involving damage-induced stress signals. This interpathway crosstalk allows for a coordinated regenerative response, where apoptosis of damaged cells and proliferation of progenitor cells are tightly balanced. Interestingly, Hippo-Yki signaling does not act in isolation but is integrated into a broader regenerative signaling network that includes EGFR, JAK/STAT, JNK, and Wnt pathways. This integration ensures a precise spatiotemporal control of ISC behavior, enabling the gut to respond dynamically to varying levels of tissue stress and damage.

In summary, the Hippo pathway in *Drosophila* midgut acts as a damage-responsive switch that modulates stem cell activity via Yki-dependent transcriptional programs. By controlling the expression of regenerative cytokines and cooperating with other mitogenic pathways, Hippo-Yki signaling ensures efficient tissue repair, homeostatic balance, and epithelial integrity in the insect gut.

5. Conclusion

Synthetic insecticides have long served as indispensable tools in modern agriculture, offering efficient and rapid solutions for managing a broad spectrum of insect pests. Their application has significantly contributed to increased crop yields and food security. However, the intensive, non-standardized, and often excessive use of these chemical agents has given rise to a number of pressing concerns. One of the most serious issues is the accumulation of pesticide residues, which can persist in agricultural products, soil, and water. These residues not only remain in raw produce, but can also make their way into processed foods and bioaccumulate through the food chain, ultimately posing serious risks to human health, including endocrine disruption, neurotoxicity, and carcinogenic effects. Moreover, these chemical residues can alter soil microbiota, reduce biodiversity, and disrupt ecological balance, highlighting the urgent need for more sustainable pest management strategies.

In parallel, insect pest populations have rapidly adapted to the selective pressures imposed by chemical pesticides, evolving various forms of insecticide resistance through genetic mutations, enhanced detoxification mechanisms, and behavioral avoidance. This growing resistance has further diminished the effectiveness of synthetic insecticides, compelling researchers and farmers alike to seek alternative and environmentally friendly solutions.

Among these alternatives, microbial biopesticides, particularly those based on the Gram-positive bacterium *Bacillus thuringiensis* (Bt), have emerged as one of the most promising tools for integrated pest management (IPM). Bt is renowned for its ability to produce insecticidal pore-forming toxins (PFTs), especially the well-characterized Cry (crystal) and Vip (vegetative insecticidal protein) families, which exhibit high specificity toward insect midgut cells, primarily targeting lepidopteran larvae. These toxins bind to specific receptors on the epithelial cells of the midgut, undergo conformational changes, oligomerize, and insert into the membrane to form pores. This pore formation disrupts ion gradients, causes cell lysis, and ultimately results in gut paralysis and insect death. Because of

their host specificity and safety to non-target organisms, Bt-derived toxins have been extensively utilized in biological control programs since the 1960s. Additionally, Bt toxin genes have been successfully engineered into genetically modified (GM) crops, such as Bt corn and Bt cotton, to provide continuous protection against targeted insect pests.

However, the long-term and widespread use of Bt-based products has led to a reduction in efficacy in certain field populations. This decline is often attributed to the evolution of resistance in insect pests, involving changes in toxin receptors, alterations in gut physiology, and suppression of toxin binding or activation. Recent studies have also begun to shed light on another crucial, yet historically underexplored, aspect of the Bt-host interaction - the insect's own defense mechanisms, particularly those mediated by the midgut epithelium, which is the primary site of Bt toxin action.

Upon exposure to sublethal doses of Bt toxins, lepidopteran insects activate a range of cellular and molecular defense responses within their midgut. These include mechanisms such as autophagy, apoptosis, cell shedding, regenerative proliferation, and the upregulation of immune pathways (e.g., JAK/STAT, EGFR, and JNK). The midgut regenerative response is especially important, as it enables the rapid replacement of damaged cells with new epithelial cells derived from intestinal stem cells (ISCs). These responses not only restore tissue integrity and functionality but may also counteract Bt toxin activity, contributing to the observed decline in mortality rates under field conditions.

Given the increasing reliance on Bt in both organic and GM crop systems, a comprehensive understanding of host defense responses against Bt toxins is becoming ever more critical. Such insights can not only help in the design of next-generation Bt toxins with improved potency but also aid in developing co-formulation strategies that suppress host defense mechanisms. Ultimately, a deeper understanding of these midgut-mediated defenses will be key to sustaining the long-term efficacy of Bt-based pest control, delaying the onset of resistance, and ensuring the ecological safety and sustainability of modern agricultural practices.

Chapter 2

Problematic, research aim, thesis outline, and experimental design

1. Problematic

Lepidoptera, the second largest insect order, includes numerous agricultural pests that cause significant damage to crops, forests, and horticultural plants. The widespread application of chemical insecticides poses risks to both the environment and human health. *Bacillus thuringiensis* (Bt) has emerged as one of the most effective microbial agents for pest control, utilized in both bio-insecticides and genetically modified crops. Its insecticidal proteins disrupt the midgut epithelium by forming pores, ultimately leading to larval mortality. The insect midgut plays a vital role in digestion and nutrient absorption while also serving as a protective barrier against pathogens and toxins. However, midgut defense mechanisms can diminish the effectiveness of Bt-based products and contribute to the emergence of resistance. Given this context, a critical question arises: How do lepidopteran pests defend against Bt insecticidal proteins, and which key genes and signaling pathways are involved in this defense?

2. Research aims

This project aims to explore the molecular mechanisms of lepidopteran pest defense against Bt insecticidal proteins, using methods from insect physiology, molecular biology, and biological chemistry. The thesis is divided into several objectives:

- To explore the specific form of midgut defense Bt insecticidal proteins in lepidopteran pests.
- To establish an efficient research system for midgut defense genes in lepidopteran insects based on RNAi.
- To explore the related genes and pathways of midgut defense Bt insecticidal proteins in lepidopteran pests.

3. Thesis outline

The following experimental chapters are designed based on the insights provided in **Chapter 1,** aiming to fill the research gap in understanding the molecular mechanisms of lepidopteran pest defense against Bt insecticidal proteins.

Chapter 3 investigates the specific midgut defense responses of lepidopteran insects against Bt insecticidal proteins.

Chapter 4 establish an efficient oral dsRNA-based research system for studying midgut defense genes in lepidopteran insects.

Chapter 5 investigates the specific genes and pathways involved in the midgut defense response of lepidopteran insects against Bt insecticidal proteins.

Finally, **Chapter 6** offers a general discussion and summary of all notable findings, providing suggestions, opinions, and perspectives.

Chapter 3

Determination of the specific forms of midgut defense Bt insecticidal proteins in Lepidopteran pests

Adapted from:

Wang, Z.,[#] Yang, Y.,[#] Li, S., Ma, W., Wang, K., Soberón, M., Shuo, Y., Frederic, F., Alejandra, B., & Zhang, J. (2024). JAK/STAT signaling regulated intestinal regeneration defends insect pests against pore-forming toxins produced by *Bacillus thuringiensis*. PLoS Pathogens, 20(1), e1011823.

Abstract

Bacillus thuringiensis (Bt) produces insecticidal Crystal (Cry) proteins that target midgut epithelial cells in insect larvae, leading to their death. However, sublethal concentrations of Cry proteins can trigger defense mechanisms in insects to counteract toxicity. This study elucidates the midgut defense mechanisms of *Chilo suppressalis* larvae against *Bacillus thuringiensis* Cry9A protein, integrating histopathological, molecular, and biochemical analyses. Using sublethal doses (LC_{20} and LC_{2}), we observed rapid Cry9Aa-induced midgut damage, characterized by 20–30% reductions in epithelial thickness and cell loss within 48 hours, followed by full recovery by 96 hours. Cell shedding was quantified via aminopeptidase N (APN) release, showing a 3.5-fold increase in lumenal activity at 24 hours. Regeneration involved intestinal stem cell (ISC) proliferation, evidenced by phospho-histone H3 (PH3) upregulation, and Notch-mediated differentiation, with *Delta* expression peaking at 72 hours (4.2-fold). Our results showed that sublethal concentration of Cry9A (LC_{20}) induced structural remodeling of midgut tissue, including epithelial cell shedding and midgut regeneration. These findings demonstrate a biphasic response - initial damage and subsequent repair - orchestrated by ISC activation, providing insights into lepidopteran adaptive strategies against Bt toxins.

Keywords: *Bacillus thuringiensis*, Cry9A, midgut defense responses, *Chilo suppressalis*, remodeling, cell shedding, midgut regeneration

1 Introduction

Synthetic pesticides have been widely used for pest control, but their excessive and improper application has led to pesticide resistance in many insect species, along with environmental and health concerns (Nougadère et al., 2011; Meftaul et al., 2020). One promising alternative is the use of microbial bioinsecticides, particularly those based on *Bacillus thuringiensis* (Bt), which produces insecticidal pore-forming toxins (PFTs) such as Cry and Vip proteins. These proteins have been widely used for the biological control of both agricultural pests and insect vectors of human diseases since the 1960s and certain toxin genes from Bt have been introduced in transgenic crops that resist insect attack. Bt bacteria produce monomeric PFTs, which oligomerize upon binding to their specific receptors and assemble into transmembrane pores permeabilizing midgut cells and facilitating bacterial infection (Crickmore et al., 2021). Bt-based insecticides have been extensively used in pest management, and certain Cry toxin genes have been successfully incorporated into transgenic crops.

However, the efficacy of Cry toxins varies among different insect species due to their ability to activate midgut defense responses, such as epithelial repair, cell shedding, and immune signaling pathways (Lee et al., 2016; Zhai et al., 2018; Tanaka et al., 2012). Previous studies suggest that these responses help maintain gut homeostasis and protect against midgut damage caused by microbial toxins. In particular, intestinal stem cells (ISCs) play a crucial role in midgut regeneration by proliferating and differentiating into new epithelial cells following toxin exposure (Pinos et al., 2021).

Although apoptosis has been proposed as a common mechanism for removing damaged cells, its role in midgut defense against Cry toxins remains unclear. Studies on other lepidopteran insects indicate that Cry toxins may not always activate apoptotic pathways. Instead, alternative mechanisms such as cell shedding and ISC-mediated regeneration may dominate the midgut repair process. This study aims to elucidate the effects of Cry9A on midgut tissue morphology in *C. suppressalis* and investigate what type of cell elimination process is involved in the toxin-induced midgut remodeling.

2 Materials and methods

2.1 Insect populations

Striped stem borer (*Chilo suppressalis*) obtained from Hubei Province in China was supplied by Shennong Inc. (Hubei, China) and fed an artificial diet (supplied by Prof. Lanzhi Han from the Institute of Plant Protection, Chinese Academy of Agricultural Sciences) and (70±5)% relative humidity (RH) with a 16 h light:8 h dark photoperiod.

2.2 Protein expression and purification

The Cry9A and non-toxic Cry9A-D125R mutant proteins were expressed in *Escherichia coli.* The recombinant plasmids pET28a-*cry9A* and pET28a-*cry9A-D125R* were transformed into BL21 DE3 *E. coli* competent cells. Under the conditions of 16℃ and 150 rpm for 12 hours, the expression of wild-type and mutant proteins was induced in BL21 containing the recombinant plasmids using 0.5 mmol/L IPTG. The bacterial cells were centrifuged at 4℃ and 6500 rpm for 10 minutes, and the supernatant was resuspended in Binding Buffer (50 mmol/L imidazole，20 mmol/L Tris-HCl，500 mmol/L NaCl，pH 8.0). The resuspended cells

were then subjected to sonication for 5 minutes (Amplitude 70%, pulse on 3 seconds, pulse off 5 seconds) to disrupt the cell walls. After sonication, the lysate was centrifuged at 4℃ and 9500 rpm for 10 minutes. The supernatants were collected and analyzed for protein expression using sodium dodecyl sulfate-polyacrylamide gel electrophoresis (SDS-PAGE). The crude Cry9A and mutant proteins were purified by affinity chromatography (Ni Sepharose 6 Fast Flow, Bio-Rad, California). The purified proteins were desalted using a Hiprep 26/10 desalting column (GE Healthcare) and protein purification system (AKTA avant 150, Cytiva) according to the manufacturers. The purified protein was finally analyzed by SDS-PAGE and the concentration was determined using a BCA protein assay kit (Solarbio Life Sciences, Beijing, China).

2.3 Insecticidal bioassays

Bioassays to determine median lethal concentration values were performed on 2-day-old and 3rd instar larvae. 5 gradient concentrations of Cry9A or its mutant protein in one mL were mixed thoroughly with 3 g artificial diet and transferred into flat glass tubes. Thirty-five larvae were placed inside each tube and three replicates were performed for each treatment. The mortality was calculated after 7 days. Lethal concentration of 20% larvae mortality (LC_{20}) and lethal concentration 2% larvae mortality (LC_2) was calculated by Probit analysis.

2.4 Intestinal thickness and cell number determination

The midgut tissues from third instar larvae that survived were dissected after feeding with 200 and 20 μg Cry9A protein per g of diet for different times (1.5-120 h) and fixed overnight in 4% paraformaldehyde at 4℃. These midgut tissues were carefully washed three times with PBS and labeled with 1:1000 Phalloidin-iFluor 647 (Abcam, Cambridge, UK) for 1 h at room temperature (RT). After washed twice with PBS, the tissues were labeled with 10 μg/ml Hoechst33342 (Solarbio Life Sciences, Beijing, China) final concentration in PBS for 5 min. The tissues were sealed with Prolong Diamond Antifade (Invitrogen, Oregon, USA) on microscopic slides after washing three times with PBS. Images were obtained using 20X objective in the confocal LSM 980 (Zeiss, Germany). Six guts were used for each treatment and six images were taken from each midgut. The intestinal thickness measurements were based on the data of the cytoskeleton stained with Phalloidin-iFluor 647 by using ImageJ software in a total of 36 images. Midgut cell numbers were counted based on number of nuclei stained with Hoechst33342 and then dividing by the gut length as the number of nuclei per μm area. Three replicates were performed for each treatment.

2.5 Analysis of APN release

Third instar larvae were treated with 200 μg/g Cry9A for 12 and 24 h. Fifteen intact midguts were dissected from alive larvae at the indicated times and transferred into 100 μL of 50 mmol/L Tris-HCl, pH 7.5. Vortexed 30 sec, centrifuged at 21,000 xg for 5 min at 4℃, and the supernatants containing contents in midgut lumen of these samples were used for APN activity analysis. Protein concentration in the samples was measured by using Bradford kit (Solarbio Life Sciences, Beijing, China). APN activity was assayed using 4 mmol/L L-leucyl-p-nitroanilide as substrate in 50 mmol/L Tris-HCl (pH 7.5) buffer. The released

p-nitroanilide by the hydrolysis of LpNA was monitored at 405 nm for 10 min using FlexStation 3 Multi-Mode Microplate Reader (Molecular Devices, USA). The higher APN enzymatic activity was the result of an increase in intestinal cell shedding that represented intestinal damage condition. In these experiments, we used as negative control (Ctrl) a non-toxic Cry9A-D125R mutant protein which the mutation site is located in domain I helix α3. This mutant lost toxicity but retains the same ability to bind to the BBMV as the Cry9A. Control and all the treatments were performed in three repetitions.

2.6 Reverse transcript quantitative PCR (RT-qPCR)

Fifteen midguts from third-instar larvae were collected together and mixed in a single sample for gene expression determination for each treatment by RT-qPCR using primers described in Table 3-1. Total RNA was extracted from the samples by using Total RNA Kit I (OMEGA Bio-tek, GA, USA). Five hundred ng RNA was used for reverse transcription by using HiScript III RT SuperMix (Vazyme, Nanjing, China). Twenty-fold dilution of cDNA was used as template for qPCR by using SYBR qPCR Master Mix (Vazyme, Nanjing, China) through QuantStudio 6 (Applied Biosystems, MA, USA). Relative gene expression was calculated in relation to a reference gene, *elongation factor-1* (*EF-1*), using the $2^{-\Delta\Delta Ct}$ method (Pfaffl and Hageleit 2001). Three replicates and three independent experiments were performed.

Table 3-1. Primers for RT-qPCR

Gene	**(5'-3') Primer sequence**
q-*EF-1*-F	TGAACCCCCATACAGCGAATCC
q-*EF-1*-R	TCTCCGTGCCAACCAGAAATAGG
q-*Delta*-F	CTCGCTCATAGTCGAAGCGT
q-*Delta*-R	CGTCGGCTATGCTCTGCTTA

2.7 Histopathological analyses

The midgut tissue were dissected from larvae of both treatments and fixed in 4% paraformaldehyde at 4℃ overnight. Then embedded in paraffin and made 5 μm thick sections. The sections were stained with hematoxylin and eosin (Solarbio, Beijing, China) in sequence, and sealed with neutral gum (Solarbio, Beijing, China). The pathological changes in midgut tissues were observed under Pannoramic 250 Flash digital microscopes (3DHISTECH, Budapest, Hungary).

2.8 Western blot

Total protein was extracted from fifteen larval midgut tissues using a Protein Kit (OMEGA Bio-tek, GA, USA) and quantified with a BCA kit (Solarbio Life Sciences, Beijing, China). For each treatment, 35 μg of protein was separated via SDS-PAGE and transferred onto PVDF membranes. After blocking with 1% non-protein blocking solution (Sangon Biotech, Shanghai, China) for 40 min at RT, the membranes were incubated for 4 h with primary

antibodies: anti-β-actin (1:30000), anti-Histone H3 (1:3000), and anti-Phospho-Histone H3 (1:1000) (all from ABclonal Technology, Wuhan, China) in PBST (PBS + 0.1% Tween-20). Following three 10-min washes with PBST, membranes were incubated with FITC-labeled goat anti-rabbit secondary antibody (1:1000, Solarbio Life Sciences, Beijing, China) for 1 h at RT. Images were captured using a Typhoon 9410 scanner (GE Healthcare, USA) and analyzed with ImageJ software.

2.9 Statistical analysis

All the experiments were repeated at least three times and the statistical analyses were performed using GraphPad Prism 7.0 software (GraphPad, San Diego, CA). Pairwise comparisons were performed by Student's t-test. One-way analysis of variance (ANOVA) was used in comparing the multiple groups, and Tukey's test was used as a post-hoc test.

3 Results

3.1 Insecticidal bioassays of *C. suppressalis* against Cry9A protein

The Cry9A-D125R protein is a mutant form of the Cry9A toxin, previously constructed in our laboratory through site-directed mutagenesis. This mutant carries a single amino acid substitution (aspartic acid to arginine at position 125), which abolishes its pore-forming ability, a key functional property of Cry toxins. As a result, Cry9A-D125R exhibits a complete loss of insecticidal activity against the target pest, *Chilo suppressalis*, and serves as an ideal negative control in functional assays to dissect toxin-induced midgut responses independent of cytotoxicity (He et al., 2024).

To produce both wild-type and mutant proteins, a prokaryotic expression system was employed. Expression was induced in *E. coli* with isopropyl β-D-1-thiogalactopyranoside (IPTG). Following induction, bacterial cells were harvested and lysed using ultrasonic disruption. The recombinant proteins were initially purified using nickel-nitrilotriacetic acid (Ni-NTA) affinity chromatography, which exploits the His-tag fused to the recombinant proteins. Further buffer exchange and removal of low-molecular-weight contaminants were performed using a HiPrep™ 26/10 desalting column.

Protein purity and integrity were confirmed by SDS-PAGE analysis. As shown in Figure 3-1A, both Cry9A and Cry9A-D125R proteins had a molecular weight of approximately 70 kDa. To evaluate the insecticidal efficacy of Cry9A, we conducted bioassays on *C. suppressalis* larvae at different developmental stages. For 2-day-old larvae, Cry9A demonstrated potent activity, with an LC_{20} of 7.5 μg/g (7.5 μg of protein per gram of diet caused 20% mortality after 7 days) (Figure 3-1B) and an LC_{50} of 51 μg/g. In contrast, third-instar larvae exhibited reduced sensitivity, with an LC_{20} of 200 μg/g and LC_{50} of 499 μg/g (Figure 3-1C).

Based on these results, we selected the sublethal dose of 200 μg/g, corresponding to the LC_{20} value for third-instar larvae, as the working concentration for subsequent experiments. This sublethal exposure allows us to investigate early host defense mechanisms, particularly focusing on midgut epithelial damage, cell shedding, and regenerative responses in the larval gut.

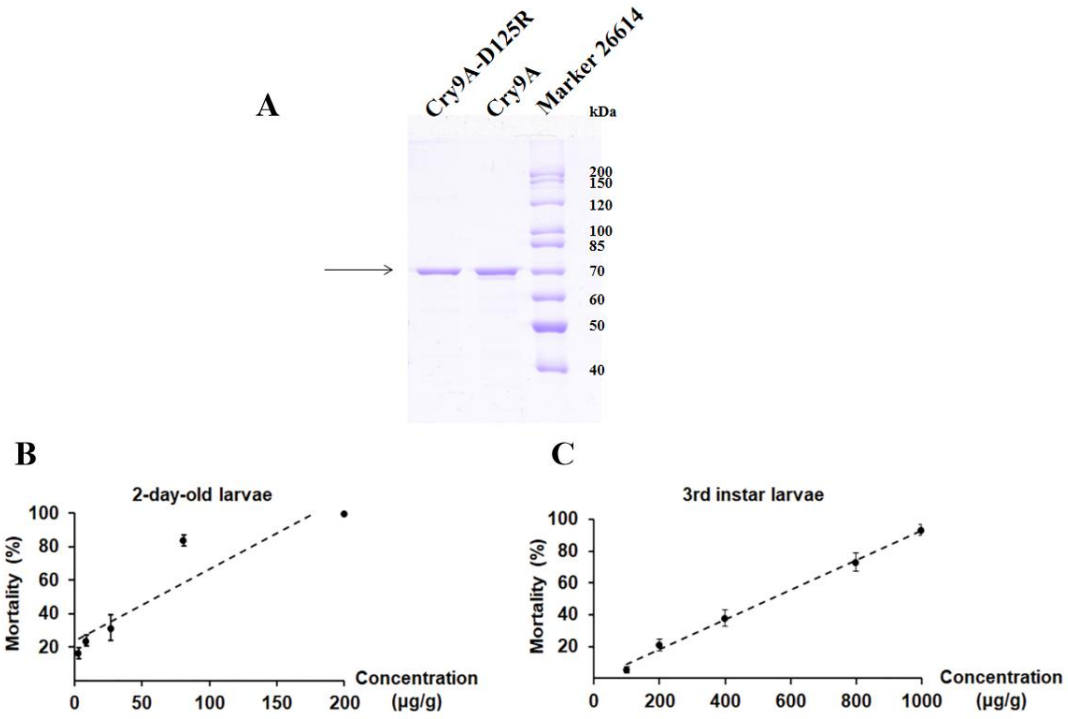

Figure 3-1. Insecticidal bioassays of *C. suppressalis* against Cry9A protein (A) Analysis results of SDS-PAGE for purified Cry9A and mutant proteins. (B and C) Insecticidal toxicity assays of Cry9A against 2-day-old (B) or 3rd instar (C) larvae of rice striped stem borer. Thirty-five larvae were analyzed with each protein concentration and three replicates were performed. The error bar represents ±SEM.

3.2 Changes in midgut tissue morphology after treatment with sublethal dose of Cry9A protein

To investigate the effects of Cry9A, a pore-forming toxin (PFT), on the midgut tissue of the *C. suppressalis*, third-instar larvae were fed a sublethal dose of Cry9A protein at a concentration of 200 μg per gram of diet, corresponding to 20% lethal concentration (LC_{20}). The morphological changes in the midgut over a period of 120 hours were examined using a laser scanning confocal microscope (LSCM), which provided high-resolution median sagittal views of intact midgut tissue (Figure 3-2A).

A significant reduction in midgut tissue thickness was observed as early as 24 hours post-ingestion, with a 20% decrease compared to the control group (P<0.0001). This reduction became more pronounced at 48 hours post-ingestion, reaching a maximum decrease of approximately 30% (P<0.0001). However, the midgut tissue gradually recovered over the following hours, and by 96 hours post-protein ingestion, the tissue thickness had returned to levels comparable to the control group (Figure 3-2A and B).

A similar trend was observed when larvae were treated with a 10-fold lower concentration of Cry9A (LC_2, 20 μg per gram of diet). Although a reduction in intestinal thickness was also detected, the degree of change was less severe, indicating a concentration-dependent effect of Cry9A on midgut tissue remodeling (Figure 3-2A and B). To determine whether these effects were specifically due to Cry9A's pore-forming activity, larvae were also treated with a

non-toxic mutant, Cry9A-D125R. Notably, no significant changes in midgut morphology were observed in the Cry9A-D125R group, further confirming that the observed tissue alterations were a direct consequence of Cry9A's toxic action.

In addition to changes in intestinal thickness, the total number of cells in the midgut epithelium exhibited a similar pattern. A significant reduction in the number of midgut epithelial cells was observed at 24 hours post-ingestion, with the lowest cell count recorded at 48 hours (P<0.0001) (Figure 3-2A and C). However, by 96 hours post-ingestion, the cell number had returned to baseline levels, indicating a recovery process similar to that observed in tissue thickness. The Cry9A-D125R mutant did not induce any noticeable reduction in cell count, reinforcing the conclusion that cell loss was a direct consequence of Cry9A toxin activity. Furthermore, larvae exposed to the lower LC_2 dose of Cry9A exhibited a milder reduction in cell count, with a faster recovery rate compared to those treated with the higher LC_{20} dose. These findings suggest that both midgut tissue thinning and epithelial cell loss are dependent on the protein's concentration and activity.

Overall, these results indicate that sublethal concentration of Cry9A protein induces significant but reversible morphological changes in the midgut of *C. suppressalis*, characterized by transient reductions in both intestinal thickness and cell count. The extent of these changes correlates with toxin concentration, suggesting a dose-dependent effect. The ability of the midgut to recover from Cry9A-induced damage highlights the potential for tissue remodeling and repair following exposure to sublethal doses of the toxin.

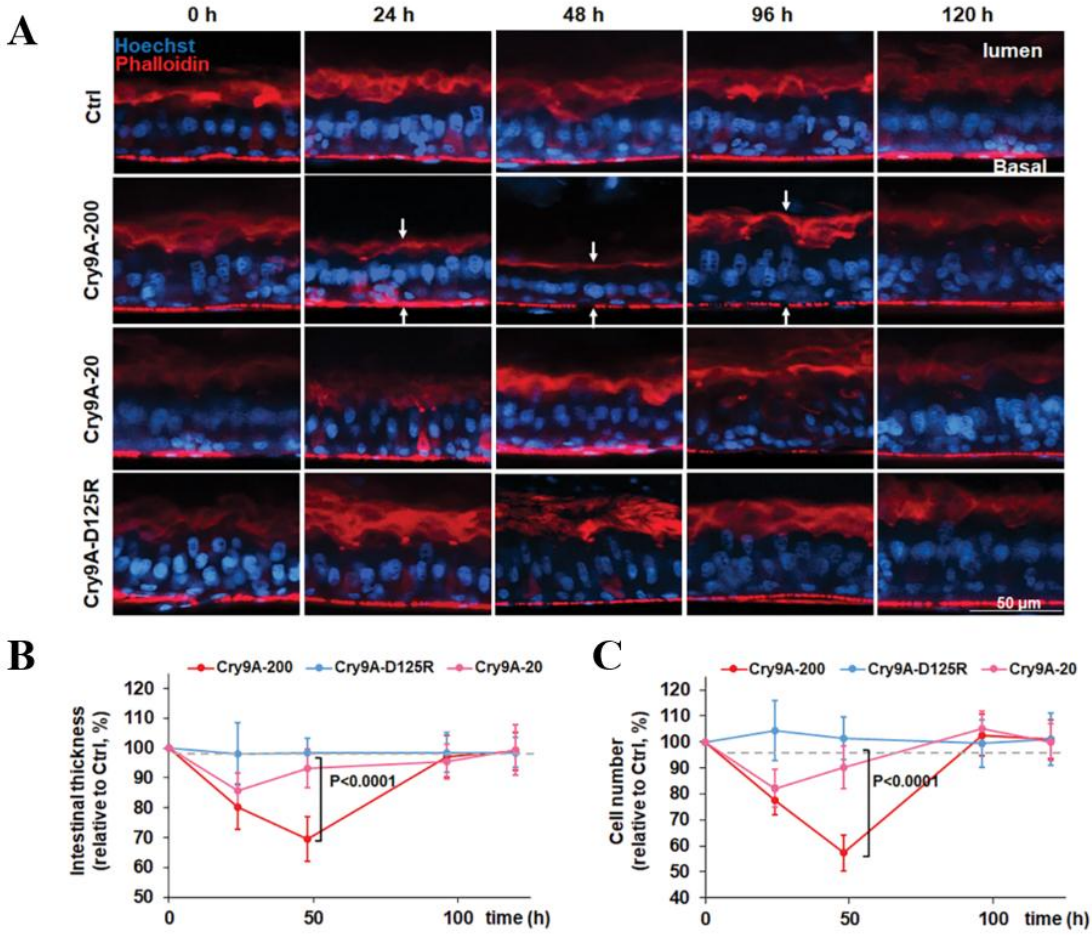

Figure 3-2. Changes in midgut tissue morphology after treatment with sublethal dose of Cry9A protein (A) Sagittal view representative images obtained from midgut tissue of rice striped stem borer larvae treated with Cry9A observed in the LSCM. Phalloidin-647 (red color) stains F-actin present in the brush border (upper arrows) and in the visceral muscles (lower arrows). Hoechst33342 (blue color) labels nuclei. Control (Ctrl) samples were treated with 50 mmol/L Na_2CO_3 buffer pH 10, that was the buffer used for solubilization of Cry9A protein. (B and C) Quantification of the fluorescent signal of intestinal thickness (B) and cell number (C).

3.3 Detection of cell shedding after treatment with sublethal concentration of Cry9A protein

To further investigate the causes of reduction in midgut tissue thickness and cell number, histopathological analyses were conducted using hematoxylin-eosin (HE) staining. This approach enabled the visualization of morphological changes in midgut architecture at various time points post-toxin ingestion. The results revealed that apical microvilli of columnar epithelial cells - structures critical for nutrient absorption and barrier function - were severely compromised as early as 3 hours after Cry9A exposure. At this stage, the microvilli appeared disorganized or completely absent, indicating rapid disruption of the apical membrane (Figure 3-3A).

As toxin exposure progressed, more profound structural alterations were observed. By 12 hours post-ingestion, the midgut epithelium displayed pronounced stratification, characterized by multiple disorganized cell layers, and the presence of epithelial cells with intact nuclei extruding into the gut lumen (Figure 3-3A and B). This suggests that, in addition to microvilli loss, Cry9A disrupts cell-cell adhesion mechanisms within the epithelium, leading to the detachment and shedding of damaged epithelial cells into the lumen. These changes reflect a breakdown of epithelial barrier integrity and suggest the initiation of tissue remodeling or regenerative responses.

To quantitatively evaluate the extent of epithelial cell shedding, we measured the release of aminopeptidase N (APN) - a GPI-anchored brush-border enzyme highly enriched on the apical membrane of midgut epithelial cells. Because APN is released into the gut lumen upon epithelial damage or cell shedding, its extracellular activity serves as a biochemical marker for epithelial cell loss, as previously described (Valaitis et al., 2008).

Following the experimental workflow depicted in Figure 3-3C, we isolated luminal contents at different time points post-Cry9A ingestion and measured APN enzymatic activity. Our analysis revealed that APN levels remained relatively unchanged at 6 hours, indicating limited early shedding. However, by 12 hours, there was a significant increase in APN activity, which further escalated by 24 hours post-treatment ($P<0.001$; Figure 3-3D). These data suggest a time-dependent escalation of epithelial damage, with cell shedding becoming a prominent response.

Taken together, our histological and biochemical evidence demonstrates that Cry9A ingestion elicits a rapid and progressive midgut injury in *Chilo suppressalis* larvae. This damage begins with the destruction of apical microvilli, followed by epithelial disorganization, and culminates in cell detachment and shedding, as evidenced by elevated APN activity. These

findings underscore the cytopathic effects of sublethal Cry9A exposure and lay the groundwork for further investigation into the insect's regenerative following midgut disruption.

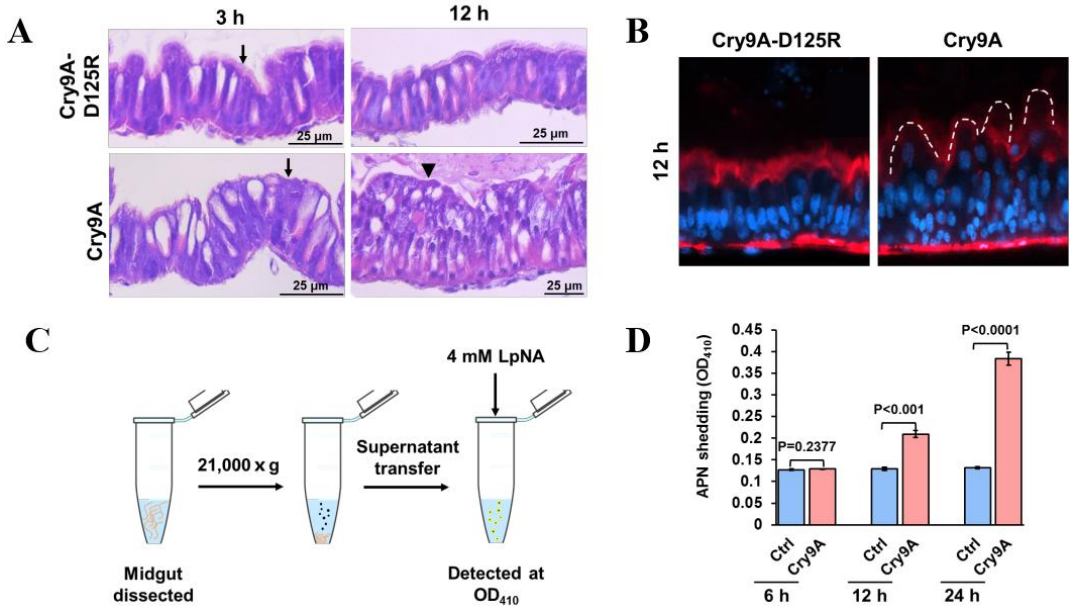

Figure 3-3. Detection of cell shedding after treatment with sublethal concentration of Cry9A protein (A) Transection of midgut stained with hematoxylin-eosin (HE). Arrows show microvilli and the arrowhead points to stratification of midgut epithelium. (B) Sagittal view of larvae midgut tissue treated with Cry9A observed by laser scanning confocal microscopy. (C) Schematic illustration of the epithelial shedding assay. (D) Analysis of *p*-nitroanalide release into the midgut lumen of larvae that were treated with Cry9A. Control (Ctrl) samples were treated with Cry9A-D125R mutant protein. *n*=15 isolated midgut tissues from 3rd instar larvae per treatment. Three biological replicate samples performed in three independent experiments were performed. *P* values were calculated by two-sided Student's t-test, $P<0.001$ shows statistically significant differences. $P>0.05$ shows no significant difference. The error bar represents ±SEM..

3.4 Detection of midgut regeneration after treatment with sublethal concentration of Cry9A protein

Pathogens or toxic agents that induce damage to midgut tissues often trigger compensatory responses, particularly the proliferation of intestinal stem cells (ISCs), which are essential for facilitating tissue repair and regeneration (Xiang et al., 2017). In insects, ISC proliferation serves as a critical mechanism to replenish damaged epithelial cells and restore gut functionality. One of the most reliable markers for assessing mitotic activity in ISCs is the phosphorylation of histone H3 (PH3), which is commonly used as an indicator of cell division (Jiang et al., 2009).

To investigate the proliferative response of ISCs following Cry9A exposure, we performed Western blot analysis on midgut tissue collected at different time points after Cry9A ingestion. Our results revealed a significant presence of PH3 in the midgut tissue from 24 to 96 hours

post-ingestion, corresponding to the observed period of cell number recovery and midgut tissue regeneration (Figure 3-4A). The presence of PH3 during this timeframe strongly indicates that ISC proliferation was actively occurring in response to Cry9A-induced midgut damage, underscoring the involvement of ISCs in the regenerative response to toxin exposure.

In addition to ISC proliferation, another critical aspect of midgut regeneration involves the differentiation of enteroblasts (EBs) into mature enterocytes (ECs). This process is essential for the restoration of the midgut epithelium and its proper functionality. Notch signaling plays a pivotal role in regulating the differentiation of ISCs into EBs and further into ECs. Specifically, ISCs express the Notch ligand *Delta*, which binds to the Notch receptor on adjacent cells, initiating downstream signaling that promotes differentiation into mature enterocytes (Martin et al., 2018).

We analyzed *delta* gene expression as a marker for Notch signaling activation. Our quantitative analysis revealed a significant upregulation of delta expression from 24 to 96 hours post-Cry9A ingestion (Figure 3-4B). This upregulation coincided with the timeframe of ISC proliferation (Figure 3-4A), further supporting the notion that ISC proliferation and differentiation are tightly coupled processes essential for effective midgut regeneration.

Collectively, these results demonstrate that midgut remodeling occurs following exposure to a sublethal dose of Cry9A, beginning with initial cell loss and tissue thinning, followed by a robust regenerative response. This regenerative response is driven by ISC proliferation, marked by histone H3 phosphorylation, and the subsequent differentiation, which is regulated by Notch signaling. By 96 hours post-ingestion, midgut integrity is fully restored, allowing for the recovery of gut function and enabling the larvae to survive despite the initial cytotoxic effects of the pore-forming Cry9A toxin.

These findings highlight the adaptive plasticity of the midgut in response to toxin exposure, providing valuable insights into the mechanisms of tissue repair and regeneration in lepidopteran pests. Understanding these processes is crucial for improving biopesticide efficacy and delaying resistance development against Cry proteins in agricultural pest management.

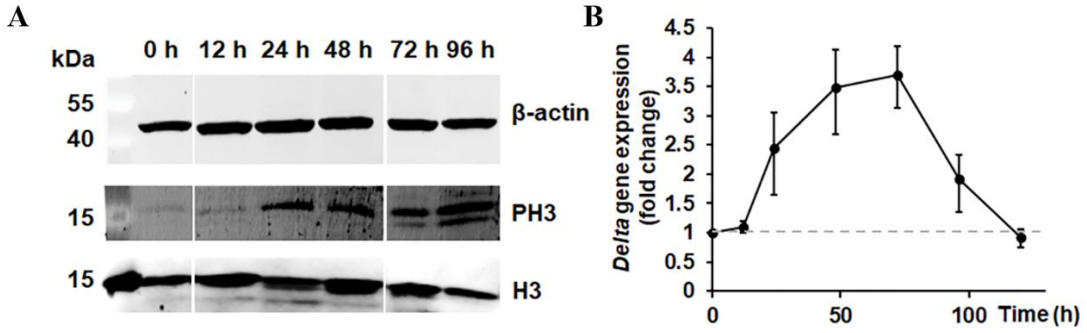

Figure 3-4. Detection of midgut regeneration after treatment with sublethal concentration of Cry9A protein (A) Western blot detection of phospho-histone H3 (PH3) and histone H3 (H3) in midgut tissue samples from fifteen larvae after Cry9A (LC_{20}) intoxication for 0-96 h. β-actin was detected as an internal reference. (B) Quantification of *delta* gene expression determined by RT-qPCR in intestines isolated from fifteen larvae treated with Cry9A (LC_{20}) for 0, 12, 24, 48, 72, 96 and 120 h. The data were normalized to uninfected control intestines

and elongation factor-1 (*EF-1*) gene was used as reference gene on three biological replicate samples performed in three independent experiments. The error bar represents ±SEM.

4. Discussion

Bacillus thuringiensis (Bt) produces insecticidal Crystal (Cry) proteins that target midgut epithelial cells in insect larvae, leading to their death. However, sublethal concentrations of Cry proteins can trigger defense mechanisms in insects to counteract toxicity. In this study, our results reveal that *Chilo suppressalis* employs a dynamic, two-phase defense strategy against Cry9Aa: (1) rapid epithelial shedding to eliminate damaged cells, and (2) ISC-driven regeneration to restore gut integrity.

Histopathological analyses provided detailed insights into the midgut remodeling process following Cry9A ingestion. Our findings show that Cry9A induces a 20-30% reduction in midgut thickness within 48 hours, followed by tissue recovery at 96 hours, illustrating a temporal pattern of damage and repair. This initial thinning of the midgut epithelium indicates significant damage, which is followed by a robust regenerative response. This structural remodeling was accompanied by a marked increase in cell shedding, as evidenced by the elevated enzymatic activity of aminopeptidase N (APN). APN is a well-established marker of epithelial turnover and its increased activity in the lumen highlights the shedding of damaged epithelial cells into the gut cavity, a protective mechanism aimed at removing damaged or dysfunctional cells from the tissue.

Additionally, we observed dose-dependent activation of the defense mechanisms. At LC_{20}, Cry9A induced a 30% reduction in midgut tissue thickness, while at LC_2, only a 15% reduction was observed. This suggests that higher doses of Cry9A lead to more extensive damage and consequently a more pronounced activation of compensatory repair mechanisms. The ability of the larvae to initiate these defense responses in a dose-dependent manner suggests a fine-tuned response, enabling the insect to adapt to varying levels of toxin exposure.

The recovery of midgut integrity was closely linked to the proliferation of intestinal stem cells (ISCs). As damage progressed, we observed increased phosphorylation of histone H3 (PH3), a well-established marker for mitotic activity in ISCs. This finding strongly indicates that ISC proliferation was actively occurring in response to the Cry9A-induced damage, contributing to tissue repair and regeneration. The increased mitotic activity of ISCs underscores their critical role in the repair process, as they serve as the primary source of new epithelial cells necessary for restoring the integrity of the gut.

In addition to proliferation, our RT-qPCR analysis demonstrated significant upregulation of genes involved in the Delta/Notch signaling pathway, a key regulator of ISC differentiation. This upregulation occurred between 24 and 96 hours post-ingestion, corresponding with the timeframe of ISC proliferation. The Notch pathway, which controls the differentiation of ISCs into mature enterocytes, was likely crucial for the replacement of damaged cells. The peak of *Delta* expression during this period further supports the idea that ISCs were actively differentiating into new epithelial cells to restore the structure and function of the gut. These findings are consistent with previous studies on *Drosophila melanogaster*, where ISC proliferation and differentiation are central to gut repair following toxin-induced damage (Jiang et al., 2009; Martin et al., 2018).

Conclusion and Implications for Pest Control

In conclusion, our study provides strong evidence that Cry9A triggers a two-phase defense response in *C. suppressalis*, characterized by epithelial shedding and ISC-driven midgut regeneration. This response helps the larvae recover from the cytotoxic effects of the toxin, allowing them to survive despite significant gut damage. The ability of the insect to repair its gut following exposure to sublethal doses of Cry9A suggests that *C. suppressalis* has developed an adaptive strategy to cope with the toxin, which may contribute to the persistence of this pest in environments where Bt-based insecticides are used.

These findings have important implications for the use of Bt-based pest control strategies. Disrupting the ISC-mediated repair mechanisms could potentially enhance the efficacy of Bt toxins by preventing the regeneration of the midgut epithelium and increasing the overall lethality of Cry9A. Targeting specific pathways involved in ISC proliferation and differentiation, such as the Delta/Notch signaling pathway, could serve as a novel approach to overcome insect resistance to Bt toxins and improve the long-term effectiveness of Bt-based biopesticides.

Future studies should explore the potential of genetic or chemical inhibitors that specifically target ISC proliferation and differentiation. These inhibitors could be used in combination with Bt treatments to increase the lethality of Bt insecticides in resistant pest populations. Furthermore, understanding the molecular mechanisms that underlie midgut regeneration in response to Bt protein will be essential for developing more targeted and effective strategies to manage resistance in agricultural pests.

Chapter 4

Establishment of an efficient RNAi-based research system for gut defense genes in Lepidopteran larvae

Adapted from:

Yang, Y.,[#], Wang, Z.,[#] Niu, X., Li, S., Frédéric, F., Shu, C., Ma, W., Zhang, J. (2024). Knockdown of *Egfr* and *Stmn4* by using an efficient oral feeding RNAi system increases the susceptibility of *Spodoptera frugiperda* larvae to Cry1F protein (Under review)

Abstract

Crystal (Cry) proteins produced by *Bacillus thuringiensis* (Bt) efficiently control many Lepidopteran pests. However, the low efficiency of RNA interference (RNAi) has limited the study of their defense mechanisms to Cry proteins in the midgut. Epidermal growth factor receptor (*Egfr*) and stathmin 4 (*Stmn4*) genes regulate stem cell proliferation and cell cycle in *Drosophila*. In this study, *SfEgfr* and *SfStmn4* both highly expressed in the midgut of 4th instar *S. frugiperda* larvae. *SfEgfr* and *SfStmn4* dsRNA synthesized in vitro showed better silencing efficiency compared to that expressed in *Escherichia coli*, especially when it was combined with star-polycation complex (SPc) nanoparticles. The highest silencing efficiency (over 75%) of those two genes were achieved at the concentration of 25 μg synthesized dsRNA-SPc per gram diet for 48 hours. Pretreatment with dsRNA for 48 h increased the mortality of larvae treated with Cry1F by more than 30%. Silencing of these two genes dampened intestinal stem cell proliferation in the midgut after Cry1F treatment, which explains the increased mortality. This study provides an efficient oral feeding RNAi system for silencing midgut genes in Lepidopteran pests, and demonstrated that *SfEgfr* and *SfStmn4* play a crucial role in the midgut defense response to Bt Cry proteins. Our findings offer a novel concept and theoretical framework for the biological management of Lepidopteran pests.

***Keywords*:** *Bacillus thuringiensis*, RNA interference, *Spodoptera frugiperda*, midgut defense response

1 Introduction

The management of agricultural pests represents a critical challenge in ensuring global food security. Current pest management strategies primarily rely on chemical pesticides and biological control agents, including *Bacillus thuringiensis* (Bt) toxins. However, the emergence of resistance to Bt proteins among Lepidopteran pests underscores the urgent need for alternative and sustainable approaches to pest control.

The Cry proteins produced by Bt are pore-forming toxins that target the midgut of susceptible insects, disrupting epithelial cells and causing osmotic imbalances that lead to mortality. The insect midgut, a critical site for nutrient digestion and absorption, also functions as a defensive barrier against pathogens and toxins (Ragasruthi et al. 2024; Li et al. 2024; Pacheco et al. 2023). When infected by pathogens, the homeostasis of the insect midgut is disrupted. The midgut enterocytes (ECs) are damaged and eliminated through processes such as apoptosis (Tanaka et al. 2012), necrosis (Singh et al. 2016), cell shedding (Zhai et al. 2018), and Erebosis (Ciesielski et al. 2022). This leads to the activation of midgut stem cell proliferation and differentiation, culminating in midgut regeneration. In *Drosophila*, the regeneration process of the midgut is regulated by multiple genes and signaling pathways, including JAK/STAT, EGFR, JNK, Hippo, and Wg (Ren et al. 2010; Zhou et al. 2015; Tian et al. 2015; Santabarbara-Ruiz et al. 2015; Cordero et al. 2012). Upon damage to the intestinal epithelial cells, several EGFR ligands are induced, leading to the activation of EGFR signaling in intestinal stem cells (ISCs). The activation of EGFR signal transduction promotes ISC division and midgut epithelial regeneration, thereby maintaining tissue homeostasis. Furthermore, ISC proliferation induced by JAK/STAT signaling depends on EGFR signal transduction (Ciesielski et al. 2022; Xiang et al. 2017; Tian et al. 2022). Stathmin, a founding member of a protein family, plays a crucial role in regulating the microtubule cytoskeleton. Overexpression or repression of *stathmin* results in reduced cell proliferation and accumulation of cells in the G2/M phase of the cell cycle (Rubin and Atweh 2004). However, the role of these pathways and regulatory proteins in Lepidopteran pests, remains poorly understood. Investigating the molecular mechanisms underlying midgut defense in Lepidopteran pests is essential for developing novel pest management strategies that exploit vulnerabilities in these defense systems.

RNA interference (RNAi) has emerged as a powerful tool for studying gene function and pest control. RNAi operates by silencing specific genes through the introduction of double-stranded RNA (dsRNA), leading to the degradation of target mRNA (Zotti and Zhang 2015). However, the efficiency of RNAi in Lepidopteran insects is limited by several factors, including the stability of dsRNA in the midgut, the delivery method, and the concentration and duration of treatment (Wang et al. 2016). Oral delivery of dsRNA has gained attention as a minimally invasive method suitable for large-scale pest control applications. However, achieving high RNAi efficiency in Lepidopteran midguts requires optimization of dsRNA synthesis, encapsulation, and administration.

In this study, we targeted the Lepidopteran pest, *S. frugiperda,* to establish an efficient research system for RNAi of midgut defense genes through oral feeding of dsRNA in Lepidopteran insects.

2 Materials and methods

2.1 Insect populations

Fall armyworm (*Spodoptera frugiperda*) was maintained in our laboratory and fed an artificial diet, the main component of which was wheat bran or soybean meal at (27±2)℃ and (70±5)% relative humidity (RH) with a 14 h light:10 h dark photoperiod.

2.2 Isolation and Purification of Insecticidal Proteins

Bt strain HD73-*Cry1F3* was grown in 1/2 liquid Luria–Bertani (LB) media until 50-60% of insecticidal crystals were released. Following centrifugation at 9000 ×g for 15 minutes at 4℃, the mixture containing crystals, spores, and debris was collected and washed with 1.0 mol/L NaCl, followed by a rinse with distilled water. The mixture was then resuspended directly in a solubilization buffer (50 mmol/L Na_2CO_3, 50 mmol/L EDTA-Na_2, and 3% β-ME, pH 10.0) and incubated on ice with shaking at 100 rpm for 2 h. After incubation, the mixture was centrifuged at 9000×g for 15 min to remove insoluble debris. The supernatant was collected, a 1/7 volume of 4 mol/L NaAc-HAc (pH 4.8) was gradually added while stirring gently. The mixture was then incubated on ice for 1 h. The resulting pellet was collected by centrifugation at 9000 ×g for 15 min, washed twice with distilled water, and dissolved in 50 mmol/L Na_2CO_3.

2.3 dsRNA Synthesis

The DNA templates for dsRNA were cloned from cDNA of larval midguts and ligated into pEasy Blunt Zero vector (TransGen Biotech, Beijing, China) using primers described in Table 4-1, enhanced green fluorescent protein gene (*egfp*) as a negative control. The different dsRNAs were synthesized from plasmid DNA using the T7 RiboMAX™ Express RNAi System (Promega, Madison, USA) according to the manufacturer's instructions. The concentration of synthetic dsRNA was determined by using NanoDrop (ThermoFisher Scientific, Oregon, USA).

For expressing dsRNA in *Escherichia coli*, the DNA was ligated into pET-2p expression vector, the confirmed plasmids (sequence consistent with the target gene) were expressed using *E. coli* HT115 (DE3) competent cells lacking RNase III. Individual colonies were cultured in Luria-Bertani culture for 4 h. Subsequently, the colonies were induced to express dsRNA using isopropyl β-D-1-thiogalactopyranoside (0.4 mmol/L) for 4 h. The bacteria were precipitated by centrifugation at 5,000 rpm for 10 min, resuspension using RNase-free water.

For obtain dsRNA expressed in *Escherichia coli*,

For obtain dsRNA in *E. coli*, the bacteria obtained as described above was resuspended in STE buffer (10 mmol/L Tris-HCl, 100 mmol/L NaCl, 1 mmol/L EDTA) and mixed thoroughly. An equal volume of phenol:chloroform:isopropanol was added, mixed thoroughly, and incubated in a 65℃ water bath for 30 min. Centrifugation was performed at 12,000 ×g for 15 min at 4℃. Without disturbing the interface, the supernatant was carefully collected into a new tube. An equal volume of isopropanol was added to the collected supernatant, and the sample was precipitated overnight at -20℃. The next day, it was centrifuged at 12,000 ×g for

5 min at 4℃ and the supernatant was discarded. The pellet was washed once with 75% ethanol, resuspension using RNase-free water.

Table 4-1. Primers for Synthesis of dsRNA

Gene	**(5'-3') Primer sequence**
ds*gfp*-kit-F	GGATCCTAATACGACTCACTATAGGGATTAAGTTCAGCGTGTC
ds*gfp*-kit-R	GGATCCTAATACGACTCACTATAGGCTAGTGATTCACCTTGAT
ds*Egfr*-kit-F	GGATCCTAATACGACTCACTATAGGCACACCCAAGTATGCTCC
ds*Egfr*-kit-R	GGATCCTAATACGACTCACTATAGGGCTCATTGTCTTCACAGC
ds*Stmn4*-kit-F	GGATCCTAATACGACTCACTATAGGCACTAAGGAGGCTCTGGA
ds*Stmn4*-kit-R	GGATCCTAATACGACTCACTATAGGGGTTGCGCAGTTTCTCTT
ds*gfp-E. coli*-F	CGGAATTCGATTAAGTTCAGCGTGTCCG
ds*gfp-E. coli*-R	GGGGTACCCTAGTGATTCACCTTGATGC
ds*Egfr-E. coli*-F	CGGAATTCCACACCCAAGTATGCTCCCT
ds*Egfr-E. coli*-R	GGGGTACCGCTCATTGTCTTCACAGCCA
ds*Stmn4-E.*	CGGAATTCCACTAAGGAGGCTCTGGACG
ds*Stmn4-E.*	GGGGTACCGGTTGCGCAGTTTCTCTTTC

2.4 dsRNA treatment and bioassays

Mixed dsRNA with Star Polycation (SPc) complex (donated by Prof. Jie Shen and Prof. Shuo Yan from China Agricultural University) (Li et al. 2019) at 1:1 mass ratio in 1 mL RNase-free water (RNase-free water as blank control). After incubated for 15 min at RT, *S. frugiperda* neonates were treated with 3 g diet mixed with the SPc-dsRNA formulation. SPc-ds*egfp* was used as negative control. For one-step method, thirty larvae were collected after 48 h for reverse transcript quantitative PCR (qRT-PCR) and the rest of the treated larvae were transferred to artificial diet containing Cry1F. 15 g artificial diet were incorporated with 15 μg Cry1F (1 μg/g) (LC_{20}) and evenly packed into 24-well culture plates. One 2-day-old larva was placed in each well. Three replicates were performed for each treatment. The percentage of mortality was calculated after 7 days. For two-step method, mixed dsRNA with Star Polycation (SPc) complex at 1:1 mass ratio. After incubated for 15 min at room template, mixed SPc-dsRNA solution with artificial diet containing Cry1F (1 μg/g) and packed into 24-well culture plates. One 2-day-old larva was placed in each well, and three replicates were performed for each treatment. The mortality was counted after 7 days.

2.5 Reverse transcript quantitative PCR (RT-qPCR)

RNAi efficiency and gene expression were evaluated by RT-qPCR using primers described in Table 4-2. Thirty 2-day-old larvae were collected as a whole for RNAi efficiency in bioassay and for gene expression determination for each treatment. Total RNA was extracted from the

2-day-old larvae or midguts by using Total RNA Kit I (OMEGA Bio-tek, GA, USA). Five hundred ng RNA was used for reverse transcription by using HiScript III RT SuperMix (Vazyme, Nanjing, China). Twenty-fold dilution of cDNA was used as template for qPCR by using SYBR qPCR Master Mix (Vazyme, Nanjing, China) through QuantStudio 6 (Applied Biosystems, MA, USA). Relative gene expression was calculated in relation to a reference gene, *ecdysoneless* (*ECD*) (Salem et al. 2014), using the $2^{-\Delta\Delta}$ Ct method (Pfaffl and Hageleit 2001). Three replicates were performed, and three independent experiments were performed.
RT-qPCR was used to detect the expression levels of *SfEgfr* and *SfStmn4* gene at different periods of egg, larvae (1^{st}-6^{th} instar larvae), pupae and adults. The whole body was collected for further experiments. For spatial expression patterns, 7 tissue samples (head, cuticle, foregut, midgut, hindgut, fat body and hemolymph) were taken from 4^{th} instar larvae. Samples were collected for RNA extraction, cDNA synthesis and RT-qPCR detection. Each sample had three biological replicates, and each replicate contained 12 larvae.

Table 4-2. Primers for RT-qPCR

Gene	**(5'-3') Primer sequence**
q-*Ecd*-F	GCCGTATCCAAAGCATGACA
q-*Ecd*-R	TGGTGACGGCCAAAGGAA
q-*Egfr*-F	AGAGACCCGGGCAGATACTT
q-*Egfr*-R	AGGACCTTCCATTGCTGACG
q-*Stmn4*-F	TCGCGTACGAAGTGATCCTG
q-*Stmn4*-R	GACAGAGGGCGTCTTCTCAG

2.6 Western blot

Total protein was extracted from the midgut tissues of 12 4^{th} instar larvae using a protein extraction kit (OMEGA Bio-tek, GA, USA). The total protein concentration of the midgut samples was quantified using a BCA protein assay kit (Solarbio Life Sciences, Beijing, China). For each treatment, 35 μg of protein was separated by SDS-PAGE and transferred onto a PVDF membrane. After blocking with 1% non-fat milk in PBS (Sangon Biotech, Shanghai, China) at room temperature for 1 h, the PVDF membrane was incubated with one of the following primary antibodies: anti-β-actin (abclone, Wuhan, China) diluted 1:30,000, anti-histone H3 (abclone, Wuhan, China) diluted 1:3,000 or anti-phospho-histone H3 (abclone, Wuhan, China) diluted 1:1,000, in PBS containing 0.1% Tween-20 (PBST) for 4 hours. The membrane was washed three times with PBST, each wash lasting 5 min, and then incubated with the corresponding FITC-conjugated goat anti-rabbit secondary antibody (Solarbio Life Sciences, Beijing, China) diluted 1:1000 in PBST. Images were captured using a Typhoon 9410 scanner (GE Healthcare, USA).

2.7 Statistical analysis

All the experiments were repeated at least three times and the statistical analyses were performed using GraphPad Prism 7.0 software (GraphPad, San Diego, CA). Pairwise

comparisons were performed by Student's t-test. One-way analysis of variance (ANOVA) was used in comparing the multiple groups, and Tukey's test was used as a post-hoc test.

3 Results

3.1 Gene expression after treated with sublethal Cry1F protein

SfEgfr (Gene ID: 118264998) and *SfStmn4* (Gene ID: 118273070) genes, which have been previously reported in *Drosophila* and are associated with cell proliferation and cell cycle, were obtained from our larval transcriptome of *S. frugiperda*. The complete ORF sequence of *SfEgfr* and *SfStmn4* genes consisted of 4347 and 870 bp, encoding 1448 and 289 amino acid residues, with predicted molecular weights of 160.08 and 33.21 kDa.

Temporal expression analysis revealed that both *SfEgfr* and *SfStmn4* were significantly upregulated in response to treatment with Cry1F protein at a sublethal concentration (LC_{20}). Specifically, the expression levels of both genes began to increase after 12 hours of exposure to Cry1F. Between 12 and 24 hours, the expression levels continued to rise, reaching their peak at 24 hours. After 24 hours, the upregulation of *SfEgfr* showed a slight decline but remained close to a two-fold increase compared to the control. In contrast, *SfStmn4* maintained an upregulation level exceeding two-fold throughout the observed period (Figure 4-1).

These findings suggest that sublethal concentrations of Cry1F protein significantly induce the upregulation of *SfEgfr* and *SfStmn4*, highlighting their crucial roles in the defense mechanisms of *S. frugiperda* against Bt insecticidal proteins. The sustained upregulation of these genes, indicates their potential involvement in mediating cellular responses to Cry1F-induced stress, possibly through regulating cell proliferation and the cell cycle.

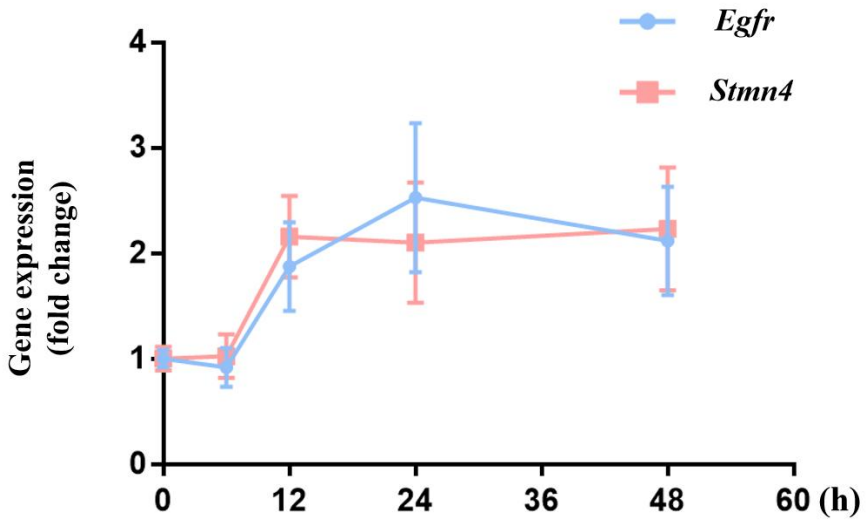

Figure 4-1. Temporal expression profiles of *SfEgfr* and *SfStmn4* genes determined by RT-qPCR in the midgut tissues of 4th instar *S. frugiperda* larvae treated with Cry1F (LC_{20}) for different time intervals (6, 12, 24 and 48 hours). The data represent the fold change in gene expression relative to the control. Three biological replicates and three independent experiments were performed. Error bars indicate the standard error of the mean (±SEM).

3.2 Spatio-temporal expression analysis of *SfEgfr* and *SfStmn4*

RT-qPCR was used to detect the expression levels of *SfEgfr* and *SfStmn4* across various different developmental stages and tissues in *S. frugiperda*. The developmental expression profiles revealed that both *SfEgfr* and *SfStmn4* were expressed at all developmental stages, with relatively similar expression patterns. Specifically, the expression of *SfEgfr* reached its peak in the 4th instar stage, reaching its highest expression level compared to other stages. Following this peak, its expression gradually declined during the 5th and 6th instar stages, as well as during the pupal and adult stages (both male and female). Similarly, *SfStmn4* also shows increased expression during larval stages, though its peak expression level is less pronounced compared to *SfEgfr*, and it follows a comparable declining trend in later stages (Figure 4-2A).

The tissue-specific expression profiles demonstrated that *SfEgfr* exhibits its highest expression in the cuticle and midgut, significantly higher than in the head, foregut, hindgut, fat body, and hemocytes. *SfStmn4* demonstrates relatively consistent expression across tissues, with its peak expression observed in the midgut, similar to *SfEgfr* (Figure 4-2B). Both genes exhibited the highest expression in the midgut, indicating their important role in this tissue.

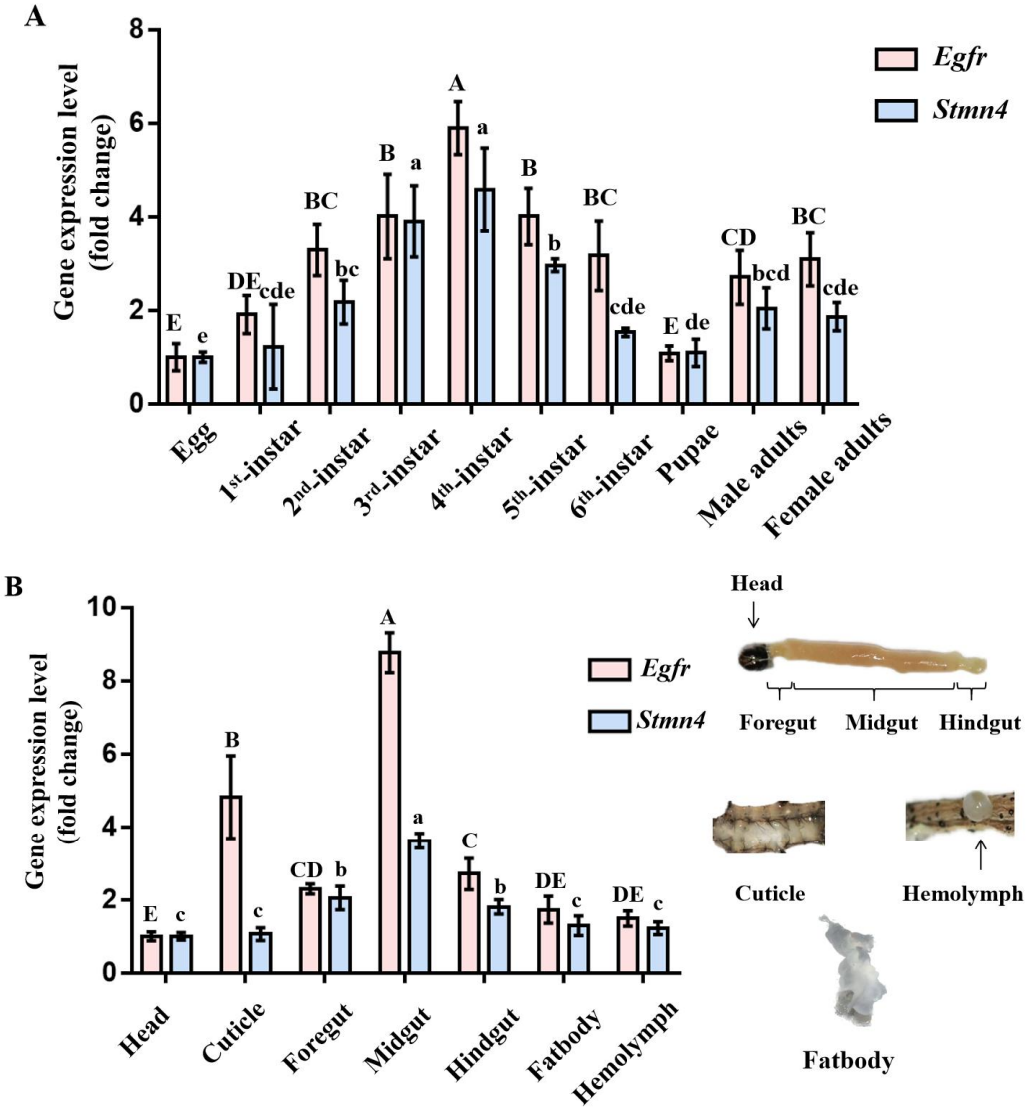

Figure 4-2. Relative expression levels of *SfEgfr* and *SfStmn4* across different developmental stages (A) and tissues (B) in *S. frugiperda*. Uppercase letters indicate significant differences in *SfEgfr* expression, and lowercase letters indicate significant differences in *SfStmn4* expression, based on one-way ANOVA followed by a least significant difference test.

3.3 Establishment of the optimal RNAi system based on oral-feeding dsRNA

To establish an efficient RNAi system for Lepidopteran insects based on oral-feeding dsRNA, we systematically compared the interference efficiency of different dsRNA synthesis methods, concentrations, and treatment durations. Initially, dsRNA was synthesized using three distinct approaches: (1) expressing dsRNA in *Escherichia coli*, (2) extracting dsRNA from *E. coli* that expressed dsRNA, and (3) *in vitro* synthesis dsRNA using T7 RiboMAX™ Express RNAi System kit. To enhance the stability and delivery efficiency of dsRNA, the synthesized dsRNA from each method was encapsulated using star-polycation complex (SPc) nanoparticles, with a control group lacking SPc encapsulation. In these experiments, a consistent dsRNA concentration of 25 μg/g was maintained, and the interference efficiency was assessed in the midgut tissues of *S. frugiperda* larvae after a 48-hour treatment period. The RT-qPCR results revealed that the interference efficiencies varied significantly depending on the synthesis method. The highest interference efficiency was achieved with *in vitro*-synthesized dsRNA, followed by dsRNA extracted from *E. coli*, and finally dsRNA expressed in *E. coli*. Notably, the encapsulation of dsRNA with SPc nanoparticles further enhanced the interference efficiency across all synthesis methods (Figure 4-3A).

Subsequently, we evaluated the impact of different treatment durations and dsRNA concentrations on interference efficiency using *in vitro*-synthesized dsRNA. The results demonstrated that the highest interference efficiency was achieved after a 48-hour treatment, outperforming both 24-hour and 72-hour treatments (Figure 4-3B). Furthermore, when comparing different dsRNA concentrations, both 50 μg/g and 25 μg/g treatments achieved approximately 80% interference efficiency. Considering the balance between interference efficacy and cost-effectiveness, 25 μg/g was identified as the optimal dsRNA concentration (Figure 4-3C).

In conclusion, the most effective RNAi strategy for Lepidopteran insects involves feeding 25 μg/g of SPc-encapsulated, *in vitro*-synthesized dsRNA for a duration of 48 hours. This approach not only maximizes gene silencing efficiency but also provides a cost-effective and practical solution for large-scale pest control applications.

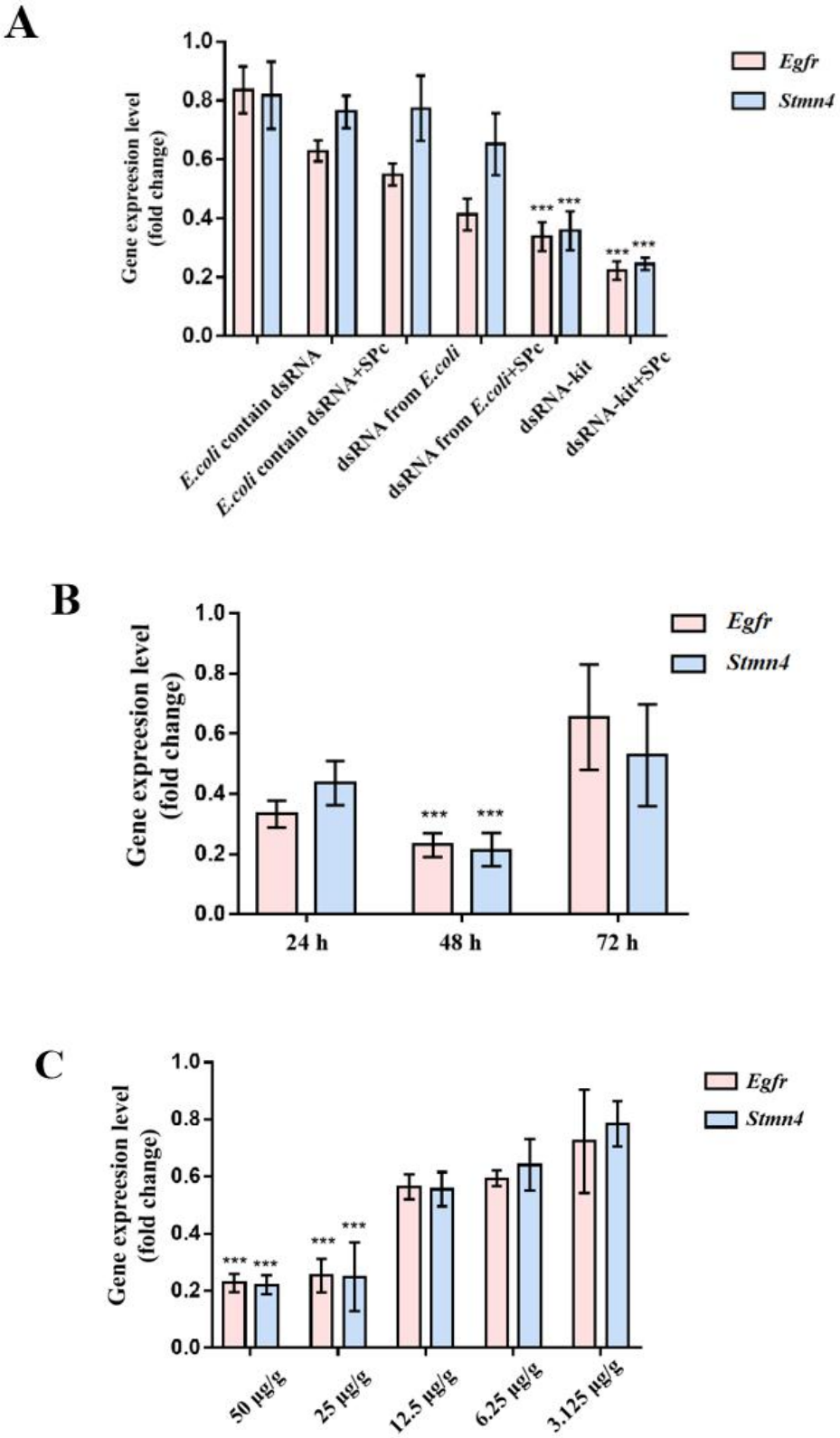

Figure 4-3. Relative expression levels of *SfEgfr* and *SfStmn4* after treatment with dsRNA synthesized by different methods (A), different treatment times (B) and different concentrations of dsRNA (C). Significant differences between the treatments and control were determined by Student's t-test (***: $P<0.001$).

3.4 Establishment of bioassay method for Bt insecticidal protein based on RNAi

To elucidate the functional roles of midgut genes in the defense mechanisms of lepidoptera insects against Bt insecticidal proteins and to enhance pest control strategies, we examined bioassay methods incorporating RNA interference. Specifically, we investigated the efficacy of two distinct approaches: (1) two-step method: feeding dsRNA followed by the introduction of Cry1F protein, and (2) one-step method, feeding a diet containing both dsRNA and Cry1F protein simultaneously.

Our findings revealed that the two-step approach, involving initial RNAi interference followed by Cry1F protein treatment, significantly enhanced the mortality rates. Specifically, the mortality rate increased from 23.3% to 66.7% and 56.6% after 7 days, representing increases of 43.4% and 33.3%, respectively. These results were statistically significant, as illustrated in Figure 4-4A. In contrast, the one-step method resulted in a more modest increase in mortality rates, from 15.0% to 41.6% and 33.3%, corresponding to increases of 26.6% and 18.3% (Figure 4-4B). Notably, only the silencing of the *SfEgfr* gene demonstrated a significant difference in mortality when using the one-step method, underscoring the superiority of the two-step approach for studying midgut functional genes involved in the defense against Bt insecticidal proteins in lepidoptera.

Furthermore, our experiments demonstrated that silencing the *SfEgfr* and *SfStmn4* genes significantly heightened the sensitivity of *S. frugiperda* larvae to the Cry1F protein. This observation highlights the critical roles these genes play in the insect's defensive response to Bt toxins, providing valuable insights for the development of more effective pest control measures.

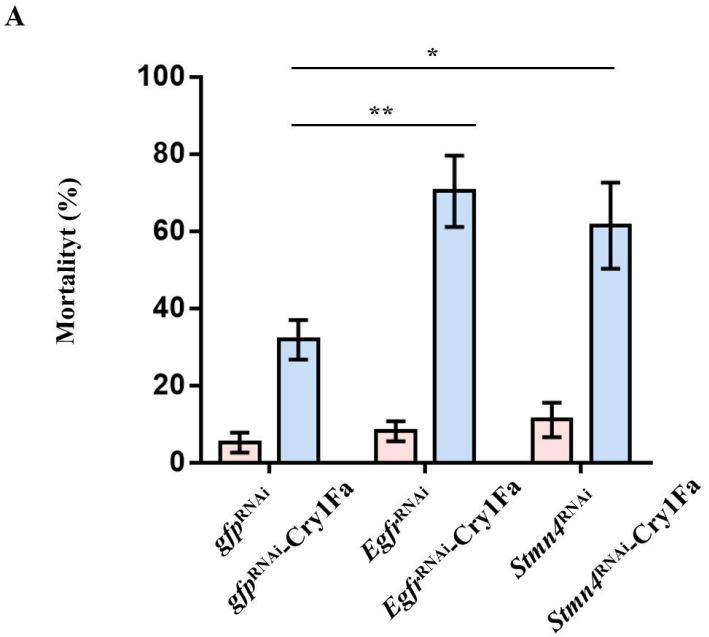

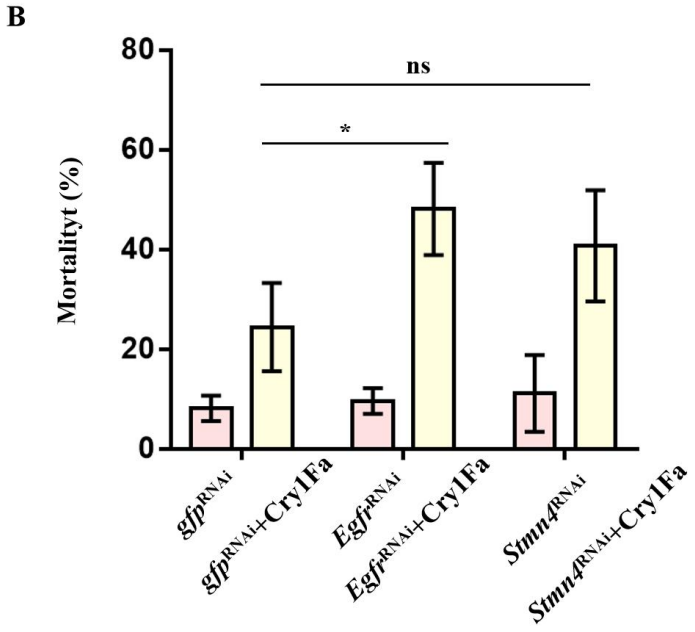

Figure 4-4. Insecticidal bioassay of Cry1F against fall armyworm larvae after treatment with dsRNA for 48 h (A) or treatment with diet containing dsRNA and Cry1F (B). Three replicates were performed. *P* values were calculated by two-sided Student's t-test (**: $P<0.01$; *: $P<0.05$; ns: $P>0.05$).

3.5 The roles of *SfEgfr* and *SfStmn4* in the defense of *S. frugiperda* midgut against Cry1F proteins

After 72 hours of exposure to a sublethal concentration (LC_{20}) of Cry1F, the treated larvae exhibited a noticeable reduction in body length compared to the control group that did not receive the protein treatment. This observation suggests that Cry1F impairs larval growth and development. Furthermore, when the genes *SfEgfr* and *SfStmn4* were silenced, the surviving larvae displayed even more pronounced stunting in body length, and their recovery process was significantly hindered. These findings indicate that *SfEgfr* and *SfStmn4* play crucial roles in the larvae's defense mechanisms against Cry1F, as their silencing exacerbated the detrimental effects of the toxin on larval growth (Figure 4-5A and B).

Histone H3, one of the five core histones, is a fundamental component of chromatin in eukaryotic cells, working in conjunction with other histones to regulate DNA packaging and gene expression. Phosphorylated histone H3 (PHH3), which peaks during the G2 and M phases of mitosis, serves as a reliable marker for mitotic activity, particularly in intestinal stem cells (ISCs) (Jiang et al., 2009). Western blot analysis revealed that exposure to Cry1F protein for 36 hours significantly increased the expression of PHH3, as detected by an anti-phospho-histone H3 antibody. This upregulation indicates that ISC proliferation was activated in response to the sublethal concentration of Cry1F, likely as a compensatory mechanism to repair midgut damage caused by the toxin. However, when *SfEgfr* and *SfStmn4* were silenced, the positive PHH3 signal was abolished, suggesting that the proliferation of ISCs was suppressed (Figure 4-5C). This suppression highlights the critical role of *SfEgfr* and *SfStmn4* in mediating the midgut's regenerative response to Cry1F-induced damage.

In summary, the results demonstrate that *SfEgfr* and *SfStmn4* are integral to the larvae's defense against Bt insecticidal proteins, particularly in facilitating midgut regeneration, *SfEgfr* or *SfStmn4* exert its defense function against Bt insecticidal proteins by affecting midgut regeneration

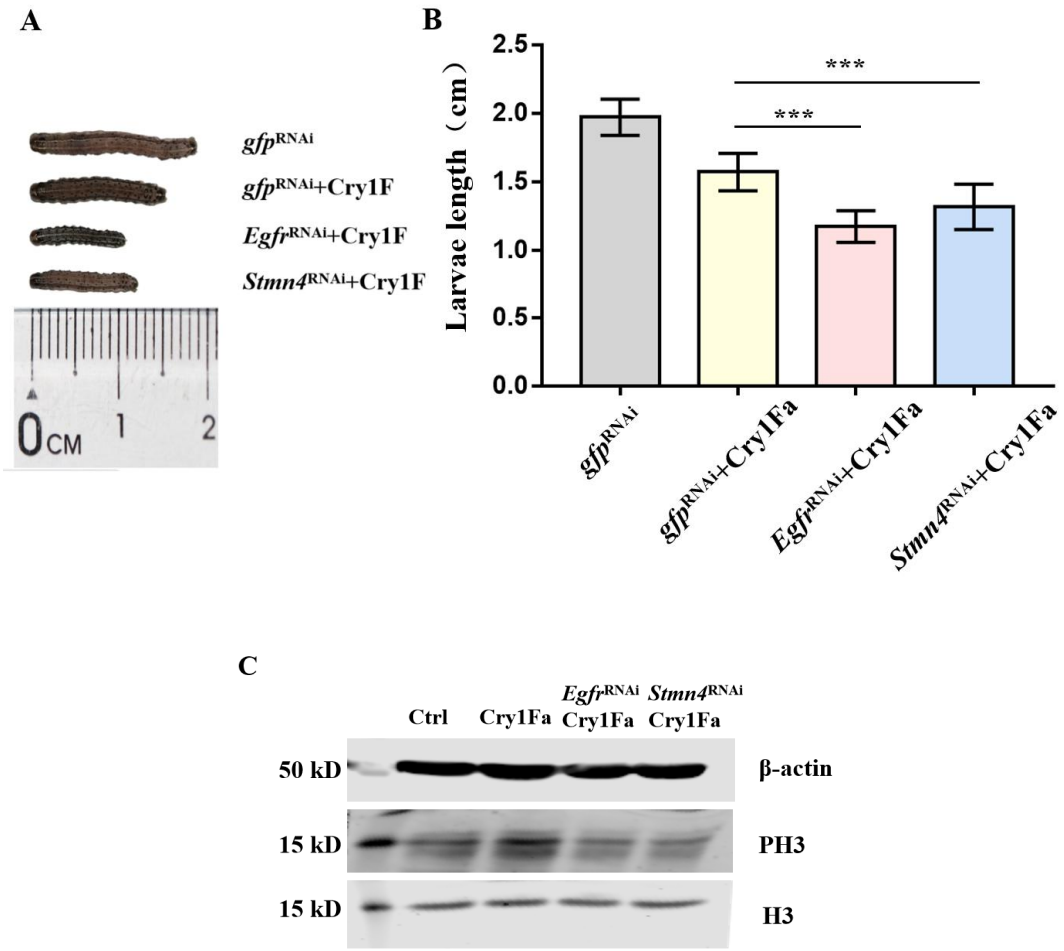

Figure 4-5. The roles of *SfEgfr* and *SfStmn4* in the defense of *S. frugiperda* midgut against Cry1F protein (A) Representative images from seventy-two 4th instar larvae treated with Cry1F (LC_{20}) for 72 h with or without silencing *SfEgfr* and *SfStmn4*. (B) Quantification of length from seventy-two 4th instar larvae treated with Cry1F (LC_{20}) for 72 h after treating with or without silencing *SfEgfr* and *SfStmn*. (C)Western blot detection of PH3 in midgut tissue samples from larvae of 4th instar fall armyworm after 36 h of Cry1F (LC_{20}) intoxication with or without dsRNA treatment. *P* values were calculated by one-way ANOVA and Tukey's test (***: $P<0.001$).

4 Discussion

The midgut epithelial cells of insects serve as a critical protective barrier, safeguarding the internal environment from external threats such as pathogenic microorganisms and insecticidal proteins. These cells play a pivotal role in defending against pathogens and toxins, ensuring the insect's survival in hostile environments. When *Bacillus thuringiensis* (Bt) and its insecticidal proteins target the midgut, the epithelial cells activate defensive responses to maintain structural integrity and mitigate damage caused by the toxins (Vega-Cabrera et al.

2014). These defense mechanisms not only influence the efficacy of Bt proteins but also contribute to the development of resistance in target pests. Therefore, understanding the molecular basis of midgut defense responses is essential for enhancing the insecticidal effects of Bt and delaying the emergence of resistance. However, the low efficiency of RNA interference (RNAi) in lepidopteran pests has hindered progress in this area, underscoring the urgent need for an efficient system to study midgut defense genes.

Oral delivery is a minimally invasive and potentially high-throughput RNAi delivery method that holds particular value for insects intolerant to injections and for the field application of RNAi-mediated pest control. The effectiveness of reaching the midgut epithelium with RNAi is influenced by various factors, including the method of dsRNA synthesis, intake concentration, processing time, and the gastrointestinal morphology and physiology, which may reduce the efficiency of RNAi in the midgut. The efficiency of RNA interference (RNAi) is primarily determined by the successful delivery and cellular uptake of intact double-stranded RNA (dsRNA). Therefore, strategies that effectively protect dsRNA molecules or enhance their cellular absorption hold significant potential for improving RNAi efficiency. Polymeric nanoparticles synthesized via wet chemical routes using natural or synthetic polymers have emerged as promising carriers due to their high stability, ease of surface modification, biodegradability, and environmental safety. These properties make them suitable for dsRNA encapsulation. In *Anopheles gambiae*, chitosan-based encapsulation of dsRNA has been shown to significantly enhance RNAi efficiency (Zhang et al., 2010). Subsequent studies have reported similar improvements in RNAi efficiency using chitosan-dsRNA complexes in other insect species, such as *Aedes aegypti* and *Ostrinia furnacalis* (He et al., 2013; Zhang et al., 2015). Moreover, other nanomaterials have also been explored for dsRNA delivery to improve RNAi outcomes. These include guanylated polymers for *Spodoptera exigua*, and branched amphiphilic peptide capsules (BAPCs) for *Myzus persicae* and *Tribolium castaneum* (Avila et al., 2018; Christians et al., 2018). Several additional polymeric materials show potential for nucleic acid encapsulation, such as dendrimers, polyethyleneimine (PEI), polyethylene glycol (PEG), poly-amino acids, and polyacrylates (Antimisiaris et al., 2017).

One particularly promising nanocarrier is the Star Polycation (SPc), a cationic dendritic macromolecule consisting of four peripheral amino acid-functionalized arms and densely packed tertiary amines (Li et al., 2019). SPc exhibits high gene transfection efficiency and can condense random nucleic acids into complexes readily taken up by cells through endocytosis (Yan et al., 2020). For future pest control, RNAi-based sprayable products could offer a practical and environmentally friendly alternative to chemical pesticides. Using such nanocarriers for dsRNA delivery via foliar spraying holds significant promise in advancing sustainable agriculture while providing substantial ecological and societal benefits (Yan et al., 2021).

To develop an efficient RNAi system for studying midgut defense genes in Lepidopteran pests, we first compared three different dsRNA synthesis methods: dsRNA synthesized in vitro using a kit, dsRNA expressed in *Escherichia coli*, and dsRNA extracted from *E. coli* that expressing dsRNA. We also evaluated the enhancing effects of nanomaterials on silencing efficiency (over 75%). The results showed that feeding dsRNA synthesized in vitro provided the best interference efficiency, which was further enhanced by SPc. Subsequently, we

compared the concentrations of dsRNA and feeding times, finding that 25 μg/g was the optimal concentration and 48 hours was the optimal duration for interference. In summary, we determined that using the nanomaterial SPc to encapsulate 25 μg/g dsRNA synthesized in vitro for a 48-hour treatment is the most effective strategy, significantly outperforming the current research in lepidoptera (Wan et al. 2021; Wang et al. 2016; Lin et al. 2023). This is a significant advancement in RNAi application for lepidoptera, addressing challenges posed by the hostile environment of the lepidopteran midgut that often reduces RNAi efficiency.

To investigate the defense genes against pore-forming proteins in lepidoptera pests, bioassays are necessary to test biological activity following the silencing of candidate genes. Currently, two bioassay methods are employed: one involves treatment with dsRNA followed by the addition of pore-forming proteins (Dutta, et al. 2023), and the other involves simultaneous treatment with dsRNA and pore-forming proteins (Pereira et al. 2024). We compared these two methods and found that the approach of interfering first then adding pore-forming proteins showed a greater increase in mortality. This could be due to additional time required for dsRNA uptake and gene silencing prior to toxin exposure the pore-forming proteins causing some degree of feeding deterrence, leading to lower intake of dsRNA and pore-forming proteins by the pests. Consequently, we established an effective research system for studying the defense against pore-forming proteins in the midgut of lepidoptera pests.

Using this system, we discovered that *SfEgfr* and *SfStmn4* are involved in the defense of *S. frugiperda* against Bt insecticidal proteins, and specifically, they function by affecting midgut regeneration, thereby confirming the reliability of this system.

In conclusion, we have successfully developed an efficient RNAi system for studying midgut defense genes in Lepidopteran pests and elucidated the roles of *SfEgfr* and *SfStmn4* in the defense against Bt toxins. This study not only advances our understanding of midgut defense mechanisms but also provides a novel theoretical framework for the biological management of lepidopteran pests. By integrating molecular insights with practical pest control strategies, our work contributes to the development of sustainable solutions for combating resistance to Bt toxins and improving agricultural productivity.

Chapter 5

Determination of the specific regulatory pathways of midgut defense Bt insecticidal proteins in Lepidopteran pests

Adapted from:

Wang, Z.,[#] Yang, Y.,[#] Li, S., Ma, W., Wang, K., Soberón, M., Shuo, Y., Frederic, F., Alejandra, B., & Zhang, J. (2024). JAK/STAT signaling regulated intestinal regeneration defends insect pests against pore-forming toxins produced by *Bacillus thuringiensis*. PLoS Pathogens, 20(1), e1011823.

Abstract

The midgut of lepidopteran larvae serves as a critical barrier against toxins, including pore-forming proteins (PFTs) produced by *Bacillus thuringiensis* (Bt). However, the molecular mechanisms of lepidopteran pests defense against Bt proteins remain poorly understood. In this study, we investigated the roles of the JNK and JAK/STAT signaling pathway in mediating midgut regeneration and defense against Bt insecticial proteins, in the striped stem borer (*Chilo suppressalis*) and fall armyworm (*Spodoptera frugiperda*). We found that sublethal concentrations of Cry9A protein activated JNK pathway. Silencing *Jnk* or inhibiting JNK pathwy activity enhanced the susceptibility of *C. suppressalis* larvae to Bt insecticidal proteins and exacerbated long-term epithelial damage, highlighting its role in tissue remodeling. Concurrently, the JAK/STAT pathway was upregulated during the recovery phase, driving intestinal stem cell (ISC) proliferation and differentiation to restore midgut integrity. RNAi-mediated silencing of *Stat92E* or inhibition of STAT phosphorylation suppressed midgut regeneration and increased larval susceptibility to Cry9A, underscoring the pathway's critical role in toxin resistance. Temporal expression analysis shows that *Jnk* activation precedes *Stat* upregulation and acts upstream of *Stat*, suggesting a regulatory cascade where JNK-mediated epithelial shedding triggers JAK/STAT activation to promote ISC-driven tissue repair. This indicates a coordinated interplay between JNK and JAK/STAT signaling in midgut regeneration. Leveraging these insights, we developed a novel nano-pesticide formulation combining Bt toxins with dsRNA targeting *Stat*, which significantly enhanced larval mortality and reduced crop damage in pot experiment. Our findings not only elucidate the molecular mechanisms of midgut regeneration and defense in lepidoptera but also provide a promising strategy for improving the efficacy of Bt-based pest control. This study highlights the potential of integrating RNAi with traditional biopesticides to combat pest resistance and promote sustainable agriculture.

***Keywords*:** *Bacillus thuringiensis*, JAK/STAT, JNK, *Chilo suppressalis*, midgut regeneration

1. Introduction

Bacillus thuringiensis (Bt) is the most successful bacterium used for pest control through microbial insecticides and genetically modified crops. Its insecticidal proteins form pores in the midgut, leading to the death of target larvae. However, the defense responses of target pests during this process remain unclear. These defense mechanisms can significantly limit the effectiveness of Bt-based pest control and even lead to resistance. Therefore, investigating the specific regulatory pathways of Bt insecticidal protein defense in pests, especially lepidopteran pests, can effectively enhance the insecticidal efficacy of Bt products.

The Janus tyrosine kinase/signal transducer and activator of transcription signaling pathway (JAK/STAT) has emerged as a major regulator of *Drosophila* midgut regeneration (Buchon et al., 2009a; Beebe et al., 2010; Lin et al., 2010; Liu et al., 2010; Zhang et al., 2022). The major substrates for JAK tyrosine phosphorylation are the STATs, which are able to bind to specific DNA sequences to activate transcription. The ligands for the JAK/STAT pathway, such as the cytokines-Unpaired Upd2 and Upd3, are transcriptionally induced in stressed or damaged ECs and EEs, promoting division of ISCs (Buchon et al., 2009a; Buchon et al., 2009b). In addition, it was shown that STAT signaling also promotes and is required for EC and EE differentiation (Beebe et al., 2010; Jiang et al., 2009). However, it is not clear whether the Upd ligands are needed for this function (Zhang et al., 2022). In *Drosophila* besides the JAK/STAT signaling pathways, the ISCs are also activated in stressed epithelium through c-Jun NH (2) terminal kinase (JNK) to promote their proliferation as stem cells (Jiang et al., 2009). JNK signaling affects both ISCs and differentiated ECs. In the ECs, JNK confers stress tolerance and promotes epithelial turnover by triggering apoptosis in the damaged ECs and compensatory ISC proliferation (Jiang et al., 2009; Herrera et al., 2019). The downstream effects of JNK signaling induce Upd3 expression in ECs, which mediates JAK/STAT-dependent proliferation in adjacent ISCs (Mundorf et al., 2019; Boumard and Bardin, 2021). JNK activation in damaged ECs can also kill these cells, potentiating midgut turnover (Herrera et al., 2019; Apidianakis et al., 2009). JNK activation in ISCs may have different functions, such as activating stress-responsive genes, protection from oxidative damage (Buchon et al., 2009a), stimulating proliferation (Buchon et al., 2009a; Biteau et al., 2008), and altering ISC differentiation by inducing Delta expression and/or promoting ISC symmetric divisions (Biteau et al., 2008; Hu et al., 2019; Rodriguez-Fernandez et al., 2020). Otherwise, early work on *Drosophila* revealed a central role for Delta/Notch signaling in directing the differentiation of ISC progeny (Micchelli et al., 2006; Ohlstein et al., 2006; Ohlstein et al., 2007; Bardin et al., 2010). High level Notch in enteroblasts (EBs) raised by Delta from ISCs, promotes EBs differentiated to ECs; low level Notch restricts cell cycle in ISCs (Boumard and Bardin, 2021). However, the potential participation of these pathways leading to midgut cell regeneration after Cry toxin intoxication in lepidopteran larvae, which are major pests of different crops, has not been analyzed.

In this work, we identified that the JNK/JAK/STAT is involved in regulating the midgut regeneration triggered by Bt PFTs pore formation in lepidopteran larvae. In addition, we showed that silencing JAK/STAT pathway by RNAi increased the toxicity of different PFT in two different lepidopteran species. Based on these findings, a novel and efficient formulation involving the mixture of Bt and ds*Stat* nano-pesticide was developed to control striped stem borer and fall armyworm larvae. This novel strategy for formulating Bt strains along with

dsRNA that repress the insect defense response could be used for the efficient control of certain crop pests that are not highly susceptible to Bt PFTs.

2. Materials and methods

2.1 Insect populations

Striped stem borer (*Chilo suppressalis*) obtained from Hubei Province in China was supplied by Shennong Inc. (Hubei, China). Fall armyworm (*Spodoptera frugiperda*) was maintained in our laboratory. Insects were fed as described above.

2.2 Protein expression and purification

The Cry9A and non-toxic Cry9A-D125R mutant proteins were expressed in *Escherichia coli*. Cry1F protein was expressed in Bt strain. The protein expression and purification process were described above.

2.3 Insecticidal bioassays

Bioassays to determine median lethal concentration values were performed on 2-day-old larvae, while additional mortality bioassays were performed on neonate larvae after two-day feeding with dsRNA by using diet incorporation assay according to previous description. For insecticidal mortality tests against striped stem borer, five gradient concentrations of Cry9A or its mutant protein in one mL were mixed thoroughly with 3-g artificial diet and transferred into flat glass tubes. Thirty-five larvae were placed inside each tube and three replicates were performed for each treatment. The mortality was calculated after 7 days. Lethal concentration of 20% larvae mortality (LC_{20}) and lethal concentration 2% larvae mortality (LC_2) was calculated by Probit analysis.

For insecticidal mortality assays against fall armyworm, a modified artificial diet based on soybean powders and wheat bran. In the bioassays, 15 g artificial diet were incorporated with 7.5 μg Cry1F (0.5 μg/g) or 15 μg Vip3Aa (1 μg/g) and evenly packed into 24-well culture plates. One 2-day-old larva was placed in each well. Three replicates were performed for each treatment. The percentage of mortality was calculated after 7 days.

2.4 RNA interference assays

The DNA templates for dsRNA were cloned from cDNA of larvae midguts (information about primers and the selected gene fragments of dsRNA are described in Table 5-1). The DNA was ligated into pEasy Blunt Zero vector (TransGen Biotech, Beijing, China). A 428-bp fragment of enhanced green fluorescent protein gene (*egfp*) was separately constructed. The different dsRNAs were synthesized from plasmid DNA using the T7 RiboMAX Express RNAi System (Promega, Madison, USA) according to the manufacturer's instructions. The concentration of synthetic dsRNA was determined by using NanoDrop (ThermoFisher Scientific, Oregon, USA). Mixed 75 μg dsRNA with Star Polycation (SPc) complex at 1:1 mass ratio in 1 mL nuclease-free water. After incubated for 15 min at RT, fifty striped stem borer or fall armyworm neonates were treated with 3 g diet mixed with the SPc-dsRNA formulation for 48 h. SPc-ds*egfp* was used as negative control. Fifteen larvae were collected

for reverse transcript quantitative PCR (qRT-PCR). Three repetitions were performed for each treatment.

Table 5-1. Primers for Synthesis of dsRNA

Gene	**(5'-3') Primer sequence**
ds*gfp*-F	GGATCCTAATACGACTCACTATAGGGATTAAGTTCAGCGTGTCCG
ds*gfp*-R	GGATCCTAATACGACTCACTATAGGCTAGTGATTCACCTTGATGC
ds*CsJnk*-F	GGATCCTAATACGACTCACTATAGGCATCGACCAGTGGAACAAGA
ds*CsJnk*-R	GGATCCTAATACGACTCACTATAGGCCTCCTGGTAGATGAGCTGC
ds*CsSocs*-F	GGATCCTAATACGACTCACTATAGGAACGATACGTAGCATTCGGG
ds*CsSocs*-R	GGATCCTAATACGACTCACTATAGGGTCCGTACTTGCGAAACGAT
ds*Cspuc*-F	GGATCCTAATACGACTCACTATAGGAGAGGCAGCTGCAAGAGTTC
ds*Cspuc*-R	GGATCCTAATACGACTCACTATAGGATACTGTGGAGGCGGTTGAC
ds*CsStat*-F	GGATCCTAATACGACTCACTATAGGATCATTGATTAAGGCAGCCG
ds*CsStat*-R	GGATCCTAATACGACTCACTATAGGGCAAACTCTCCTGTGGAAGC
ds*CsEgfr*-F	GGATCCTAATACGACTCACTATAGGGCGAAACACACTACCGGAAT
ds*CsEgfr*-R	GGATCCTAATACGACTCACTATAGGTGGCAATTTTCAGGTCCTTC
ds*SfStat*-F	GGATCCTAATACGACTCACTATAGGCCCTGTGGTGTGATCATCTG
ds*SfStat*-R	GGATCCTAATACGACTCACTATAGGGCATTTCGTTTTCGGGTTTA

2.5 RT-qPCR

RNAi efficiency and gene expression were evaluated by RT-qPCR using primers described in Table 5-2. Thirty 2-day-old larvae or fifteen midguts from third-instar larvae were collected together and mixed in a single sample for analysis of RNAi efficiency and for gene expression determination for each treatment. Total RNA was extracted from the samples by using Total RNA Kit I (OMEGA Bio-tek, GA, USA). Five hundred ng RNA was used for reverse transcription by using HiScript III RT SuperMix (Vazyme, Nanjing, China). Twenty-fold dilution of cDNA was used as template for qPCR by using SYBR qPCR Master Mix (Vazyme, Nanjing, China) through QuantStudio 6 (Applied Biosystems, MA, USA). Relative gene expression was calculated in relation to a reference gene, *elongation factor-1* (*EF-1*) for striped stem borer and *ecdysoneless* (*ECD*) for fall armyworm larvae, using the $2^{-\Delta\Delta}$ Ct method. Three replicates and three independent experiments were performed.

Table 5-2. Primers for RT-qPCR

Gene	**(5'-3') Primer sequence**
q-*CsEF-1*-F	TGAACCCCCATACAGCGAATCC

q-*CsEF-1*-R	TCTCCGTGCCAACCAGAAATAGG
q-*CsJnk*-F	TGTACCAGATGCTATGCGGC
q-*CsJnk*-R	CACCACTATGTTGGACGGCT
q-*CsSocs*-F	GCATAGAGCACTACCGGCAT
q-*CsSocs*-R	CGCTGGGTCCTTGTAATGGT
q-*Cspuc*-F	TTACCTGTGCATCATGGCGT
q-*Cspuc*-R	TGCTGCATGGATGAAGTCGT
q-*CsStat*-F	AAACTGAACGTGCTGGTTGC
q-*CsStat*-R	GATAAGCTCTTCGTCCAACA
q-*CsEgfr*-F	GCGAGGTGACCGGCTATTTA
q-*CsEgfr*-R	TTTCCACAACTTGGCGTCCT
q-*CsDelta*-F	CTCGCTCATAGTCGAAGCGT
q-*CsDelta*-R	CGTCGGCTATGCTCTGCTTA
q-*SfEcd*-F	GCCGTATCCAAAGCATGACA
q-*SfEcd*-R	TGGTGACGGCCAAAGGAA
q-*SfStat*-F	TGTGAAACCCGTGTTGGTGA
q-*SfStat*-R	ATCAGTTTGGGCCGGTGTAG

2.6 Intestinal thickness and cell number determination

The midgut tissues from third instar larvae that survived were dissected after feeding with 200 μg Cry9A protein per g of diet for different times (1.5–120 h) and fixed overnight in 4% paraformaldehyde at 4°C. These midgut tissues were carefully washed three times with PBS and labeled with 1:1000 Phalloidin-iFluor 647 (Abcam, Cambridge, UK) for 1 h at room temperature (RT). After washed twice with PBS, the tissues were labeled with 10 μg/ml Hoechst33342 (Solarbio Life Sciences, Beijing, China) final concentration in PBS for 5 min. The tissues were sealed with Prolong Diamond Antifade (Invitrogen, Oregon, USA) on microscopic slides after washing three times with PBS. Images were obtained using 20X objective in the confocal LSM 980 (Zeiss, Germany). Six guts were used for each treatment and six images were taken from each midgut. The intestinal thickness measurements were based on the data of the cytoskeleton stained with Phalloidin-iFluor 647 by using ImageJ software in a total of 36 images. Midgut cell numbers were counted based on number of nuclei stained with Hoechst33342 and then dividing by the gut length as the number of nuclei per μm area. Three replicates were performed for each treatment.

2.7 Immunofluorescence microscopy

Six midgut tissues for each treatment were dissected from the larvae and fixed in 4 % paraformaldehyde overnight at 4 ℃. After washed three times with PBS, they were carefully permeabilized with 2 % Triton X-100 in PBS for 2 h at room temperature. Primary antibodies

were added and incubated for 2 h at room temperature, their concentrations were as follows: anti-Phospho-Histone H3 antibody 1:50 dilution (Abclonal Technology, China). After washing with PBS for three times and 5 min for each time, a secondary goat anti-rabbit-FITC antibody (1:100 dilution) (Solarbio Life Sciences, Beigjing, China) was added and incubated at RT for 2 h (Qin et al., 2018). After washing with PBS for three times and 5 min for each time, the midgut tissues were labeled with phalloidin-iFluor 647 and Hoechst33342 as describe above. Images were obtained using confocal LSM 980 microscope. Measurements of fluorescence intensity were done by using Image J software.

2.8 Western blot

Total protein of fifteen midgut tissues obtained from larvae was extracted by using Protein Kit (OMEGA Bio-tek, GA, USA). The amount of total protein from midgut samples was quantified using a BCA kit (Solarbio Life Sciences, Beigjing, China). Then 35 μg protein for each treatment were resolved on SDS-PAGE gels and electrotransferred to PVDF filters. After blocking in 1% non-protein blocking solution (Sangon Biotech, Shanghai, China) for 40 min at RT, the PVDF filters were incubated for 4 h with one of the following primary antibodies anti-β-actin (ABclonal Technology, Wuhan, China) at 1: 30000 dilution, anti-Histone H3 (ABclonal Technology, Wuhan, China) at 1: 3000 dilution and anti-Phospho-Histone H3 (ABclonal Technology, Wuhan, China) at 1:1000 dilution in PBS containing 0.1% Tween-20 (PBST). After washing with PBST three times for 10 min each, the PVDF filters were incubated with corresponding secondary Goat anti-rabbit antibody labelled with FITC (Solarbio Life Sciences, Beigjing, China) in PBST at 1:1000 dilution for 1 h at RT. Images were obtained with a Typhoon 9410 scanner (GE Healthcare, USA) and analyzed with Image J software.

2.9 Pot experiment

Two rice seedlings (*Oryza sativa* L.) at four-leaf stage per pot were utilized for spraying assay. Five mL formulation containing $1.8x10^9$ cfu Bt serovar *fukuokaensis* strain with *cry9A* gene preserved in our laboratory mixed with 60 μg dsRNA samples embedded in SPc at 1:1 mass ratio as previously reported were sprayed on the seedlings. After 1 h, six second-instar striped stem borer larvae were placed on each plant. Two pots were used for each treatment. Three replicates were performed. We analyzed wormholes and dead insects daily, and calculated the plant heights on the seventh day.

2.10 Statistical analysis

All the experiments were repeated at least three times and the statistical analyses were performed using Graphpad Prism 7.0 software (Graphpad, San Diego, CA). Pairwise comparisons were performed by Student's t-test. One-way analysis of variance (ANOVA) was used in comparing the multiple groups, and Tukey's test was used as a post-hoc test (percentages via log transformation).

3. Results

3.1 Analysis of the role of JAK/STAT in *C. suppressalis* against Cry9A protein

3.1.1 Analysis of the activation of JAK/STAT pathway after Cry9A treatment

The JAK/STAT pathway is a conserved signaling pathway in *D. melanogaster*. It was shown that JAK kinase promotes the translocation of a STAT3-like transcription factor (STAT92E) into the nucleus for regulating transcriptional targets such as *Socs36E* (Herrera et al., 2019). In the present study, we analyzed the expression levels of *Stat92E* and *Socs36E* in the midgut tissue of *C. suppressalis* larvae following exposure to Cry9A protein to determine the potential involvement of the JAK/STAT pathway in toxin response.

The results indicate that after feeding on a sublethal concentration (LC_{20}, 200 μg/g) of Cry9A for 6 h, there were no significant changes in the expression levels of either *Stat* or *Socs* ($P>0.05$). However, after a 48 h recovery period, the expression of both genes was significantly upregulated ($P<0.01$ for *Stat* and $P<0.001$ for *Socs*), as shown in Figure 5-1. This suggests that the JAK/STAT pathway may play a role in the late-stage recovery process following Cry9A protein exposure, although the specific mechanisms involved require further investigation.

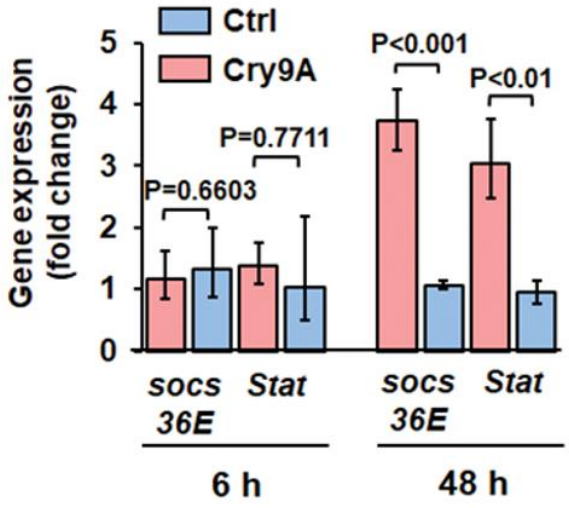

Figure 5-1. JAK/STAT pathway gene expression in the intestine from 15 larvae of striped stem borer after treatment with Cry9A (LC_{20}) for different times (6 and 48 h) determined by RT-qPCR. Control (Ctrl) were larvae treated with non-toxic Cry9A-D125R. The data were normalized to control on biological triplicate samples. Three independent experiments were performed. *P* values were calculated by two-sided Student's t-test, $P<0.01$ shows statistically significant differences. $P>0.05$ shows no significant difference. The error bar represents ±SEM.

3.1.2 Bioassays after silencing JAK/STAT pathway genes or adding inhibitor

To investigate whether the JAK/STAT signaling pathway mediates *C. suppressalis* defense mechanisms against Bt insecticidal proteins, we performed bioassays after silencing *Stat* and

Socs by RNAi (Figure 5-2A). Furthermore, we employed STAT inhibition nifuroxazide, an inhibitor that represses the constitutive phosphorylation of STAT (Nelson et al., 2008), to assess its potential role in modulating the sensitivity of *C. suppressalis* larvae to Bt insecticidal proteins (Figure 5-2B).

RNAi was used to silence *Stat* and *Socs* expression in *C. suppressalis* larvae, as shown in Figure 5-2A, larvae subjected to *Stat* or *Socs* knockdown exhibited significantly increased mortality following Cry9A treatment compared to the control group (P<0.0001) (Figure 5-2A). This suggests that both genes are involved in the protective response against Cry9A-induced toxicity.

Furthermore, pharmacological inhibition of STAT signaling using nifuroxazide, a well-characterized STAT inhibitor, resulted in a significant increase in larval mortality upon Cry9A exposure compared to larvae that untreated with inhibition (P<0.001) (Figure 5-5B). These findings collectively indicate that the JAK/STAT pathway plays a crucial role in defense mechanism of *C. suppressalis* larvae against Bt insecticidal proteins.

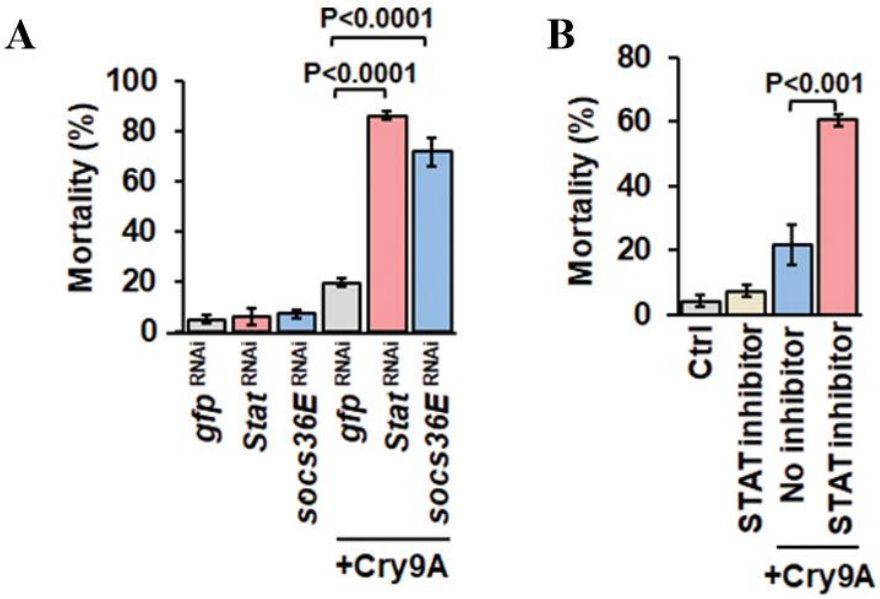

Figure 5-2. Bioassays after silencing JAK/STAT pathway genes or adding inhibitor. (A) Insecticidal toxicity assay of Cry9A against neonate larvae of striped stem borer after silencing JAK/STAT pathway genes (*Stat* and *Socs* genes) by RNAi for 48 h. Thirty-five neonates were analyzed with each treatment. Three replicates were performed. P<0.0001 shows statistically significant difference (two-sided Student's t-test). The error bar represents ±SEM. (B) Insecticidal toxicity assay of Cry9A against neonates of striped stem borer after treatment with JAK/STAT pathway inhibitor Nifuroxazide for 48 h. Thirty-five neonates were analyzed with each treatment. Three replicates were performed. P<0.001 shows statistically significant difference (two-sided Student's t-test). The error bar represents ±SEM. Control (Ctrl) were larvae treated with non-toxic Cry9A-D125R. The error bar represents ±SEM

3.1.3 Changes in midgut tissue morphology after silencing JAK/STAT pathway genes or adding inhibitor

To elucidate the specific role of the JAK/STAT pathway in *C. suppressalis*' defense against Bt insecticidal proteins, we employed RNAi-mediated *Stat* knockdown and pharmacological

inhibitors nifuroxazide followed by morphological analysis of Cry9A-treated midgut tissues. Initial observations revealed that neither *Stat* silencing nor nifuroxazide treatment affected the primary epithelial response to Cry9A intoxication. At 48 hours post-exposure, both *Stat*-RNAi and inhibitor-treated larvae exhibited comparable midgut epithelial thickness and cellularity to those receiving Cry9A alone, indicating that knockdown of STAT or JAK/STAT pathway blockade does not directly modulate Cry9A-induced primary epithelial damage.

Notably, during later recovery phases (72-96 h), control larvae demonstrated progressive restoration of midgut architecture, evidenced by increasing epithelial thickness and cellular repopulation. In stark contrast, both knockdown of *Stat* and pharmacological inhibition of JAK/STAT signaling significantly attenuated these midgut regenerative processes (Figure 5-3). These findings establish that while JAK/STAT inhibition doesn't prevent the initial cytotoxic effects of Cry9A, this pathway plays an indispensable role in facilitating post-injury midgut recovery.

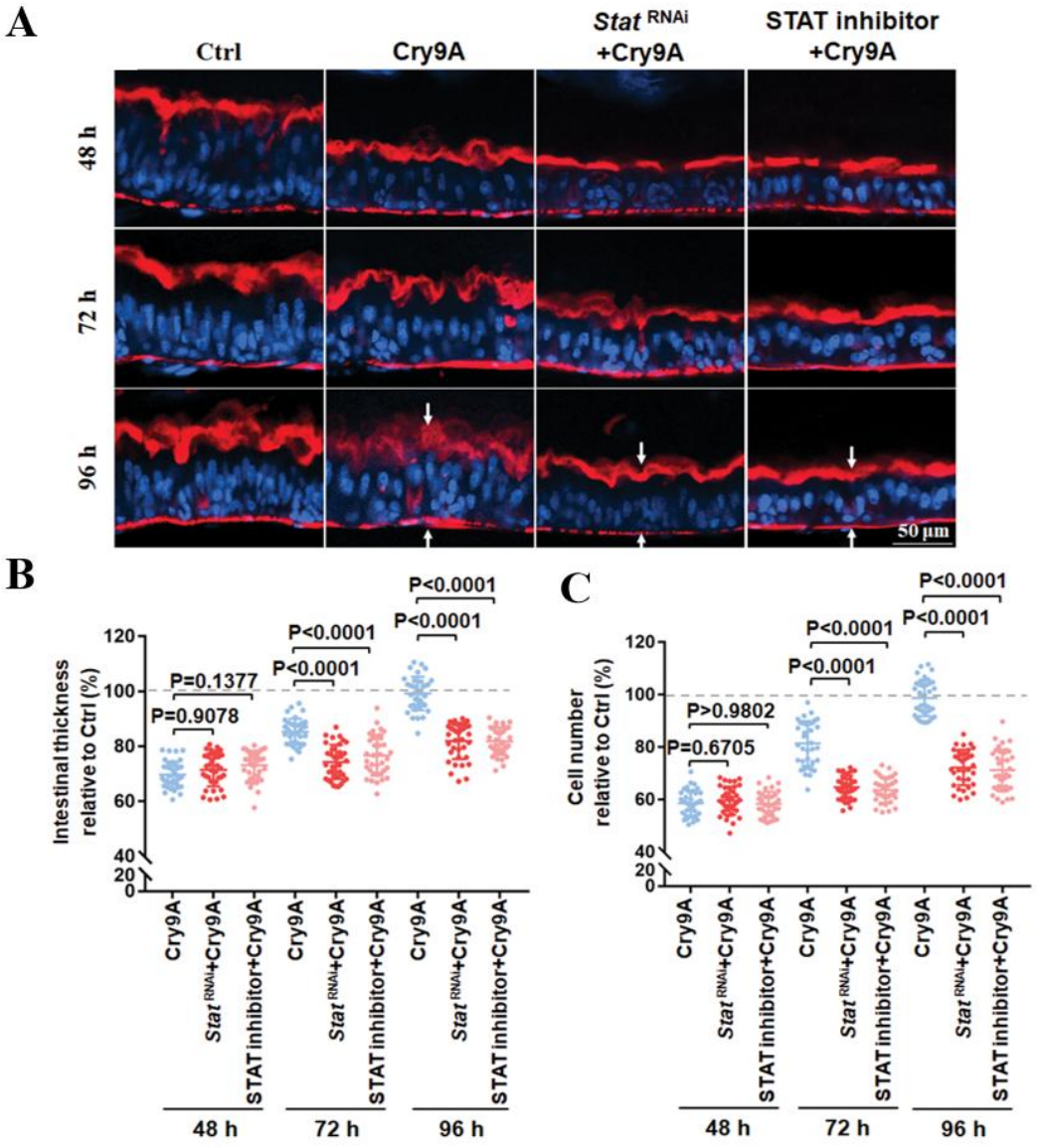

Figure 5-3. Changes in midgut tissue morphology after silencing JAK/STAT pathway genes or adding inhibitor. (A) Sagittal view representative images of larvae midgut tissues isolated from larvae treated with Cry9A with or without *Stat* dsRNA or nifuroxazide treatment observed in the LSCM. Hoechst33342 (blue color) labels nuclei. Phalloidin-647 (red color) labels F-actin. Control (Ctrl) were larvae treated with non-toxic Cry9A-D125R. (B and C) Quantification of the fluorescent signal of intestinal thickness (B) and cell number (C). Control (Ctrl) are midguts treated with the non-toxic Cry9A-D125R mutant. Toxin-free treated intestine was measured as 100%. n=36 images per treatment. P values were calculated by two-sided Student's t-test, P<0.0001 shows statistically significant differences. P>0.05 shows no significant difference. The large bar corresponds to the mean, whereas the smaller ones represent ±SEM.

3.2 Analysis of the role of JNK in *C. suppressalis* against Cry9A protein

3.2.1 Analysis of the activation of JNK and EGFR pathway after Cry9A treatment

It was previously shown that JNK pathway, a mitogen activated MAPK-type kinase cascade, is activated in response to cellular stress and is also involved in compensatory cell proliferation following injury of *Drosophila* intestine (Mundorf et al., 2019; Zhang et al., 2022; Boumard and Bardin, 2021). In *Drosophila*, the *puckered* (*puc*) gene encodes a Jun N-terminal kinase phosphatase which is a potent target downstream of JNK signaling (Martín-Blanco et al., 1998).

To determine whether the JNK signaling pathway is involved in the defense mechanisms of *C. suppressalis* against Bt insecticidal proteins, we first analyzed the expression levels of *Jnk* and *puc* in the midgut tissue of *C. suppressalis* larvae following exposure to Cry9A protein. The results showed that both *Jnk* and *puc* genes were upregulated in midgut tissue of the larvae after 6 h treatment with of Cry9A and the expression levels of both genes were reduced to similar levels found in the control larvae after 48 h (Figure 5-4), indicating that JNK may participate in the midgut defense response at an early stage.

In addition, it was previously shown that upon midgut epithelial damage or stress, multiple EGFR ligands and rhomboids are induced, leading to the activation of EGFR signaling in ISCs. This activation promotes ISC division and facilitates epithelial regeneration, ensuring tissue homeostasis((Jiang et al., 2011). To comprehensively evaluate the involvement of EGFR signaling in the insect's response to Bt insecticidal proteins, we conducted RT-qPCR analyses to measure the transcriptional alterations of key EGFR pathway genes after Cry9A (LC_{20}) treatment. Consistently, *Egfr* expression was markedly upregulated at 6 h post-treatment but normalized to control levels by 48 h, implying its functional involvement in *C. suppressalis* defence against Bt insecticidal proteins (Figure 5-4).

Overall, these data support that JNK and EGFR pathway may play crucial role in the defense mechanism of *C. suppressalis* against Cry9A protein.

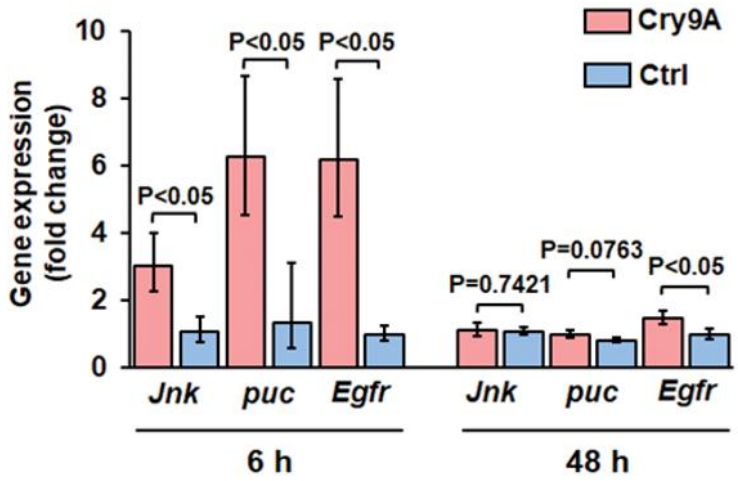

Figure 5-4. Analysis of the activation of JNK and EGFR pathway after Cry9A treatment. *Jnk*, *puc* and *Egfr* genes expression in the intestine from fifteen 3rd instar larvae of striped stem borer after treatment with Cry9Aa (LC_{20}) for different times determined by RT-qPCR. Control (Ctrl) were larvae treated with non-toxic Cry9A-D125R. The data were normalized to uninfected control and *EF-1* gene was used as reference gene. The data were from triplicate biological samples performed in three independent experiments. *P* values were calculated by two-sided Student's t-test, $P<0.05$ shows significant difference. $P>0.05$ shows no significant difference. The error bar represents ±SEM.

3.2.2 Bioassays after silencing JNK and EGFR pathway genes

Previous results demonstrated that the Cry9Aa protein (LC_{20}) can induce significant upregulation of key genes in both JNK and EGFR pathways during early treatment. To further elucidate the specific roles of these pathways in *C. suppressalis* defense against Bt insecticidal proteins, we conducted bioassays following RNAi-mediated knockdown of *Jnk* and *Egfr*. The results showed that silencing *Jnk* by using dsRNA incorporated into SPc nanoparticles, increased the mortality of the larvae to Cry9A toxin treatment (Figure 5-5), indicating that JNK pathway participates in the defense response to Cry9Aa action. However, RNAi silencing of *Egfr* did not modify the larval mortality to Cry9Aa, although up-regulation of *Egfr* gene expression was observed at early stage (6 h) of Cry9Aa intoxication.

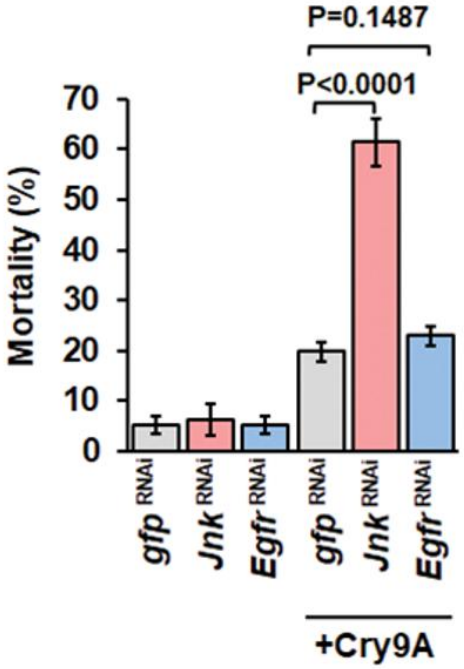

Figure 5-5. Bioassays after silencing JNK and EGFR pathway genes. Insecticidal toxicity assay of Cry9Aa against neonate larvae of striped stem borer after silencing JAK/STAT pathway genes (*Jnk* and *Egfr*) by RNAi. Thirty-five neonates were analyzed with each treatment. Silencing *gfp* was used as negative control. Three replicates were performed. $P<0.001$ shows statistically significant difference (one-way ANOVA and Tukey's test). The error bar represents ±SEM.

3.2.3 Bioassays after adding JNK inhibitor

Furthermore, we employed SP600125 (an anthrapyrazole inhibitor of JNK inhibitor) (Bennett et al., 2001), to assess its potential role in modulating the sensitivity of *C. suppressalis* larvae to Bt insecticidal proteins (Figure 5-6). The results demonstrated that repression of JNK activity with the SP600125 increased larval mortality under Cry9Aa toxin treatment, further confirming the critical role of the JNK pathway.

In summary, our results indicate that JNK signaling pathway, instead of EGFR pathway, is involved in the defensive response of *C. suppressalis* larvae against Bt insecticidal proteins.

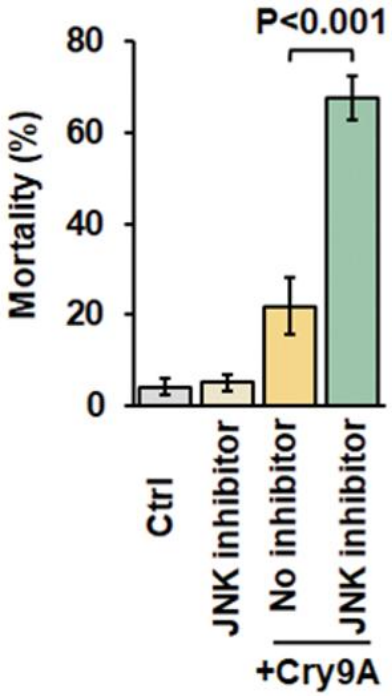

Figure 5-6. Bioassays after adding JNK inhibitor. Insecticidal toxicity assay of Cry9Aa (LC_{20}) against neonates of striped stem borer after treatment with JNK pathway inhibitor SP600125. Thirty-five neonates were analyzed with each treatment. Three replicates were performed. $P<0.001$ shows statistically significant difference (two-sided Student's t-test). The error bar represents ±SEM. Control (Ctrl) were larvae treated with non-toxic Cry9A-D125R.

3.2.4 Changes in midgut tissue morphology after silencing *Jnk* or adding inhibitor

To analyze the role of JNK pathway in the defense of Cry9A protein of *C. suppressalis*, we treated third-instar larvae with dsRNA (encapsulated with SPc) or the JNK inhibitor SP600125 for 48 hours. After this pretreatment, the larvae were transferred to a diet containing LC_{20} Cry9A. At various time points post-treatment, the midgut tissues were dissected and observed to assess the effects of Cry9A exposure on midgut morphology and cellular responses.

Analysis of midgut morphology after treatment with Cry9A showed that knockdown of *Jnk* by RNAi, as well as the addition of the JNK inhibitor SP600125, did not affect the initial response of the midgut epithelial tissue to Cry9A treatment. Specifically, at 48 hours post-treatment, both intestinal thickness and cell number in the midgut tissue of larvae subjected to *Jnk* RNAi or SP600125 treatment remained comparable to those treated with Cry9A alone. These findings suggest that neither *Jnk* depletion nor JNK inhibition has an immediate impact on Cry9A-induced damage in the midgut epithelium.

However, at later time points (72 and 96 hours post-treatment), significant differences were observed. In larvae treated with Cry9A alone, the intestinal thickness of the midgut gradually increases, and the number of cells significantly rises, indicating that the midgut is recovering. In contrast, both *Jnk* knockdown and JNK inhibition significantly mitigated these effects, as reflected by the intestinal thickness and cell number compared to Cry9A treatment alone (Figure 5-7). These results indicate that while JNK pathway does not prevent the initial midgut response to Cry9A intoxication, it plays a critical role in limiting long-term epithelial

damage, likely by interfering with pathways involved in midgut regeneration and tissue homeostasis.

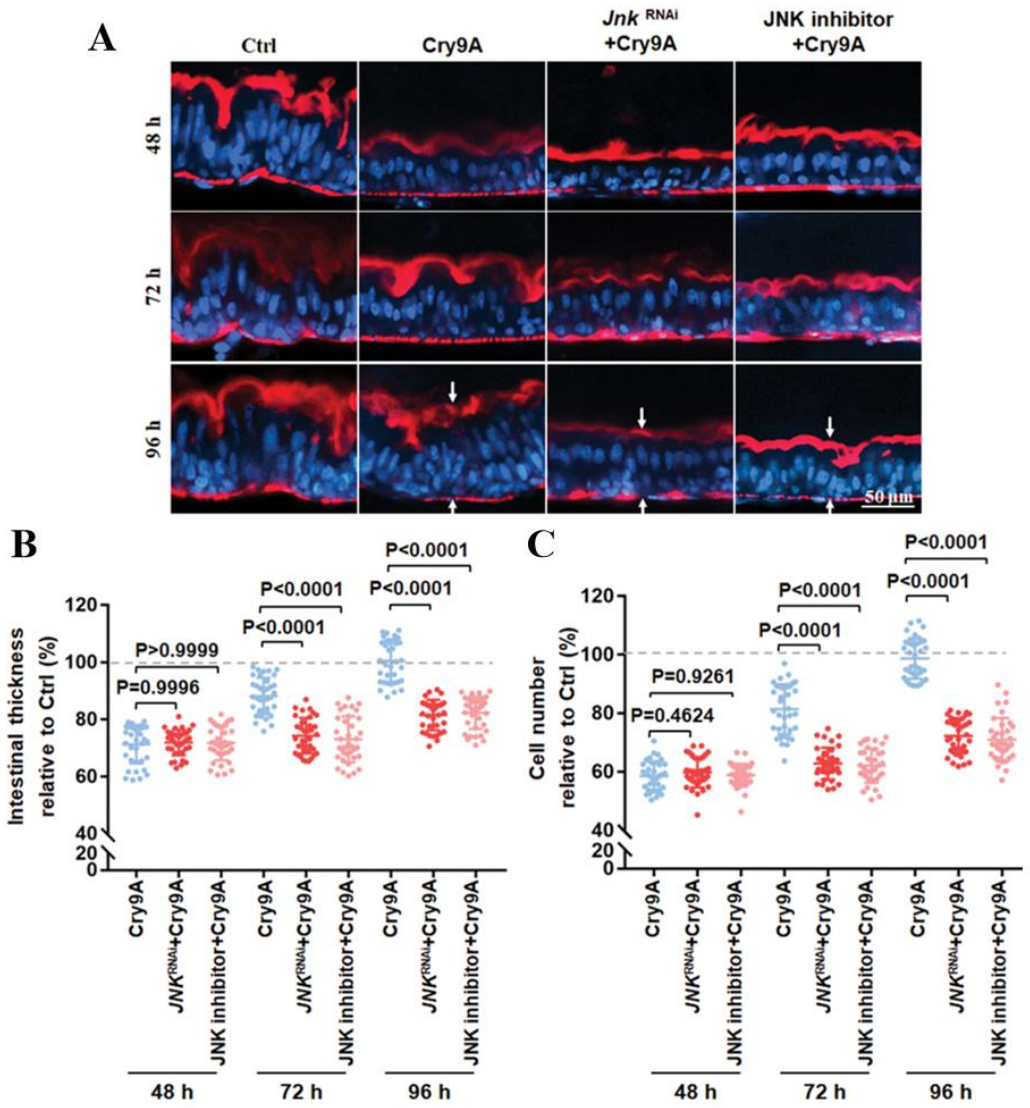

Figure 5-7. Changes in midgut tissue morphology after silencing *Jnk* or adding inhibitor. (A) Sagittal view representative images of midgut tissues isolated from 3rd instar alive striped stem borer larvae treated with Cry9Aa (LC_{20}) with or without *Jnk* dsRNA or SP600125 inhibitor treatment observed in the LSCM. Hoechst33342 (blue color) labels nuclei. Phalloidin-647 (red color) stains F-actin present in the brush border (upper arrows) and in the visceral muscles (lower arrows). Control (Ctrl) were larvae treated with non-toxic Cry9A-D125R. (B and C) Quantification of the fluorescent signal of intestinal thickness (B) and cell number (C) obtained after Cry9Aa (LC_{20}) with or without *Jnk* dsRNA or SP600125 inhibitor treatment. Control (Ctrl) are midguts treated with the non-toxic Cry9A-D125R mutant. Toxin-free treated intestine was measured as 100%. n = 36 images per treatment. P values were calculated by one-way ANOVA and Tukey's test, $P<0.0001$ shows statistically significant differences. $P>0.05$ shows no significant difference. The large bar corresponds to the mean, whereas the smaller ones represent ±SEM.

3.3 Analysis of the relationship between JNK and JAK/STAT in *C. suppressalis* against Cry9A protein

3.3.1 Analysis of the upstream and downstream relationship between JNK and JAK/STAT

JNK and the JAK/STAT pathway exhibit similar roles in the defense response of *C. suppressalis* against Bt insecticidal proteins. To investigate potential cross-regulation between JNK and JAK/STAT pathways in *C. suppressalis*' defense against Bt toxins, we conducted a comparative analysis of their expression patterns.

The results showed that *Jnk* was up-regulated in 3rd instar larvae of striped stem borer after 1.5 h of LC_{20} (200 μg/g) Cry9A ingestion and reached its highest expression value after 12 h (Figure 5-8A). The expression of *Stat* gene increased after the *Jnk* gene expression and the peak of higher expression of *Stat* gene was observed at 48 h corresponding with the midgut recovery. According to the observed gene expression patterns, the relationship between *Stat* and *Jnk* was further analyzed through RNAi at their corresponding time points. The expression of *Stat* after treatment with Cry9A for 48 h in the larval midgut was suppressed after silencing *Jnk* by RNAi, while the expression of *Jnk* after treatment with Cry9A toxin for 6 h was not affected when *Stat* gene was silenced by RNAi (Figure 5-8B), indicating that JNK regulates JAK/STAT pathway.

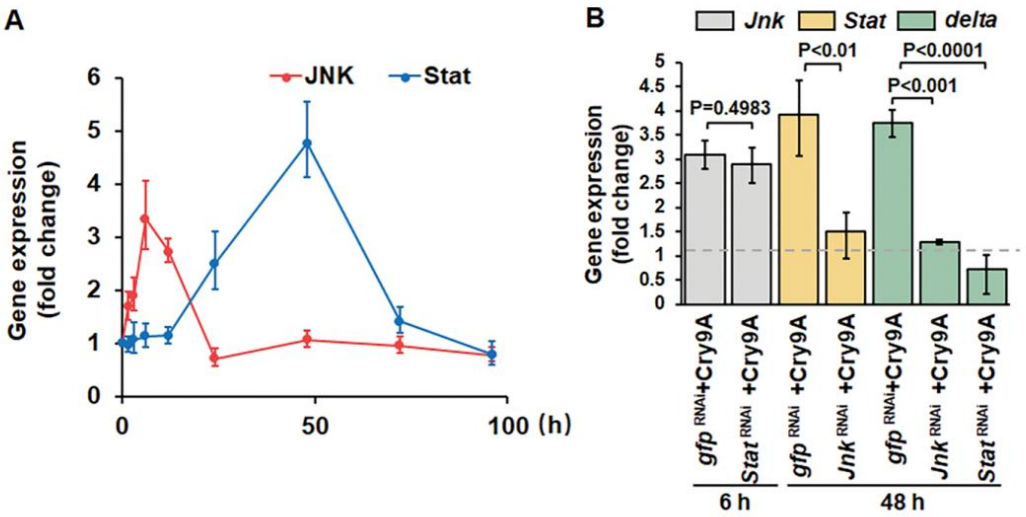

Figure 5-8. Analysis of the upstream and downstream relationship between JNK and JAK/STAT. (A) Quantification of gene expression determined by RT-qPCR in intestines isolated from 15 larvae treated with Cry9A (LC_{20}) for time series. The data were normalized to uninfected control on biological triplicate samples and three independent experiments were performed. The error bar represents ±SEM. (B) Quantification of gene expression determined by RT-qPCR in intestines isolated from 15 silenced larvae treated with Cry9A (LC_{20}) for 6 and 48 h. Gene expression detected in toxin-free treated intestine was measured as 100%. Fifteen larvae were analyzed after silencing for each treatment. The data were normalized to

uninfected control on biological triplicate samples and three independent experiments were performed. *P* values were calculated by two-sided Student's t-test, $P<0.05$ shows statistical differences. $P>0.05$ shows no significant difference. The error bar represents ±SEM.

3.3.2 Role of JNK and JAK/STAT in midgut regeneration induced by Cry9A

Finally, the role of Delta/Notch pathway in ISC proliferation and differentiation was analyzed. It was proposed that Notch activation in ISC was due to the production of the Notch-ligand "Delta" in the adjacent EC cells (Boumard and Bardin, 2021). Here we found that *Delta* was highly expressed 48 hours after Cry9A treatment. Silencing *Jnk* and *Stat* by RNAi, resulted in down-regulation of *Delta* mRNA level (Figure 5-8B), indicating that *Delta* expression may be regulated by JNK and JAK/STAT, which activated epithelial cell differentiation once cell shedding happened. Furthermore, immunofluorescence analysis showed that PH3 was detected in ISCs using an anti-phospho-histone H3 antibody 48 hours after Cry9A toxin treatment (Figure 5-9A). However, when *Jnk* or *Stat* was silenced by RNAi, the PH3 signal disappeared. Western blot experiments confirmed these data (Figure 5-9B), indicating that Cry9A-induced ISC mitotic activation is regulated by both the JNK and JAK/STAT signaling pathways. These data support that after intoxication with sublethal dose of PFT the larvae respond with a defense mechanism involving a non-apoptotic epithelial shedding of midgut cells that activated JNK/JAK/STAT pathway that participate in promoting the intestinal regeneration of the larvae by activating proliferation and differentiation of ISCs.

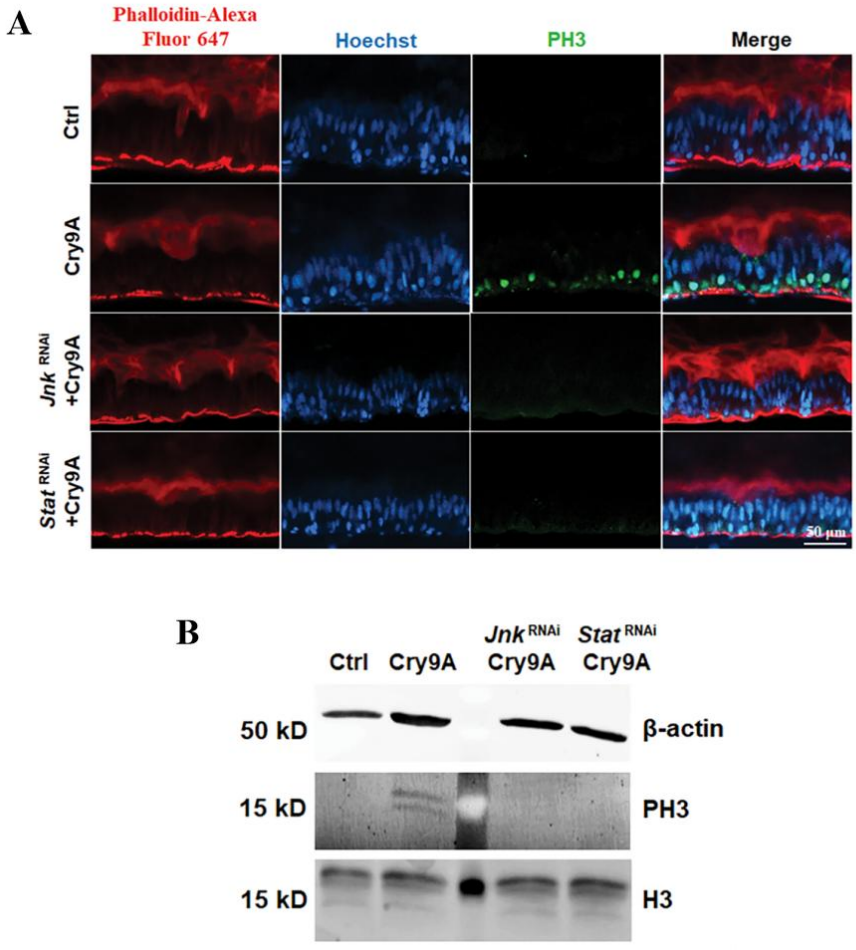

Figure 5-9. Role of JNK and JAK/STAT in midgut regeneration induced by Cry9A. (A) Sagittal view representative images of midgut tissues isolated from Cry9Aa (LC_{20}) treated 3rd instar alive striped stem borer larvae pretreated with or without *Jnk* or *Stat* dsRNA treatment observed in LSCM. Six midgut tissues were analyzed and phospho-histone H3 (PH3) was detected by using a specific anti-PH3 antibody followed by FITC labeled secondary antibody (green color). Hoechst33342 (blue color) labels nuclei. Phalloidin-647 (red color) labels cytoskeleton. Control (Ctrl) were larvae treated with the non-toxic Cry9Aa-D125R. (B) Western blot detection of PH3 in midgut tissue samples from fifteen 3rd instar larvae after Cry9A (LC_{20}) intoxication after pretreatment with or without *Jnk* or *Stat* dsRNA. β-actin was detected as an internal reference. Histone H3 (H3) was detected to show that the loading quantity of H3 was similar. Control (Ctrl) were larvae treated with non-toxic Cry9A-D125R.

3.3.3 Role of JNK and JAK/STAT in defense responses induced by Cry9A

Quantitative analysis revealed significant growth retardation in *C. suppressalis* larvae following 120-hour exposure to sublethal Cry9Aa (LC_{20}), despite the restoration of intestinal homeostasis by 96 hours (Figure 5-10). This phenotypic disparity suggests a substantial metabolic investment in detoxification processes, as evidenced by a 23.7% reduction in larval body length compared to non-toxin controls. Strikingly, RNAi-mediated silencing of *Jnk* or *Stat* genes exacerbated growth suppression, with larvae exhibiting 38.2% and 41.5% length reductions, respectively ($P<0.001$), demonstrating their non-redundant roles in mitigating Cry9Aa toxicity. The data imply that JNK and JAK/STAT pathways mediate cellular defense mechanisms.

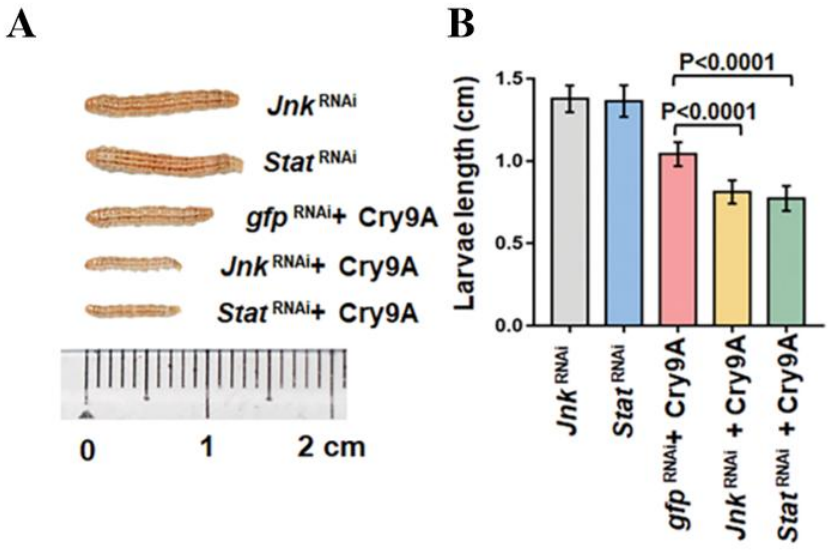

Figure 5-10. Role of JNK and JAK/STAT in defense responses induced by Cry9A. Representative images of seventy-two larvae treated with Cry9Aa (LC_{20}) for 120 h after treating with or without silencing *Jnk* or *Stat*. Negative control (Ctrl) was treated with the non-toxic Cry9A-D125R. (F) Quantification of length of seventy-two larvae treated with Cry9Aa (LC_{20}) for 120 h after treating with or without silencing *Jnk* or *Stat*. *P* values were calculated by one-way ANOVA and Tukey's test, $P<0.0001$ shows statistically significant differences.

3.4 Analysis of the role of JAK/STAT in another insect pest against Bt insecticial protein

3.4.1 Insecticidal bioassays of *S. frugiperda* against Bt insecticial protein

To investigate whether the JAK/STAT-mediated defense mechanism is conserved, we tested toxicity of other PFTs such as Cry1F or Vip3A after treatment with dsRNA of *Stat* in a different lepidopteran pest, the fall armyworm (*Spodoptera frugiperda*) larvae, a harmful corn insect pest.

The data showed that silencing *Stat* is effective to increase toxicity of both PFTs (Cry1F and Vip3A) (Figure 5-11), indicating that *Stat* also plays a crucial role in the defense of *S. frugiperda* against Cry1F and Vip3 proteins. Our results demonstrate that the JAK/STAT-mediated midgut regeneration defense mechanism is evolutionarily conserved among lepidopteran pests.

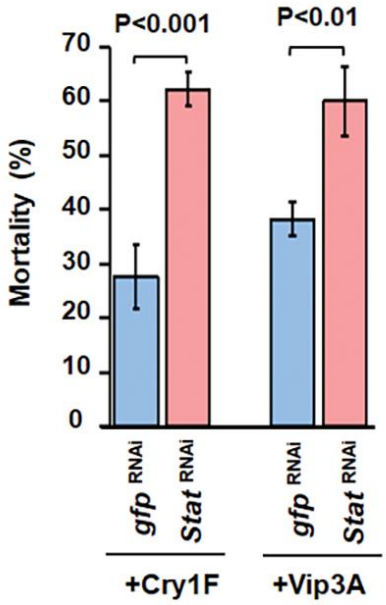

Figure 5-11. Insecticidal bioassays of *S. frugiperda* against Bt insecticial protein. Insecticidal bioassay of Cry1Fa and Vip3Aa against neonate fall armyworm larvae that were pretreated with dsRNA of *Stat*. Thirty-five two-day-old larvae were analyzed in each treatment. Three replicates were performed. *P* values were calculated by two-sided Student's t-test, $P<0.0001$ shows statistically significant differences. $P>0.05$ shows no significant difference. The error bar represents ±SEM.

3.4.2 Changes in midgut tissue morphology after silencing *Stat*

To further determine the role of JAK/STAT pathway in the defense of Bt insecticidal protein in the fall armyworm, the intestinal regeneration after treatment with low dose of Cry1F was also observed in the larvae of fall armyworm (Figure 5-12A). Quantitative analysis revealed that both intestinal thickness (Figure 5-12B) and epithelial cell number (Figure. 5-12C) in *Stat*-silenced larvae were significantly reduced compared to non-silenced control larvae after 72 hours of Cry1F exposure, indicating that the regenerative capacity was severely impaired when the *Stat* gene was silenced through RNA interference. These results provide compelling

evidence that the JAK/STAT signaling pathway plays a crucial role in mediating midgut epithelial regeneration following Cry toxin-induced damage.

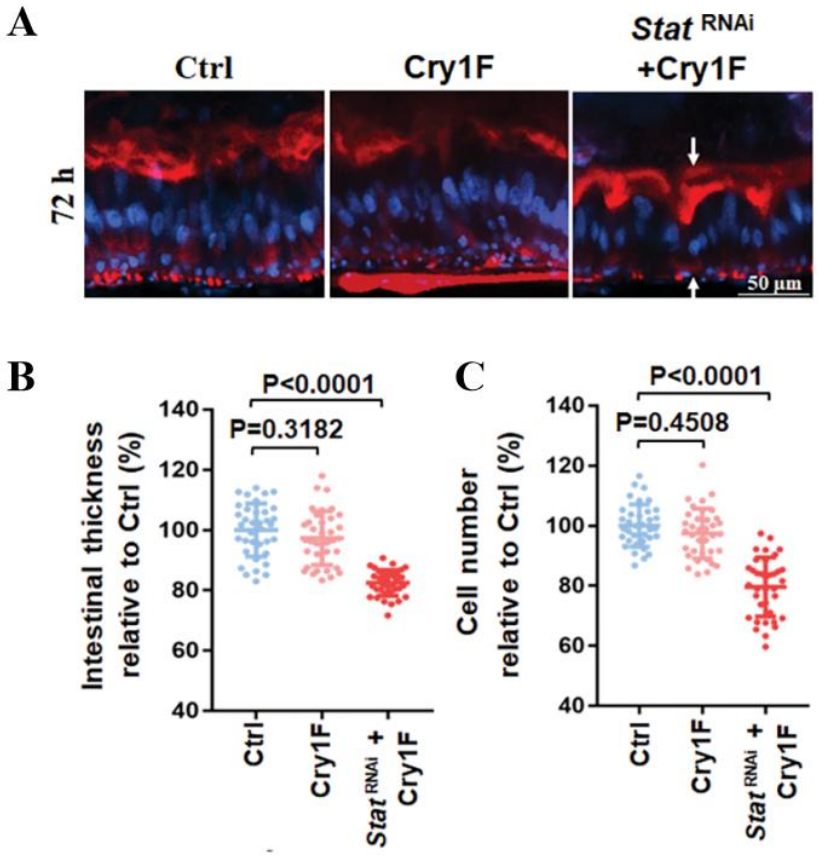

Figure 5-12. Changes in midgut tissue morphology after silencing *Stat*. (A) Sagittal view representative images of 4th instar fall armyworm larvae midgut tissues isolated after 72h of Cry1F (LC_{20}) treatment with or without *Stat* dsRNA pretreatment observed in the LSCM. Hoechst33342 (blue color) labels nuclei. Phalloidin-647 (red color) stains F-actin present in the brush border (upper arrows) and in the visceral muscles (lower arrows). Control (Ctrl) were larvae treated with diet without Cry1F toxin. (B and C) Quantification of the fluorescent signal of intestinal thickness (B) and cell number (C) obtained after 72h of Cry1F (LC_{20}) with or without *Stat* dsRNA pretreatment. Control (Ctrl) are midguts treated with the toxin-free artificial diet. Toxin-free treated intestine was measured as 100%. n=36 images per treatment. P values were calculated by one-way ANOVA and Tukey's test, P<0.0001 shows statistically significant differences. P>0.05 shows no significant difference. The large bar corresponds to the mean, whereas the smaller ones represent ±SEM.

3.4.3 Analysis of the midgut regeneration after silencing *Stat*

We further investigated the role of the JAK/STAT signaling pathway in midgut regeneration during *Spodoptera frugiperda*'s defense against Bt insecticidal proteins using immunofluorescence and Western blot techniques.

PH3 was also detected in the intestine after Cry1F treatment, suggesting that ISC proliferation was activated (Figure 5-13A) and the ISC proliferation was dampened by silencing *Stat* expression. The western-blot results confirmed these data, showing that the phosphorylation of histone-H3 was depressed after *Stat* knockdown (Figure 5-13B). Finally, delta gene

expression induced by Cry1F and Vip3Aa was also downregulated after silencing *Stat* (Figure 5-13C). The larvae survived after 72 h of treatment with sublethal doses Cry1F grew faster than the larvae pretreated with *Stat* dsRNA (Figure 5-13D and E) suggesting that the JAK/STAT signaling affects global growth of the larvae through regulation of intestinal regeneration. Hence, these data indicate that JAK/STAT signaling participates inducing a broad response through intestinal regeneration after treatment with different PFTs in different lepidopteran species.

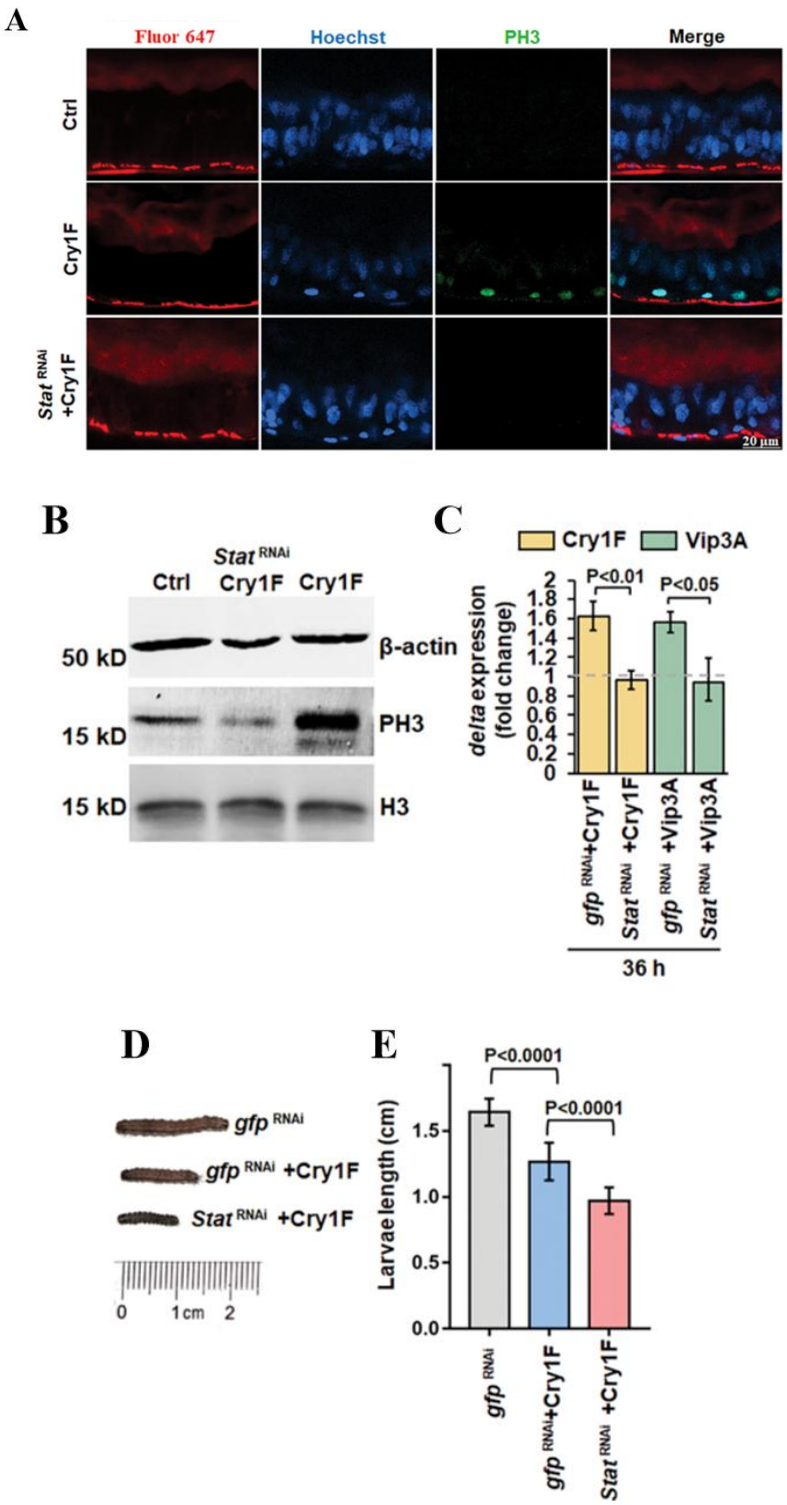

Figure 5-13. Analysis of the midgut regeneration after silencing *Stat*. (A) Sagittal view representative images of midgut tissues isolated after 36 h of Cry1F (LC_{20}) treatment from 4th instar alive fall armyworm larvae with or without *Stat* dsRNA pretreatment observed in LSCM. Six midgut tissues were analyzed and phospho-histone H3 (PH3) was detected by using a specific anti-PH3 antibody followed by FITC labeled secondary antibody (green color). Hoechst33342 (blue color) labels nuclei. Phalloidin-647 (red color) labels cytoskeleton. Control (Ctrl) were larvae treated without toxin. (B) Western blot detection of PH3 in midgut tissue samples from fifteen larvae of 4th instar fall armyworm after 36 h of Cry1F (LC_{20}) intoxication with or without *Stat* dsRNA treatment. β-actin was detected as an internal reference. Histone H3 (H3) was detected to show that the loading quantity of H3 was similar. Control (Ctrl) were larvae treated without toxin. (C) *Delta* gene expression determined by RT-qPCR in intestines isolated from fifteen 4th instar fall armyworm larvae treated with Cry1F or Vip3A (LC_{20}) for 36 h. The error bar represents ±SEM. *P* values were calculated by two-sided Student's t-test, $P<0.05$ shows statistical difference. (D) Representative images from seventy-two 4th instar larvae treated with Cry1F (LC_{20}) for 72 h with or without silencing *Stat*. Negative control (Ctrl) was treated without toxin. (E) Quantification of length from seventy-two 4th instar larvae treated with Cry1F (LC_{20}) for 72 h after treating with or without silencing *Stat*. *P* values were calculated by one-way ANOVA and Tukey's test, $P<0.0001$ shows statistically significant differences.

3.5 Analysis of the synergistic insecticidal activity between silencing *Stat* and Bt for pesticide protecting rice seedlings from damage by striped stem borer

To test the potential use of silencing the *Stat* gene expression in combination with Bt toxins for efficient insect pest control, the *Stat*-dsRNA was incorporated into SPc nanoparticles and sprayed onto the stems and leaves of rice seedlings simultaneously with Bt serovar *fukuokaensis* strain that produces Cry9A, Cry1I, Cry9E and Vip3A proteins before inoculation of striped stem borer larvae (Wang et al., 2020). This formulation containing both the Bt strain and SPc-ds*Stat* controlled the larvae more effectively than the control plants sprayed only with the Bt strain (Figure 5-14A). The toxicity of the formulation reached up to 80% mortality within three days and dead larvae were observed on the soil nearby the stems after three days of treatment. Our data show that the seedlings sprayed by ds*Stat* combined with Bt strain grew much healthier and stronger than the other treatments, showing bigger leaves (Figure 5-14B), fewer wormholes on the stems (Figure 5-14C) and higher plant height (Figure 5-14D). In contrast, the seedlings without treatment or treated only with the dsRNA were not protected. The control where ds*gfp* was used in a mixture with Bt strain, showed some protection due to Bt toxins action since fewer dried and frizzled leaves, and fewer wormholes on the stems were found when compared with controls without Bt strain treatment.

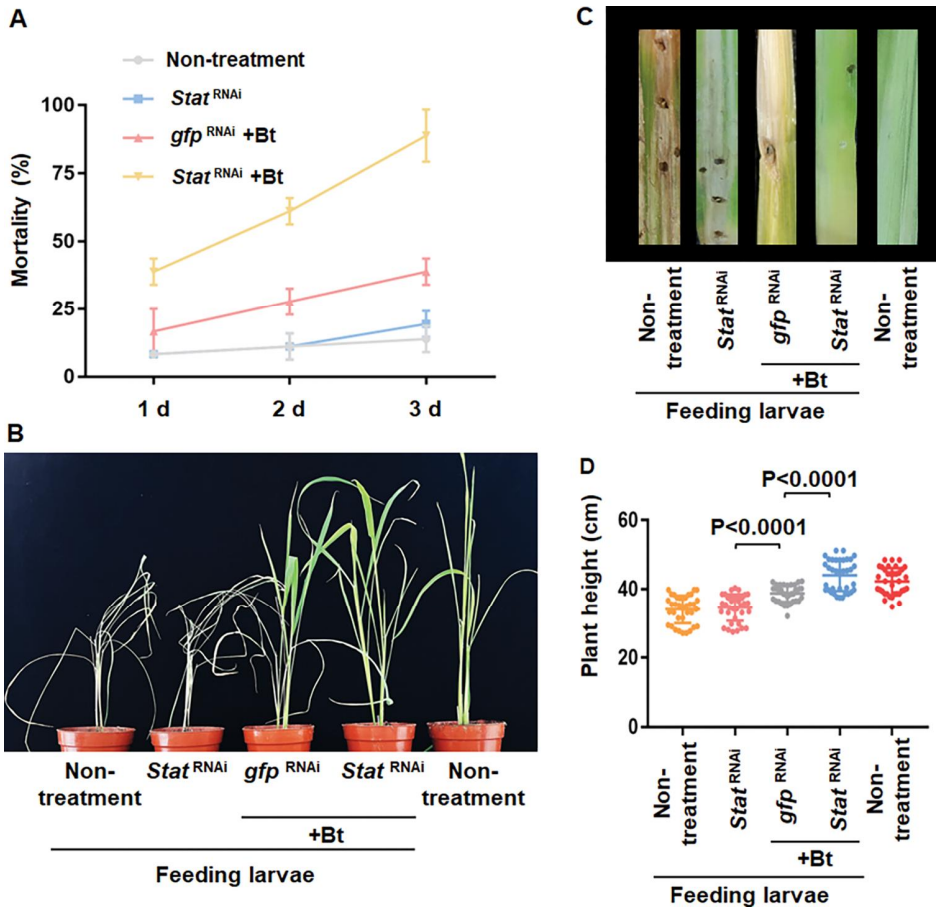

Figure 5-14. Analysis of the synergistic insecticidal activity between silencing *Stat* and Bt for pesticide protecting rice seedlings from damage by striped stem borer. (A) Mortality of 2nd instar larvae of striped stem borer (six larvae per plant) on rice seedlings sprayed with the mixture of Bt *fukuokaensis* strain and *Stat*-dsRNA or *gfp*-dsRNA combined nanoparticles. Representative larvae treated with Bt strain for 3 days with or without silencing *Stat*. Negative control were plants sprayed without Bt strain. The error bar represents ±SEM. (B) Growth of rice seedlings sprayed with or without the mixture of Bt pesticide and *Stat*-dsRNA combined nanoparticles. Negative control were plants sprayed with Bt strain and *gfp*-dsRNA combined nanoparticles. Two rice seedlings at four-leaf stage per pot and two pots per treatment, with three replicates were performed. (C) Representative images of wormholes produced by the larvae that damage the rice stems, especially near the ground. The different treatments were indicated in the figure. (D) Quantification of plant height of rice seedlings sprayed with or without mixture of Bt strain and *Stat*-dsRNA combined nanoparticles and the infected with striped stem borer larvae. *P* values were calculated by one-way ANOVA and Tukey's test. $P<0.0001$ indicates statically significant difference. The large bar corresponds to the mean, whereas the smaller ones represent ±SEM.

4. Discussion

The present study elucidates the intricate roles of the JAK/STAT signaling pathway and JNK in mediating midgut regeneration and defense mechanisms in lepidopteran larvae exposed to Cry9A, a pore-forming toxin (PFT) produced by *Bacillus thuringiensis* (Bt). Our findings reveal a coordinated interplay between these pathways, balancing tissue repair and apoptotic responses to mitigate toxin-induced damage. Furthermore, the development of a novel

nano-pesticide combining Bt toxins and dsRNA targeting *Stat* demonstrates significant potential for improving pest control efficacy. Below, we discuss these results in the context of existing literature, their implications for pest management, and future research directions.

JNK and JAK/STAT: Coordinating Midgut Regeneration

The JAK/STAT pathway emerged as a central regulator of midgut regeneration in *Chilo suppressalis* and *Spodoptera frugiperda*. Following Cry9A intoxication, JAK/STAT activation promoted intestinal stem cell (ISC) proliferation and differentiation, facilitating epithelial repair. This aligns with findings in *Drosophila*, where JAK/STAT drives ISC proliferation in response to tissue damage (Jiang et al., 2009; Zhou et al., 2015). Notably, our temporal expression analysis revealed that *Stat92E* and *Socs36E* peaked during the recovery phase (48 h post-treatment), coinciding with ISC-driven tissue regeneration. Silencing *Stat92E* or inhibiting STAT phosphorylation suppressed midgut regeneration and increased larval mortality, underscoring the pathway's critical role in toxin resistance.

In parallel, JNK was identified as a key player in managing Cry9A-induced stress. Silencing *Jnk* or inhibiting JNK enhanced the susceptibility of *C. suppressalis* larvae to Bt insecticidal proteins and exacerbated long-term epithelial damage, highlighting its role in tissue remodeling. Crucially, the interplay between JAK/STAT and JNK defines a feedback loop governing midgut regeneration. JNK activation preceded STAT upregulation, and *Stat92E* expression was suppressed upon *Jnk* knockdown. This suggests JNK acts upstream of JAK/STAT, potentially via cytokine release from damaged cells, which in turn activates STAT to drive ISC proliferation. Such cross-talk highlights the evolutionary conservation of stress-response mechanisms but also underscores unique adaptations in lepidopterans, where rapid midgut repair is critical for surviving toxin exposure.

Delta/Notch Signaling: Bridging JNK and JAK/STAT

Our study further implicates the Delta/Notch pathway in midgut regeneration. *Delta* expression surged post-Cry9A treatment, peaking at 48 h, and was downregulated upon silencing *Jnk* or *Stat92E*. This aligns with the proposed model where JNK-mediated epithelial shedding triggers Delta production in enterocytes (ECs), activating Notch in adjacent ISCs to promote differentiation (Boumard and Bardin, 2021). STAT signaling may amplify this process by upregulating *Delta*, thereby coupling ISC proliferation to differentiation. This mechanism ensures efficient replacement of damaged cells while maintaining epithelial integrity - a strategy likely conserved across lepidoptera but previously uncharacterized.

Synergistic Nano-Pesticides

Bt insecticides have been used for over 60 years, and improving and sustaining their insecticidal efficacy remains a major research focus. Among current strategies, the combined application of Bt insecticides with RNA interference (RNAi) technology has emerged as a promising trend. In laboratory settings, silencing key insect genes via RNAi has been shown to significantly enhance the insecticidal activity of Bt (Rodríguez et al., 2010; Guan et al., 2019; Wang et al., 2024). In addition, transforming RNAi vectors into Bt strains to create engineered Bt strains capable of expressing dsRNA represents a novel approach. For instance, fragments of the arginine kinase gene from *Plutella xylostella* (*PxAK*) were introduced into Bt strains 8010 and BMB171, resulting in engineered Bt strains 8010AKi and BMB171AKi that express *PxAK*-targeting dsRNA. When mixed with wild-type Bt 8010 at various ratios, both engineered strains exhibited significantly enhanced insecticidal activity against *P. xylostella*

larvae (Jiang et al., 2022). Furthermore, the co-application of nanomaterials and biocontrol agents has also shown potential. For example, the star polycation (SPc), a type of nanocarrier, has been used to simultaneously deliver dsRNA and cellobiose (a plant immune inducer that effectively activates plant defense signals), enhancing antimicrobial activity by simultaneously suppressing pathogens and boosting plant defenses. Through hydrophobic and electrostatic interactions, SPc self-assembles with dsRNA and cellobiose to form a novel nano-scale multi-component biological agent. This multi-functional nanomaterial demonstrated significant protective effects under both greenhouse and field conditions, achieving control efficacy comparable to commercial fungicides and enabling sustainable green management of potato late blight (Wang et al., 2023).

The development of a SPc-dsRNA/Bt nano-pesticide may represents a breakthrough in pest control. By silencing *Stat*, we disrupted the insect's regenerative capacity, amplifying Cry9A toxicity. Field trials demonstrated 80% larval mortality within three days, with rice seedlings showing reduced damage and enhanced growth. This approach overcomes a major limitation of Bt toxins - evolving pest resistance - by targeting host defense pathways. Similar efficacy against Cry1F and Vip3A in *S. frugiperda* suggests broad applicability across lepidoptera.

Overall, our data show that the JNK and JAK/STAT pathways are involved in midgut tissue regeneration following PFT damage. Furthermore, JAK/STAT is a conserved pathway that regulates the defense of two different lepidopteran pests (striped stem borer and fall armyworm) against two different Bt PFTs (Cry9A, Cry1F). As mentioned earlier, the main goal of this work is to identify target genes that knock out the intestinal regeneration response to enhance the toxicity of Bt Cry insecticidal proteins. Our data suggest that silencing the *Stat* gene inhibits midgut regeneration after exposure to Cry insecticidal proteins, thereby enhancing the toxicity of Cry proteins to at least two different pests. Additionally, we demonstrate that spraying this novel formulation on plants helps prevent pest damage. Therefore, this represents a new strategy to enhance the toxicity of Cry proteins against different pests. Furthermore, co-expression of *Stat* dsRNA and Cry toxins in transgenic plants or topical formulations could provide a method for effectively controlling pests that are less sensitive to Cry toxins or have developed resistance to these insecticidal proteins.

Chapter 6

General discussion and conclusions

1. General discussion

Synthetic pesticides are useful tools for protecting crops against different insect pests. However, their nonstandard use and abuse have resulted in increased pesticide residues, which remain in food, plants and soil, appearing also in processed commodities and food chain, leading to serious threats to human health and to the ecosystem balance (Nougadère et al., 2011; Meftaul et al., 2020; Xu et al., 2022). In addition, several insect pests have evolved resistance to synthetic pesticides (Rajmohan et al., 2020). One of the most promising alternatives for the reduction of synthetic pesticides in pest control is the use of microbial bioinsecticides based on the Gram-positive bacterium *Bacillus thuringiensis* (Bt). Bt is well known for producing different insecticidal pore-forming toxins (PFTs) such as Cry and Vip toxins that attack the larval midgut cells (Crickmore et al., 2021). These proteins have been widely used for the biological control of both agricultural pests and insect vectors of human diseases since the 1960s and certain toxin genes from Bt have been introduced in transgenic crops that resist insect attack (Tabashnik et al., 2017). Bt bacteria produce monomeric PFTs, which oligomerize upon binding to their specific receptors and assemble into transmembrane pores permeabilizing midgut cells and facilitating bacterial infection (Bravo et al., 2013). The midgut of insects plays a critical role in digestion and nutrient absorption, but it is also a primary target for microbial toxins and insecticidal proteins such as Cry9A. This toxin, produced by Bt, forms pores in the midgut epithelium, disrupting cellular integrity and leading to significant tissue damage. Understanding how insect midgut cells respond to such stressors is crucial for both basic insect physiology and the development of effective pest control strategies.

The research presented in this dissertation explores the intricate defense mechanisms of lepidopteran pests against pore-forming toxins (PFTs) produced by *Bacillus thuringiensis* (Bt), with a focus on the midgut's role in mitigating toxin-induced damage. The study spans three main chapters, each addressing specific aspects of midgut defense responses, including morphological and cellular changes, the establishment of an efficient RNA interference (RNAi) system, and the identification of key regulatory pathways. Below, we synthesize these findings, discuss their implications for pest control, and outline future research directions. Furthermore, we explore the broader ecological and evolutionary implications of midgut responses to Cry toxins and how they can be leveraged in future biotechnological applications.

1.1 Midgut defense responses to Bt proteins: midgut remodeling

In this work, we show that the midgut tissue of lepidopteran larvae experienced two rounds of morphological changes after treatment with sublethal dose of PFT produced by Bt. The microvilli of damaged midgut cells shed into the midgut lumen. These data are in agreement with previous publications showing damage of lepidopteran midgut tissue after ingestion of Cry1A toxins (Bravo et al., 1992). We show here that after damage in the midgut tissue, the intestinal epithelial cells were extruded and shed into midgut lumen. These results are different with those previously described in *D. melanogaster* after infection with other PFTs such as hemolysin from *Serratia marcescens* or cholesterol-dependent cytolysins, where a limited extrusion of apical cytoplasm containing some organelles was observed (Lee et al.,

2016; Romero et al., 2017; Brito et al., 2019). The reasons for the different responses observed in *D. melanogaster* and *C. suppressalis* to PFT are not known but differences may be caused by the variation of the pore size and the toxin characteristics. This remains to be analyzed.

It was previously shown that Cry1A toxin may induced apoptosis in midgut of *B. mori* larvae, where Bm-Apaf1 was upregulated (Tanaka et al., 2012). Instead, we found a cell shedding of epithelial cells caused by PFT: histopathological analyses showed that Cry9A ingestion led to apical microvilli loss and epithelial stratification, with cells extruding into the gut lumen. This was quantified by increased aminopeptidase N (APN) activity in the lumen, a marker for epithelial shedding.

Cell shedding is followed by midgut regeneration. Western blot analysis detected phosphorylated histone H3 (PH3), a mitotic marker, in midgut tissues during the recovery phase (24–96 h post-treatment). This indicates ISC proliferation as a compensatory mechanism for toxin-induced damage. The upregulation of *Delta* gene expression during recovery suggests that Notch activation in ISCs drives their differentiation into mature enterocytes, restoring midgut integrity. This pathway is conserved across insects and critical for epithelial repair (Buchon et al., 2009b).

These findings highlight that lepidopteran pests employ midgut remodeling mechanisms, such as cell shedding and ISC-mediated regeneration, to counteract Bt toxins. Targeting these pathways could enhance the efficacy of Bt-based pest control by disrupting midgut repair processes.

However, the specific regulatory mechanisms of genes and pathways involved in midgut remodeling remain unclear. The most straightforward and effective technique for screening defense-related genes is RNA interference (RNAi). However, the relatively low RNAi efficiency in the midgut of lepidoptera limits these studies. Therefore, establishing an efficient RNAi-based screening system for midgut defense genes in lepidopteran pests is of paramount importance.

1.2 Establishment of an efficient RNAi system for midgut defense genes

The crystal proteins (Cry) produced by *Bacillus thuringiensis* (Bt) have been widely used for the effective control of various lepidopteran pests. However, the low efficiency of RNA interference (RNAi) in lepidoptera has hindered research on the midgut defense mechanisms against Cry proteins. To address this limitation, we focused on the homologous genes of Epidermal Growth Factor Receptor (*Egfr*) and Stathmin 4 (*Stmn4*), which have been reported to regulate stem cell proliferation and cell cycle progression in *Drosophila*, and applied them to *Spodoptera frugiperda*, a major migratory agricultural pest, to establish an efficient RNAi-based system for studying midgut defense genes in lepidopteran pests.

In this study, we systematically evaluated the gene silencing efficiency by analyzing different dsRNA synthesis methods (dsRNA expressed in *Escherichia coli*, dsRNA extracted from *E. coli*, and *in vitro* synthesized dsRNA), different feeding durations of dsRNA, and different dsRNA concentrations. Additionally, we assessed the effectiveness of different bioassay methods in screening defense-related genes (pre-feeding dsRNA before transferring to Bt

protein-containing diet versus simultaneous feeding of dsRNA and Cry protein-containing diet). We also explored the specific roles of *SfEgfr* and *SfStmn4* in the midgut defense response to Bt Cry proteins.

Our results demonstrated that, compared to the *E. coli*-expressed dsRNA, *in vitro* synthesized dsRNA exhibited significantly higher gene silencing efficiency, especially when complexed with star polycation (SPc) nanoparticles. When fed at a concentration of 25 μg/g for 48 hours, the gene silencing efficiency reached over 75%. Pre-treatment with dsRNA for 48 hours increased the larval mortality rate by more than 30% following Cry1F exposure, outperforming the simultaneous feeding method of dsRNA and Cry1F protein. Furthermore, the silencing of *SfEgfr* and *SfStmn4* inhibited the proliferation of midgut stem cells after Cry1F exposure, leading to an increased mortality rate.

This study successfully established a highly efficient, oral dsRNA-based RNAi system for investigating midgut defense genes in lepidopteran pests. Moreover, it confirmed the critical roles of *SfEgfr* and *SfStmn4* in the midgut defense response against Bt Cry proteins. These findings provide new insights and a theoretical framework for the biological control of lepidopteran pests.

1.3 Midgut defense responses mediated by midgut regeneration are regulated by the JNK/JAK/STAT pathway.

JAK-STAT signaling pathway is considered as a major regulator of *Drosophila* midgut regeneration (Lin et al., 2010; Liu et al., 2010). We demonstrated that JAK-STAT signaling regulates intestinal regeneration in lepidopteran larvae against PFTs. It was previously shown that in *Drosophila* stressed or damaged ECs stimulates regeneration of ISC by triggering a rapid, powerful JAK/STAT signaling response in which Upd2 and Upd3 are transcriptionally induced in ECs and EEs, triggering STAT signaling in ISCs, promoting their division (Buchon et al., 2009b). STAT signaling is also involved in EC and EE differentiation (Jiang et al., 2009; Beebe et al., 2010). Surprisingly, no significant similarity to Upd genes were found in the genome of striped stem borer. One possibility is that there are another kind of molecules delivering signals from ECs to ISCs. Secondly, it is possible that the detached ECs was sensed by ISCs through the loss of E-cadherin as a kind of cell-cell communication (Liang et al., 2017).

In addition, we showed that JNK was upregulated at early stage after infection and silencing *Jnk* by RNAi inhibited the STAT response of striped stem borer larvae, suggesting that JNK signaling may initiate STAT response during intestinal regeneration. These data correlate with previous works showing that upon infection by pathogens that directly damage the gut epithelium, such as *Pseudomonas*, JNK signaling is activated in ECs (Jiang et al., 2009; Apidianakis et al., 2009). Our data cannot distinguish if STAT activation by JNK is direct or indirect, more studies are required to solve this question. Also, the localization of JNK and STAT signaling and identification of responsible cells remains to be determined. This information will be useful to understand the participation of this pathway in the defense response to Cry9Aa toxin.

Likewise, it was previously shown that the EGFR/Ras/MAPK pathway is required to induce EE/EC growth in *Drosophila* after midgut damage caused by the PFT haemolysin produced

by *Pseudomonas entomophila* (Xiang et al., 2017). However, we found that RNAi for Egfr did not change the mortality of striped stem borer larvae to Cry9Aa toxin, although *Egfr* was upregulated in early stage of PFT intoxication. We hypothesized that in the case of larval midgut tissue exposed to Bt Cry9Aa PFT, EGFR may be functioning independently from JNK/JAK/STAT pathway. Also, we cannot discard that EGFR is involved also in the intestinal regeneration in lepidopteran insects but other pathways compensate the silencing of *Egfr* explaining the lack of phenotype in the silenced larvae. This remains to be studied in the future.

Overall, our data shows that JNK and JAK/STAT pathways are involved in midgut tissue regeneration after damage by PFT. Also, that JAK/STAT is a conserved pathway to regulate defense in two different insect lepidopteran pests, striped stem borer and fall armyworm, to different Bt PFTs (Cry9Aa, Cry1Fa). As mentioned previously, the main objective of this work was to identify target genes to knockdown the intestine regeneration response in order to increase the toxicity of Bt Cry insecticidal proteins. Our data shows that silencing Stat gene inhibits the intestine regeneration after exposure to Cry insecticidal proteins enhancing the toxicity of Cry proteins to at least two different insect pests. Furthermore, we demonstrated that spraying this novel formulation into plants helps to prevent the damage of the insect pest. Thus, this is a novel strategy that may be used for enhancing Cry toxicity to different insect pests. Furthermore, the simultaneous expression of *Stat* dsRNA and Cry toxins in transgenic plants or in a topic formulation could provide means for an efficient control of pests that show low susceptibility to Cry toxins or to insects that have evolved resistance to these insecticidal proteins.

2. Conclusions

One of the most promising alternatives to synthetic insecticides in pest control is the use of microbial biopesticides based on the Gram-positive bacterium *Bacillus thuringiensis* (Bt). Bt is well known for producing various insecticidal pore-forming toxins (PFTs), such as Cry and Vip toxins, which target the midgut epithelial cells of insect larvae. The insect midgut, as one of the most critical organs, can activate multiple defense responses in reaction to these pore-forming toxins. These defensive responses significantly affect the efficacy of Bt-based biopesticides; however, they remain poorly understood in lepidopteran pests. Based on this research gap, we conducted a study on the midgut defense mechanisms of lepidopteran insects and obtained the following results：

The first key finding of this study is that sublethal concentrations of Cry9A toxin induce significant structural changes in the midgut epithelium of *C. suppressalis*. Larvae exhibit a rapid midgut remodeling characterized by cell shedding and intestinal stem cell (ISC)-driven regeneration. This challenges the conventional view that apoptosis is the primary mechanism for removing toxin-damaged cells in lepidopteran midguts. These findings demonstrate a biphasic response - elimination of damaged cells and subsequent repair - orchestrated by ISC activation, providing insights into lepidopteran adaptive strategies against Bt toxins.

The second major contribution of this work is the development of an optimized RNAi system for silencing midgut defense genes in lepidopteran pests. This system addresses the longstanding challenge of low RNAi efficiency in lepidoptera. Compared to the *E. coli*-expressed dsRNA, in vitro synthesized dsRNA exhibited significantly higher gene silencing efficiency, especially when complexed with star polycation (SPc) nanoparticles.

When fed at a concentration of 25 μg/g for 48 hours, the gene silencing efficiency reached over 75%. Pre-treatment with dsRNA for 48 hours increased the larval mortality rate by more than 30% following Cry1F exposure, outperforming the simultaneous feeding method of dsRNA and Cry1F protein. Furthermore, the silencing of SfEgfr and SfStmn4 inhibited the proliferation of midgut stem cells after Cry1F exposure, leading to an increased mortality rate. Our findings offer a novel concept and theoretical framework for the biological management of lepidopteran pests.

The third key finding elucidates the roles of JNK and the JAK/STAT pathway in midgut regeneration and defense against Bt toxins. Cry9A-induced intestinal regeneration is regulated by Jun N-terminal kinase (JNK) and the Janus kinase/signal transducer and activator of transcription (JAK/STAT) signaling pathway. These factors mediate gut regeneration by promoting intestinal stem cell proliferation and differentiation, offering protection against three different Bt proteins, including Cry9A, Cry1F, and Vip3A, in *Chilo suppressalis* and *Spodoptera frugiperda*. To enhance pesticide efficacy, a nano-biopesticide was developed by combining *Stat* double-stranded RNA (dsRNA) nanoparticles with Bt strains. This formulation demonstrated superior pest control, suggesting its potential to reduce reliance on synthetic insecticides in agricultural environments.

Overall, we identified that the JNK/JAK/STAT pathway regulates midgut regeneration in lepidopteran larvae following pore formation induced by Bt pore-forming toxins (PFTs). Furthermore, we demonstrated that RNAi-mediated silencing of the JAK/STAT pathway enhances the toxicity of different PFTs in two distinct lepidopteran species. Based on these findings, we developed a novel and effective formulation combining Bt and dsStat nanopesticides for controlling *Chilo suppressalis* and *Spodoptera frugiperda* larvae. This innovative strategy, which integrates Bt strains with dsRNA targeting insect defense mechanisms, offers a promising approach for managing crop pests that exhibit low susceptibility to Bt PFTs.

3. Perspectives

The research presented in this dissertation has significantly advanced our understanding of lepidopteran midgut defense mechanisms against *Bacillus thuringiensis* (Bt) toxins, particularly focusing on midgut remodeling, RNA interference (RNAi)-based gene silencing, and the regulatory roles of the JNK and JAK/STAT pathways in epithelial repair. While these findings provide a strong foundation for improving Bt-based pest control, numerous questions remain unanswered, and several promising avenues for future research have emerged. This section outlines key research directions that could further enhance the efficacy of Bt biopesticides, delay resistance evolution, and promote sustainable agricultural practices. The discussion is structured into six major themes: (1) Elucidating species-specific defense mchanisms; (2) Deciphering JNK and JAK/STAT cross-talk in midgut regeneration; (3) Optimizing RNAi delivery for field applications; (4) Mapping the cellular atlas of the lepidopteran insect midgut by single-cell RNA sequencing. (5) Elucidating the molecular mechanisms by which lepidopteran pests defend against pore-forming toxins through single-cell RNA sequencing. (6) Investigating which metabolites are involved in the defense of lepidopteran pests against pore-forming toxins. (7) Investigating whether the defense process of lepidopteran pests against pore-forming toxins is associated with microorganisms.

(1) Our findings demonstrate that the EGFR pathway plays a non-critical role in *Chilo suppressalis* defense against Cry9Aa protein, whereas it is essential for *Spodoptera frugiperda* resistance to Cry1F toxin. The underlying causes of this species-specific divergence warrant further investigation. In this process we can employ the RNAi system that we established in this study to investigate the redundant mechanisms of the EGFR signaling pathway in the defense responses of different species.

(2) When midgut tissue of *Drosophila* was stressed or damaged, ECs stimulates regeneration of ISC by triggering JAK/STAT signaling response in which Upd2 and Upd3 are transcriptionally induced in ECs and EEs, triggering STAT signaling in ISCs, promoting their divisionIn response to damage. However, homologs of *Drosophila* intercellular communication signaling molecule Upd have not been identified in the genomes of lepidopteran pests such as *Spodoptera frugiperda* or *Chilo suppressalis*. This suggests that alternative signaling molecules may mediate communication between damaged cells and stem cells in lepidoptera, activating the JAK/STAT pathway in stem cells and regulating midgut regeneration, further studies are needed to identify and characterize the signaling molecules involved in this process.

(3) We designed a nano-biopesticide based on a combination of *Stat* double-stranded RNA (dsRNA) nanoparticles and Bt strains to enhance pesticide efficacy. This formulation demonstrated improved pest control effectiveness in indoor pot experiments, suggesting its potential for reducing the use of synthetic insecticides in agricultural environments. The next step is to evaluate the performance of the nano-biopesticide under real-world conditions, including its environmental persistence and non-target effects. Regarding stability, we need to compare the optimal ratio of dsRNA to Bt formulation. Moreover, because the application is carried out outdoors, it will be necessary to investigate additional stabilizers to protect against ultraviolet irradiation. At the same time, we must explore the best formulation type for the Bt product. In parallel, a thorough safety evaluation is required, including experiments on natural enemy insects, pollinators, soil organisms, and other non-target species.

(4) Using single-cell RNA sequencing to dissect the cellular composition of the lepidopteran insect midgut. Currently, the midgut cell types of lepidopterans remain unclear, most studies have focused on the *Drosophila midgut*. By applying single-cell transcriptomics, we can first resolve the full complement of midgut cell types in lepidopteran insects. Next, by examining the temporal patterns of gene expression, we can infer the developmental trajectories and differentiation order of each cell population. Furthermore, leveraging cell-type–specific gene-expression signatures, we can elucidate the distinct functions of each cell type. These insights will provide a critical theoretical foundation for future lepidopteran pest-management research.

(5) We can apply single-cell transcriptomic sequencing to the midgut of lepidopteran insects treated with sublethal concentrations of pore-forming toxins; this approach will reveal which specific cell types mount a response and which genes and signaling pathways are engaged, thereby informing targeted strategies for lepidopteran pest control. At the same time, we can integrate these results with the findings of this study to investigate in which specific cell types the JNK and JAK/STAT pathways are activated, thereby elucidating the signaling transmission routes.

(6) We have discussed the genes involved in the defense of lepidopteran pests against pore-forming toxins, but we are still unclear about which metabolites are involved in this process. Therefore, we propose to conduct a metabolomic study on the midgut of lepidopteran insects treated with sublethal concentrations of Bt insecticidal proteins. This will help us identify the metabolites involved in the defense response. Additionally, by integrating transcriptomic data, we aim to construct a comprehensive gene–pathway–metabolite regulatory network underlying the defense mechanism of lepidopteran pests against pore-forming toxins.

(7) It is widely accepted that Bt insecticidal proteins attack the insect midgut epithelial cells and ultimately cause insect death through septicemia. However, there is currently no direct evidence demonstrating the involvement of microorganisms in this process. Therefore, we propose to use microbiome analysis to examine whether the microbial composition changes during the defense response. Furthermore, we aim to isolate specific microorganisms and perform functional validation to determine their roles. This approach will help elucidate the potential contribution of microorganisms to the defense mechanisms of lepidopteran pests against pore-forming toxins.

References

Abou El Asrar R, Cools D, Broeck J V. Role of peptide hormones in insect gut physiology[J]. Current Opinion in Insect Science, 2020, 41: 71-78.

Adegawa S, Yamaguchi N, Sato R. The base and root of domain II loops of Cry toxins contribute to binding to *Bombyx mori* ABC transporter C2[J]. The FEBS Journal, 2022, 289(4): 965-984.

Antimisiaris S, Mourtas S, Papadia K. Targeted si-RNA with liposomes and exosomes (extracellular vesicles): How to unlock the potential[J]. international Journal of pharmaceutics, 2017, 525(2): 293-312.

Apidianakis Y, Pitsouli C, Perrimon N, et al. Synergy between bacterial infection and genetic predisposition in intestinal dysplasia[J]. Proceedings of the National Academy of Sciences, 2009, 106(49): 20883-20888.

Arbouzova N I, Zeidler M P. JAK/STAT signalling in *Drosophila*: insights into conserved regulatory and cellular functions[J]. 2006: 2605-2616.

Avila L A, Chandrasekar R, Wilkinson K E, et al. Delivery of lethal dsRNAs in insect diets by branched amphiphilic peptide capsules[J]. Journal of controlled release, 2018, 273: 139-146.

Azuma M, Harvey W R, Wieczorek H. Stoichiometry of K^+/H^+ antiport helps to explain extracellular pH 11 in a model epithelium[J]. FEBS letters, 1995, 361(2-3): 153-156.

Baldwin K M, Hakim R S. Growth and differentiation of the larval midgut epithelium during molting in the moth, *Manduca sexta*[J]. Tissue and cell, 1991, 23(3): 411-422.

Banyuls N, Hernández-Martínez P, Quan Y, et al. Artefactual band patterns by SDS-PAGE of the Vip3Af protein in the presence of proteases mask the extremely high stability of this protein[J]. International Journal of Biological Macromolecules, 2018, 120: 59-65.

Bardin A J, Perdigoto C N, Southall T D, et al. Transcriptional control of stem cell maintenance in the *Drosophila* intestine[J]. Development, 2010, 137(5): 705-714.

Baudron F, Zaman-Allah M A, Chaipa I, et al. Understanding the factors influencing fall armyworm (*Spodoptera frugiperda* JE Smith) damage in African smallholder maize fields and quantifying its impact on yield. A case study in *Eastern Zimbabwe*[J]. Crop protection, 2019, 120: 141-150.

Beebe K, Lee W C, Micchelli C A. JAK/STAT signaling coordinates stem cell proliferation and multilineage differentiation in the *Drosophila* intestinal stem cell lineage[J]. Developmental biology, 2010, 338(1): 28-37.

Benguettat O, Jneid R, Soltys J, et al. The DH31/CGRP enteroendocrine peptide triggers intestinal contractions favoring the elimination of opportunistic bacteria[J]. PLoS Pathogens, 2018, 14(9): e1007279.

Bennett B L, Sasaki D T, Murray B W, et al. SP600125, an anthrapyrazolone inhibitor of Jun N-terminal kinase[J]. Proceedings of the National Academy of Sciences, 2001, 98(24): 13681-13686.

Berliner E. Über die Schlaffsucht der Mehlmottenraupe (Ephestia kühniella Zell.) und ihren Erreger *Bacillus thuringiensis* n. sp[J]. Zeitschrift für angewandte Entomologie, 1915, 2(1): 29-56.

Billingsley P F, Lehane M J. Structure and ultrastructure of the insect midgut[M]//Biology of the insect midgut. Dordrecht: Springer Netherlands, 1996: 3-30.

Biteau B, Hochmuth C E, Jasper H. JNK activity in somatic stem cells causes loss of tissue homeostasis in the aging *Drosophila* gut[J]. Cell stem cell, 2008, 3(4): 442-455.

Biteau B, Jasper H. EGF signaling regulates the proliferation of intestinal stem cells in *Drosophila*[J]. Development, 2011, 138(6): 1045-1055.

Boonserm P, Davis P, Ellar D J, et al. Crystal structure of the mosquito-larvicidal toxin Cry4Ba and its biological implications[J]. Journal of molecular biology, 2005, 348(2): 363-382.

Boonserm P, Mo M, Angsuthanasombat C, et al. Structure of the functional form of the mosquito larvicidal Cry4Aa toxin from *Bacillus thuringiensis* at a 2.8-angstrom resolution[J]. Journal of Bacteriology, 2006, 188(9): 3391-3401.

Boumard B, Bardin A J. An amuse-bouche of stem cell regulation: Underlying principles and mechanisms from adult *Drosophila* intestinal stem cells[J]. Current Opinion in Cell Biology, 2021, 73: 58-68.

Bravo A, Gill S S, Soberón M, et al. *Bacillus thuringiensis* mechanisms and use[J]. Comprehensive Molecular Insect Science [Gilbert, LI, Kostas, I., Gill, SS (ed.)][175–206](Elsevier, Netherlands, 2005), 2010.

Bravo A, Gill S S, Soberón M. Mode of action of *Bacillus thuringiensis* Cry and Cyt toxins and their potential for insect control[J]. Toxicon, 2007, 49(4): 423-435.

Bravo A, Gómez I, Conde J, et al. Oligomerization triggers binding of a *Bacillus thuringiensis* Cry1Ab pore-forming toxin to aminopeptidase N receptor leading to insertion into membrane microdomains[J]. Biochimica et Biophysica Acta (BBA)-Biomembranes, 2004, 1667(1): 38-46.

Bravo A, Gómez I, Porta H, et al. Evolution of *Bacillus thuringiensis* Cry toxins insecticidal activity[J]. Microbial biotechnology, 2013, 6(1): 17-26.

Brito C, Cabanes D, Sarmento Mesquita F, et al. Mechanisms protecting host cells against bacterial pore-forming toxins[J]. Cellular and Molecular Life Sciences, 2019, 76: 1319-1339.

Broderick N A, Raffa K F, Handelsman J. Midgut bacteria required for *Bacillus thuringiensis* insecticidal activity[J]. Proceedings of the National Academy of Sciences, 2006, 103(41): 15196-15199.

Buchon N, Broderick N A, Chakrabarti S, et al. Invasive and indigenous microbiota impact intestinal stem cell activity through multiple pathways in *Drosophila*[J]. Genes & development, 2009a, 23(19): 2333-2344.

Buchon N, Broderick N A, Kuraishi T, et al. *Drosophila* EGFR pathway coordinates stem cell proliferation and gut remodeling following infection[J]. BMC biology, 2010, 8: 1-19.

Buchon N, Broderick N A, Poidevin M, et al. *Drosophila* intestinal response to bacterial infection: activation of host defense and stem cell proliferation[J]. Cell host & microbe, 2009b, 5(2): 200-211.

CABI Spodoptera frugiperda (Fall Armyworm) Datasheet. Invasive Species Compendium. [(accessed on 11 May 2021)]. Available online: https://www.cabi.org/isc/datasheet/29810

Caccia S, Casartelli M, Tettamanti G. The amazing complexity of insect midgut cells: types, peculiarities, and functions[J]. Cell and Tissue research, 2019, 377: 505-525.

Cao B, Shu C, Geng L, et al. Cry78Ba1, one novel crystal protein from *Bacillus thuringiensis* with high insecticidal activity against rice planthopper[J]. Journal of agricultural and food chemistry, 2020, 68(8): 2539-2546.

Cao D, Xiao C, Fu Q, et al. The Combination Analysis Between *Bacillus thuringiensis* Sip1Ab Protein and Brush Border Membrane Vesicles in Midgut of *Colaphellus bowringi* Baly[J]. Frontiers in Microbiology, 2022, 12: 802035.

Cao H, Zhang S, Zhu L, et al. The digestive proteinase trypsin, alkaline A contributes to anti-BmNPV activity in silkworm (*Bombyx mori*)[J]. Developmental and Comparative Immunology, 2021, 119: 104035.

Chen H, Kao C, Liu B, Huang SW, Kuo CJ, Ruan JW, Lin YH, Huang CR, Chen YH, Wang HD, Aroian RV, Chen CS, 2017. HLH-30/TFEB-mediated autophagy functions in a cell-autonomous manner for epithelium intrinsic cellular defense against bacterial pore-forming toxin in *C. elegans*. Autophagy, 13(2):371 - 385.

Chen Q, Wang H, Ren T, et al. Interaction between non-structural protein Pns10 of rice dwarf virus and cytoplasmic actin of leafhoppers is correlated with insect vector specificity[J]. Journal of General Virology, 2015, 96(4): 933-938.

Chen X, Zhu R, Zhong J, et al. Mosaic composition of RIP1–RIP3 signalling hub and its role in regulating cell death[J]. Nature cell biology, 2022, 24(4): 471-482.

Chiang A S, Yen D F, Peng W K. Defense reaction of midgut epithelial cells in the rice moth larva (*Corcyra cephalonica*) infected with *Bacillus thuringiensis*[J]. Journal of Invertebrate Pathology, 1986, 47(3): 333-339.

Christiaens O, Tardajos M G, Martinez Reyna Z L, et al. Increased RNAi efficacy in *Spodoptera exigua* via the formulation of dsRNA with guanylated polymers[J]. Frontiers in physiology, 2018, 9: 316.

Christich A, Kauppila S, Chen P, et al. The damage-responsive *Drosophila* gene sickle encodes a novel IAP binding protein similar to but distinct from reaper, grim, and hid[J]. Current biology, 2002, 12(2): 137-140.

Ciesielski H M, Nishida H, Takano T, et al. Erebosis, a new cell death mechanism during homeostatic turnover of gut enterocytes[J]. PLoS Biology, 2022, 20(4): e3001586.

Coates B S, Deleury E, Gassmann A J, et al. Up-regulation of apoptotic-and cell survival-related gene pathways following exposures of western corn rootworm to *B. thuringiensis* crystalline pesticidal proteins in transgenic maize roots[J]. BMC genomics, 2021, 22: 1-27.

Cong R, Hou J T, Yamamoto T. High-throughput screening for novel *Bacillus thuringiensis* insecticidal proteins revealed evidence that the bacterium exchanges Domain III to enhance its insecticidal activity[J]. Journal of Pesticide Science, 2024, 49(3): 148-158.

Crickmore N, Berry C, Panneerselvam S, et al. A structure-based nomenclature for *Bacillus thuringiensis* and other bacteria-derived pesticidal proteins[J]. Journal of invertebrate pathology, 2021, 186: 107438.

Dal Peraro M, van der Goot FG, 2016. Pore-forming toxins: ancient, but never really out of fashion. Nature Reviews Microbiology, 14(2):77 - 92.

Day R, Abrahams P, Bateman M, et al. Fall armyworm: impacts and implications for Africa[J]. Outlooks on Pest Management, 2017, 28(5): 196-201.

De Maagd R A, Bravo A, Berry C, et al. Structure, diversity, and evolution of protein toxins from spore-forming entomopathogenic bacteria[J]. Annual review of genetics, 2003, 37(1): 409-433.

Degterev A, Boyce M, Yuan J. A decade of caspases[J]. Oncogene, 2003, 22(53): 8543-8567.

Domínguez-Arrizabalaga M, Villanueva M, Escriche B, et al. Insecticidal activity of *Bacillus thuringiensis* proteins against coleopteran pests[J]. Toxins, 2020, 12(7): 430.

Dow J A T. pH gradients in lepidopteran midgut[J]. Journal of Experimental Biology, 1992, 172(1): 355-375.

Dulmage H T. Insecticidal activity of HD-1, a new isolate of *Bacillus thuringiensis* var. alesti[J]. Journal of Invertebrate Pathology, 1970, 15(2): 232-239.

Dutta T K, Santhoshkumar K, Veeresh A, et al. RNAi-based knockdown of candidate gut receptor genes altered the susceptibility of *Spodoptera frugiperda* and *S. litura* larvae to a chimeric toxin Cry1AcF[J]. PeerJ, 2023, 11: e14716.

Estruch J J, Warren G W, Mullins M A, et al. Vip3A, a novel *Bacillus thuringiensis* vegetative insecticidal protein with a wide spectrum of activities against lepidopteran insects[J]. Proceedings of the National Academy of Sciences, 1996, 93(11): 5389-5394.

FAO FAW Map|Global Action for fall Armyworm Control | Food and Agriculture Organization of the United Nations. [(accessed on 4 May 2021)]. Available online: http://www.fao.org/fall-armyworm/monitoring-tools/faw-map/en/

Felix R C, Trindade M, Pires I R P, et al. Unravelling the evolution of the allatostatin-type A, KISS and galanin peptide-receptor gene families in bilaterians: insights from Anopheles mosquitoes[J]. PloS one, 2015, 10(7): e0130347.

Fillinger U, Knols B G J, Becker N. Efficacy and efficiency of new *Bacillus thuringiensis* var. *israelensis* and *Bacillus sphaericus* formulations against *Afrotropical anophelines* in Western Kenya[J]. Tropical Medicine & International Health, 2003, 8(1): 37-47.

Food and Agriculture Organization of the United Nations (FAO). 2018. Integrated management of the fall armyworm on maize: a guide for farmer field schools in Africa. http://www.fao.org/family-farming/detail/en/c/1112643/ (Accessed 10 May 2021).

Franzetti E, Romanelli D, Caccia S, et al. The midgut of the silkmoth *Bombyx mori* is able to recycle molecules derived from degeneration of the larval midgut epithelium[J]. Cell and tissue research, 2015, 361: 509-528.

Galluzzi L, Vitale I, Aaronson S A, et al. Molecular mechanisms of cell death: recommendations of the Nomenclature Committee on Cell Death 2018[J]. Cell Death & Differentiation, 2018, 25(3): 486-541.

Gayen S, Hossain M A, Sen S K. Identification of the bioactive core component of the insecticidal Vip3A toxin peptide of *Bacillus thuringiensis*[J]. Journal of Plant Biochemistry and Biotechnology, 2012, 21: 128-135.

Gervais L, Bardin A J. Tissue homeostasis and aging: new insight from the fly intestine[J]. Current opinion in cell biology, 2017, 48: 97-105.

Goergen G, Kumar P L, Sankung S B, et al. First report of outbreaks of the fall armyworm *Spodoptera frugiperda* (JE Smith)(Lepidoptera, Noctuidae), a new alien invasive pest in West and Central Africa[J]. PloS one, 2016, 11(10): e0165632.

Goldberg L J, Margalit J. A bacterial spore demonstrating rapid larvicidal activity against *Anopheles sergentii*, *Uranotaenia unguiculata*, *Culex univitattus*, *Aedes aegypti* and *Culex pipiens*[J]. 1977.

Gomes F M, Carvalho D B, Machado E A, et al. Ultrastructural and functional analysis of secretory goblet cells in the midgut of the lepidopteran *Anticarsia gemmatalis*[J]. Cell and tissue research, 2013, 352(2): 313-326.

Gómez I, Ocelotl J, Sánchez J, et al. *Bacillus thuringiensis* Cry1Ab domain III β-22 mutants with enhanced toxicity to *Spodoptera frugiperda* (JE Smith)[J]. Applied and Environmental Microbiology, 2020, 86(22): e01580-20.

Goto S, Takeda M, Loeb M J, et al. Immunohistochemical detection of a putative insect cytokine, midgut differentiation factor 1 (MDF-1) in midgut columnar cells of *Heliothis virescens*[J]. Invertebrate reproduction & development, 2001, 40(2-3): 117-124.

Grochulski P, Masson L, Borisova S, et al. *Bacillus thuringiensis* CrylA (a) insecticidal toxin: crystal structure and channel formation[J]. Journal of molecular biology, 1995, 254(3): 447-464.

Guan R, Chen Q, Li H, et al. Knockout of the *HaREase* gene improves the stability of dsRNA and increases the sensitivity of *Helicoverpa armigera* to *Bacillus thuringiensis* toxin[J]. Frontiers in Physiology, 2019, 10: 1368.

Guo J, Zhao J, He K, et al. Potential invasion of the crop-devastating insect pest fall armyworm *Spodoptera frugiperda* to China[J]. 2018.

Gupta M, Kumar H, Kaur S. Vegetative insecticidal protein (Vip): a potential contender from *Bacillus thuringiensis* for efficient management of various detrimental agricultural pests[J]. Frontiers in microbiology, 2021, 12: 659736.

Hamadou-Charfi D B, Boukedi H, Abdelkefi-Mesrati L, et al. Agrotis segetum midgut putative receptor of *Bacillus thuringiensis* vegetative insecticidal protein Vip3Aa16 differs from that of Cry1Ac toxin[J]. Journal of invertebrate pathology, 2013, 114(2): 139-143.

Hay B A, Guo M. Caspase-dependent cell death in *Drosophila*[J]. Annual Review of Cell and Developmental Biology, 2006, 22(1): 623-650.

He B, Chu Y, Yin M, et al. Fluorescent nanoparticle delivered dsRNA toward genetic control of insect pests[J]. Advanced Materials, 2013, 25(33): 4580-4584.

He L, Eslamfam S, Ma X, et al. Autophagy and the nutritional signaling pathway[J]. Frontiers of Agricultural Science and Engineering, 2016, 3(03): 222-230.

He X, Yang Y, Soberón M, et al. *Bacillus thuringiensis* Cry9Aa insecticidal protein domain I helices α3 and α4 are two core regions involved in oligomerization and toxicity[J]. Journal of Agricultural and Food Chemistry, 2024, 72(2): 1321-1329.

Hernandez-Martinez P, Gomis-Cebolla J, Ferre J, Escriche B, 2017. Changes in gene expression and apoptotic response in *Spodoptera exigua* larvae exposed to sublethal concentrations of Vip3 insecticidal proteins. Scientific Reports, 7:16245.

Herrera S C, Bach E A. JAK/STAT signaling in stem cells and regeneration: from *Drosophila* to vertebrates[J]. Development, 2019, 146(2): dev167643.

Herrera S C, Bach E A. The emerging roles of JNK signaling in *Drosophila* stem cell homeostasis[J]. International Journal of Molecular Sciences, 2021, 22(11): 5519.

Herrero S, Bel Y, Hernández-Martínez P, et al. Susceptibility, mechanisms of response and resistance to *Bacillus thuringiensis* toxins in *Spodoptera* spp[J]. Current opinion in insect science, 2016, 15: 89-96.

Hibi M, Lin A, Smeal T, et al. Identification of an oncoprotein-and UV-responsive protein kinase that binds and potentiates the c-Jun activation domain[J]. Genes & development, 1993, 7(11): 2135-2148.

Hill C, Dellar E R, Baena-Lopez L A. Caspases help to spread the message via extracellular vesicles[J]. The FEBS Journal, 2023, 290(8): 1954-1972.

Holmes V R, Johnston J S. Differential gene expression of innate immune response genes consequent to *Solenopsis invicta* virus-3 infection[J]. Genes, 2023, 14(1): 188.

Hopkins T L, Harper M S. Lepidopteran peritrophic membranes and effects of dietary wheat germ agglutinin on their formation and structure[J]. Archives of Insect Biochemistry and Physiology, 2001, 47(2): 100-109.

Hou X, Han L, An B, et al. Autophagy induced by Vip3Aa has a pro-survival role in *Spodoptera frugiperda* Sf9 cells[J]. Virulence, 2021, 12(1): 509-519.

Hu D J K, Jasper H. Control of intestinal cell fate by dynamic mitotic spindle repositioning influences epithelial homeostasis and longevity. Cell Reports. 2019, 28, 2807–2823.

Huang J, Wu W, Fang X, et al. *Zizania latifolia* cell wall polysaccharide metabolism and changes of related enzyme activities during postharvest storage[J]. Foods, 2022, 11(3): 392.

Huang Y, Crim J W, Nuss A B, et al. Neuropeptide F and the corn earworm, *Helicoverpa zea*: a midgut peptide revisited[J]. Peptides, 2011, 32(3): 483-492.

Ibrahim M A, Griko N, Junker M, et al. *Bacillus thuringiensis*: a genomics and proteomics perspective[J]. Bioengineered bugs, 2010, 1(1): 31-50.

Ignoffo C M. Effects of entomopathogens on vertebrates[J]. Annals of the New York Academy of Sciences, 1973, 217(1): 141-164.

Ikmi A, Gaertner B, Seidel C, et al. Molecular evolution of the Yap/Yorkie proto-oncogene and elucidation of its core transcriptional program[J]. Molecular biology and evolution, 2014, 31(6): 1375-1390.

Ishiwata S. On a kind of severe flacherie (sotto disease)[J]. Dainihon Sanshi Kaiho, 1901, 114: 1-5.

Jackson R E, Marcus M A, Gould F, et al. Cross-resistance responses of Cry1Ac-selected *Heliothis virescens* (Lepidoptera: Noctuidae) to the *Bacillus thuringiensis* protein Vip3A[J]. Journal of Economic Entomology, 2007, 100(1): 180-186.

Jiang H, Grenley M O, Bravo M J, et al. EGFR/Ras/MAPK signaling mediates adult midgut epithelial homeostasis and regeneration in *Drosophila*[J]. Cell stem cell, 2011, 8(1): 84-95.

Jiang H, Patel P H, Kohlmaier A, et al. Cytokine/Jak/Stat signaling mediates regeneration and homeostasis in the *Drosophila* midgut[J]. Cell, 2009, 137(7): 1343-1355.

Jiang K, Hou X, Han L, et al. Fibroblast growth factor receptor, a novel receptor for vegetative insecticidal protein Vip3Aa[J]. Toxins, 2018, 10(12): 546.

Jiang K, Hou X, Tan T, et al. Scavenger receptor-C acts as a receptor for *Bacillus thuringiensis* vegetative insecticidal protein Vip3Aa and mediates the internalization of Vip3Aa via endocytosis[J]. PLoS pathogens, 2018, 14(10): e1007347.

Jiang K, Mei S, Wang T, et al. Vip3Aa induces apoptosis in cultured *Spodoptera frugiperda* (Sf9) cells[J]. Toxicon, 2016, 120: 49-56.

Jiang Y X, Chen J Z, Li M W, et al. The combination of *Bacillus thuringiensis* and its engineered strain expressing dsRNA increases the toxicity against *Plutella xylostella*[J]. International Journal of Molecular Sciences, 2021, 23(1): 444.

Jiang Y, Liu J, Xie M, et al. Observation on law of diffusion damage of *Spodoptera frugiperda* in China in 2019. Chin Plant Prot. 45: 10–19.

Jin M, Shan Y, Peng Y, et al. An integrative analysis of transcriptomics and proteomics reveals novel insights into the response in the midgut of *Spodoptera frugiperda* larvae to Vip3Aa[J]. Toxins, 2022, 14(1): 55.

Jisha V N, Smitha R B, Benjamin S. An overview on the crystal toxins from *Bacillus thuringiensis*[J]. Advances in Microbiology, 2013, 3(05): 462.

Jordão B P, Capella A N, Terra W R, et al. Nature of the anchors of membrane-bound aminopeptidase, amylase, and trypsin and secretory mechanisms in *Spodoptera frugiperda* (Lepidoptera) midgut cells[J]. Journal of Insect Physiology, 1999, 45(1): 29-37.

Jurat-Fuentes J L, Adang M J. Cry toxin mode of action in susceptible and resistant *Heliothis virescens* larvae[J]. Journal of invertebrate pathology, 2006, 92(3): 166-171.

Kerr J F R, Winterford C M, Harmon B V. Apoptosis. Its significance in cancer and cancer therapy[J]. Cancer, 1994, 73(8): 2013-2026.

Kerr J F R, Wyllie A H, Currie A R. Apoptosis: a basic biological phenomenon with wideranging implications in tissue kinetics[J]. British journal of cancer, 1972, 26(4): 239-257.

Khalid M Z, Ahmad S, Ngegba P M, et al. Role of endocrine system in the regulation of female insect reproduction[J]. Biology, 2021, 10(7): 614.

King M J, Chan A, Roe R, et al. Two different glycosyltransferase defects that result in GalNAcα-O-peptide (Tn) expression[J]. 1994.

Krieg A, Huger A M, Langenbruch G A, et al. *Bacillus thuringiensis* var. *tenebrionis*: ein neuer, gegenüber Larven von Coleopteren wirksamer Pathotyp[J]. Zeitschrift für angewandte Entomologie, 1983, 96(1-5): 500-508.

Kumela T, Simiyu J, Sisay B, et al. Farmers' knowledge, perceptions, and management practices of the new invasive pest, fall armyworm (*Spodoptera frugiperda*) in Ethiopia and Kenya[J]. International journal of pest management, 2019, 65(1): 1-9.

Kurtz R W, McCaffery A, O'Reilly D. Insect resistance management for Syngenta's VipCot™ transgenic cotton[J]. Journal of invertebrate pathology, 2007, 95(3): 227-230.

Lee K S, Kim B Y, Choo Y M, et al. Dual role of the serine protease homolog BmSPH-1 in the development and immunity of the silkworm *Bombyx mori*[J]. Developmental & Comparative Immunology, 2018, 85: 170-176.

Lehane M J. Peritrophic matrix structure and function[J]. Annual review of entomology, 1997, 42(1): 525-550.

Lemaitre B, Miguel-Aliaga I. The digestive tract of *Drosophila* melanogaster[J]. Annual review of genetics, 2013, 47(1): 377-404.

Lemos A J J M, Siqueira H A A, Wanderley-Teixeira V, et al. Effect of sub-lethal doses of *Bacillus thuringiensis* subsp. *Aizawai* and deltamethrin with regard to fertility and organ

toxicity in pregnant albino rats[J]. Experimental and Toxicologic Pathology, 2013, 65(5): 489-495.

Levy S M, Falleiros A M F, Gregório E A, et al. The larval midgut of *Anticarsia gemmatalis* (Hübner)(Lepidoptera: Noctuidae): light and electron microscopy studies of the epithelial cells[J]. Brazilian Journal of Biology, 2004, 64: 633-638.

Li G, Zhou Q, Qiu L, et al. Serine protease Bm-SP142 was differentially expressed in resistant and susceptible *Bombyx mori* strains, involving in the defence response to viral infection[J]. PLoS One, 2017, 12(4): e0175518.

Li J, Carroll J, Ellar D J. Crystal structure of insecticidal δ-endotoxin from *Bacillus thuringiensis* at 2.5 Å resolution[J]. Nature, 1991, 353(6347): 815-821.

Li J, Qian J, Xu Y, et al. A facile-synthesized star polycation constructed as a highly efficient gene vector in pest management[J]. ACS Sustainable Chemistry & Engineering, 2019, 7(6): 6316-6322.

Li K, Chen M, Shi J, et al. An overview of the production and use of *Bacillus thuringiensis* toxin[J]. Open Life Sciences, 2024, 19(1): 20220902.

Li Y, Hallerman E M, Wu K, et al. Insect-resistant genetically engineered crops in China: development, application, and prospects for use[J]. Annual review of entomology, 2020, 65(1): 273-292.

Liang J, Balachandra S, Ngo S, et al. Feedback regulation of steady-state epithelial turnover and organ size[J]. Nature, 2017, 548(7669): 588-591.

Lin G, Xu N, Xi R. Paracrine unpaired signaling through the JAK/STAT pathway controls self-renewal and lineage differentiation of *drosophila* intestinal stem cells[J]. Journal of molecular cell biology, 2010, 2(1): 37-49.

Liu H, Li Y, Tang X, et al. A midgut-specific serine protease, BmSP36, is involved in dietary protein digestion in the silkworm, *Bombyx mori*[J]. Insect Science, 2017, 24(5): 753-767.

Liu W, Singh S R, Hou S X. JAK–STAT is restrained by Notch to control cell proliferation of the *Drosophila* intestinal stem cells[J]. Journal of cellular biochemistry, 2010, 109(5): 992-999.

Liu Y, Wang Y, Shu C, et al. Cry64Ba and Cry64Ca, two ETX/MTX2-type *Bacillus thuringiensis* insecticidal proteins active against hemipteran pests[J]. Applied and Environmental Microbiology, 2018, 84(3): e01996-17.

Lockshin R A, Williams C M. Programmed cell death—IV. The influence of drugs on the breakdown of the intersegmental muscles of silkmoths[J]. Journal of Insect Physiology, 1965, 11(6): 803-809.

Loeb M J, Coronel N, Natsukawa D, et al. Implications for the functions of the four known midgut differentiation factors: an immunohistologic study of *Heliothis virescens* midgut[J]. Archives of Insect Biochemistry and Physiology: Published in Collaboration with the Entomological Society of America, 2004, 56(1): 7-20.

Loeb M J, Hakim R S, Martin P, et al. Apoptosis in cultured midgut cells from *Heliothis virescens* larvae exposed to various conditions[J]. Archives of Insect Biochemistry and Physiology: Published in Collaboration with the Entomological Society of America, 2000, 45(1): 12-23.

Loeb M J, Hakim R S, Martin P, Narang N, Goto S, Takeda M, 2000. Apoptosis in cultured midgut cells from heliothis virescens larvae exposed to various conditions. Arch. Insect Biochem. Physiol., 45(1):12 - 23.

Loeb M J, Jaffe H. Peptides that elicit midgut stem cell differentiation isolated from chymotryptic digests of hemolymph from Lymantria dispar pupae[J]. Archives of Insect Biochemistry and Physiology: Published in Collaboration with the Entomological Society of America, 2002, 50(2): 85-96.

Luo H, Xiong J, Zhou Q, et al. The effects of *Bacillus thuringiensis* Cry6A on the survival, growth, reproduction, locomotion, and behavioral response of *Caenorhabditis elegans*[J]. Applied microbiology and biotechnology, 2013, 97: 10135-10142.

Martin J L, Sanders E N, Moreno-Roman P, et al. Long-term live imaging of the *Drosophila* adult midgut reveals real-time dynamics of division, differentiation and loss[J]. Elife, 2018, 7: e36248.

Martín-Blanco E, Gampel A, Ring J, et al. puckered encodes a phosphatase that mediates a feedback loop regulating JNK activity during dorsal closure in *Drosophila*[J]. Genes & development, 1998, 12(4): 557-570.

Maysinger D, Zhang I, Shiao T C, et al. Guidelines for the use and interpretation of assays for monitoring autophagy[J]. 2016.

McClintock J T, Schaffer C R, Sjoblad R D. A comparative review of the mammalian toxicity of *Bacillus thuringiensis*-based pesticides[J]. Pesticide Science, 1995, 45(2): 95-105.

McHugh P, Turina M. Apoptosis and necrosis: a review for surgeons[J]. Surgical Infections, 2006, 7(1): 53-68.

Meftaul I M, Venkateswarlu K, Dharmarajan R, et al. Pesticides in the urban environment: A potential threat that knocks at the door[J]. Science of the Total Environment, 2020, 711: 134612.

Mendesil E, Tefera T, Blanco C A, et al. The invasive fall armyworm, *Spodoptera frugiperda*, in Africa and Asia: responding to the food security challenge, with priorities for integrated pest management research[J]. Journal of Plant Diseases and Protection, 2023, 130(6): 1175-1206.

Mendoza-Almanza G, Esparza-Ibarra E L, Ayala-Luján J L, et al. The cytocidal spectrum of *Bacillus thuringiensis* toxins: from insects to human cancer cells[J]. Toxins, 2020, 12(5): 301.

Meng F W, Biteau B. A Sox transcription factor is a critical regulator of adult stem cell proliferation in the *Drosophila* intestine[J]. Cell reports, 2015, 13(5): 906-914.

Meng M, Shen C, Lin M, et al. Characterization of the individual domains of the *Bacillus thuringiensis* Cry2Aa implicates Domain I as a possible binding site to *Helicoverpa armigera*[J]. Journal of Invertebrate Pathology, 2024, 205: 108129.

Micchelli C A, Perrimon N. Evidence that stem cells reside in the adult *Drosophila* midgut epithelium[J]. Nature, 2006, 439(7075): 475-479.

Misra J R, Irvine K D. The Hippo signaling network and its biological functions[J]. Annual review of genetics, 2018, 52(1): 65-87.

Mizuki E, Park Y S, Saitoh H, et al. Parasporin, a human leukemic cell-recognizing parasporal protein of *Bacillus thuringiensis*[J]. Clinical Diagnostic Laboratory Immunology, 2000, 7(4): 625-634.

Mizushima N. Autophagy: process and function[J]. Genes & development, 2007, 21(22): 2861-2873.

Moazamian E, Bahador N, Azarpira N, et al. Anti-cancer parasporin toxins of new *Bacillus thuringiensis* against human colon (HCT-116) and blood (CCRF-CEM) cancer cell lines[J]. Current microbiology, 2018, 75: 1090-1098.

Moffett D F, Koch A. The insect goblet cell: a problem in functional cytoarchitecture[J]. Physiology, 1992, 7(1): 19-23.

Mohanty P, Rajadurai G, Mohankumar S, et al. Interactions between insecticidal cry toxins and their receptors[J]. Current Genetics, 2025, 71(1): 1-28.

Mommaerts V, Jans K, Smagghe G. Impact of *Bacillus thuringiensis* strains on survival, reproduction and foraging behaviour in bumblebees (*Bombus terrestris*)[J]. Pest Management Science: Formerly Pesticide Science, 2010, 66(5): 520-525.

Montezano D G, Sosa-Gómez D R, Specht A, et al. Host plants of *Spodoptera frugiperda* (Lepidoptera: Noctuidae) in the Americas[J]. African entomology, 2018, 26(2): 286-300.

Morse R J, Yamamoto T, Stroud R M. Structure of Cry2Aa suggests an unexpected receptor binding epitope[J]. Structure, 2001, 9(5): 409-417.

Mundorf J, Donohoe C D, McClure C D, et al. Ets21c governs tissue renewal, stress tolerance, and aging in the *Drosophila* intestine[J]. Cell reports, 2019, 27(10): 3019-3033. e5.

Nagoshi R N, Silvie P, Meagher R L, et al. Identification and comparison of fall armyworm (Lepidoptera: Noctuidae) host strains in Brazil, Texas, and Florida[J]. Annals of the Entomological Society of America, 2007, 100(3): 394-402.

Nelson E A, Walker S R, Kepich A, et al. Nifuroxazide inhibits survival of multiple myeloma cells by directly inhibiting STAT3[J]. Blood, The Journal of the American Society of Hematology, 2008, 112(13): 5095-5102.

Nordstrom W, Chen P, Steller H, et al. Activation of thereaperGene during Ectopic Cell Killing in *Drosophila*[J]. Developmental biology, 1996, 180(1): 213-226.

Nougadère A, Reninger J C, Volatier J L, et al. Chronic dietary risk characterization for pesticide residues: a ranking and scoring method integrating agricultural uses and food contamination data[J]. Food and Chemical Toxicology, 2011, 49(7): 1484-1510.

Nougadère A, Reninger J C, Volatier J L, et al. Chronic dietary risk characterization for pesticide residues: a ranking and scoring method integrating agricultural uses and food contamination data[J]. Food and Chemical Toxicology, 2011, 49(7): 1484-1510.

Núñez-Ramírez R, Huesa J, Bel Y, et al. Molecular architecture and activation of the insecticidal protein Vip3Aa from *Bacillus thuringiensis*[J]. Nature communications, 2020, 11(1): 3974.

Oh H, Irvine K D. In vivo analysis of Yorkie phosphorylation sites[J]. Oncogene, 2009, 28(17): 1916-1927.

Ohba M, Aizawa K. Insect toxicity of *Bacillus thuringiensis* isolated from soils of Japan[J]. Journal of Invertebrate Pathology, 1986, 47(1): 12-20.

Ohba M, Iwahana H, Asano S, et al. A unique isolate of *Bacillus thuringiensis* serovar *japonensis* with a high larvicidal activity specific for scarabaeid beetles[J]. Letters in Applied Microbiology, 1992, 14(2): 54-57.

Ohba M, Mizuki E, Uemori A. Parasporin, a new anticancer protein group from *Bacillus thuringiensis*[J]. Anticancer research, 2009, 29(1): 427-433.

Ohlstein B, Spradling A. Multipotent *Drosophila* intestinal stem cells specify daughter cell fates by differential notch signaling[J]. Science, 2007, 315(5814): 988-992.

Ohlstein B, Spradling A. The adult *Drosophila* posterior midgut is maintained by pluripotent stem cells[J]. Nature, 2006, 439(7075): 470-474.

Osman D, Buchon N, Chakrabarti S, et al. Autocrine and paracrine unpaired signaling regulate intestinal stem cell maintenance and division[J]. Journal of cell science, 2012, 125(24): 5944-5949.

Pacheco S, Gómez I, Peláez-Aguilar A E, et al. Structural changes upon membrane insertion of the insecticidal pore-forming toxins produced by *Bacillus thuringiensis*[J]. Frontiers in Insect Science, 2023, 3: 1188891.

Palma L, Muñoz D, Berry C, et al. *Bacillus thuringiensis* toxins: an overview of their biocidal activity[J]. Toxins, 2014, 6(12): 3296-3325.

Pardo-López L, Gómez I, Rausell C, et al. Structural changes of the Cry1Ac oligomeric pre-pore from *Bacillus thuringiensis* induced by N-acetylgalactosamine facilitates toxin membrane insertion[J]. Biochemistry, 2006, 45(34): 10329-10336.

Pardo-López L, Soberón M, Bravo A. *Bacillus thuringiensis* insecticidal three-domain Cry toxins: mode of action, insect resistance and consequences for crop protection[J]. FEMS microbiology reviews, 2013, 37(1): 3-22.

Park M G, Kim W J, Choi J Y, et al. Development of a *Bacillus thuringiensis* based dsRNA production platform to control sacbrood virus in *Apis cerana*[J]. Pest Management Science, 2020, 76(5): 1699-1704.

Pereira A E, Paddock K J, Corcoran J A, et al. Knockdown of an ATP-binding cassette transporter in resistant western corn rootworm larvae partially reverses resistance to eCry3. 1Ab protein[J]. Scientific Reports, 2024, 14(1): 31508.

Perveen F K, Khan A. Introductory chapter: Lepidoptera. Lepidoptera, InTech, 2017.

Pfaffl M W, Hageleit M. Validities of mRNA quantification using recombinant RNA and recombinant DNA external calibration curves in real-time RT-PCR[J]. Biotechnology letters, 2001, 23: 275-282.

Pigott C R, Ellar D J. Role of receptors in *Bacillus thuringiensis* crystal toxin activity[J]. Microbiology and molecular biology reviews, 2007, 71(2): 255-281.

Pinos D, Andrés-Garrido A, Ferré J, et al. Response mechanisms of invertebrates to *Bacillus thuringiensis* and its pesticidal proteins[J]. Microbiology and Molecular Biology Reviews, 2021, 85(1): 10.1128/mmbr. 00007-20.

Portugal L, Muñóz-Garay C, de Castro D L M, et al. Toxicity of Cry1A toxins from *Bacillus thuringiensis* to CF1 cells does not involve activation of adenylate cyclase/PKA signaling pathway[J]. Insect biochemistry and molecular biology, 2017, 80: 21-31.

Powell J A. Lepidoptera: moths, butterflies[M]//Encyclopedia of insects. Academic Press, 2009: 559-587.

Qin L, Shi H, Xia H, et al. Comparative proteomic analysis of midgut proteins from male and female *Bombyx mori* (Lepidoptera: Bombycidae)[J]. Journal of insect science, 2014, 14(1): 226.

Ragasruthi M, Balakrishnan N, Murugan M, et al. *Bacillus thuringiensis* (Bt)-based biopesticide: Navigating success, challenges, and future horizons in sustainable pest control[J]. Science of The Total Environment, 2024: 176594.

Rahman M, Glatz R, Roush R, et al. Developmental penalties associated with inducible tolerance in *Helicoverpa armigera* to insecticidal toxins from *Bacillus thuringiensis*[J]. Applied and Environmental Microbiology, 2011, 77(4): 1443-1448.

Rajmohan K S, Chandrasekaran R, Varjani S. A review on occurrence of pesticides in environment and current technologies for their remediation and management[J]. Indian journal of microbiology, 2020, 60(2): 125-138.

Raymond B, Johnston P R, Nielsen-LeRoux C, et al. *Bacillus thuringiensis*: an impotent pathogen?[J]. Trends in microbiology, 2010, 18(5): 189-194.

Reiher W, Shirras C, Kahnt J, et al. Peptidomics and peptide hormone processing in the *Drosophila* midgut[J]. Journal of proteome research, 2011, 10(4): 1881-1892.

Ren F, Wang B, Yue T, et al. Hippo signaling regulates *Drosophila* intestine stem cell proliferation through multiple pathways[J]. Proceedings of the National Academy of Sciences, 2010, 107(49): 21064-21069.

Rodríguez-Cabrera L, Trujillo–Bacallao D, Borrás–Hidalgo O, et al. RNAi-mediated knockdown of a *Spodoptera frugiperda* trypsin-like serine-protease gene reduces susceptibility to a *Bacillus thuringiensis* Cry1Ca1 protoxin[J]. Environmental microbiology, 2010, 12(11): 2894-2903.

Rodriguez-Fernandez I A, Tauc H M, Jasper H. Hallmarks of aging *Drosophila* intestinal stem cells[J]. Mechanisms of Ageing and Development, 2020, 190: 111285.

Roller L, Daubnerová I, Mizoguchi A, et al. Expression analysis of peptidergic enteroendocrine cells in the silkworm *Bombyx mori*[J]. Cell and Tissue Research, 2022, 389(3): 385-407.

Romero M, Keyel M, Shi G, et al. Intrinsic repair protects cells from pore-forming toxins by microvesicle shedding[J]. Cell Death & Differentiation, 2017, 24(5): 798-808.

Rubin C I, Atweh G F. The role of stathmin in the regulation of the cell cycle[J]. Journal of cellular biochemistry, 2004, 93(2): 242-250.

Rubio-Infante N, Moreno-Fierros L. An overview of the safety and biological effects of *Bacillus thuringiensis* Cry toxins in mammals[J]. Journal of applied toxicology, 2016, 36(5): 630-648.

Ryoo H D, Bergmann A, Gonen H, et al. Regulation of *Drosophila* IAP1 degradation and apoptosis by reaper and ubcD1[J]. Nature cell biology, 2002, 4(6): 432-438.

Sanahuja G, Banakar R, Twyman R M, et al. *Bacillus thuringiensis*: a century of research, development and commercial applications[J]. Plant biotechnology journal, 2011, 9(3): 283-300.

Saud S, Wang D, Fahad S, et al. Comprehensive impacts of climate change on rice production and adaptive strategies in China[J]. Frontiers in Microbiology, 2022, 13: 926059.

Sebé-Pedrós A, Zheng Y, Ruiz-Trillo I, et al. Premetazoan origin of the hippo signaling pathway[J]. Cell reports, 2012, 1(1): 13-20.

Sedlakova A, Kohut A, Kalina I. Biochemical changes in apoptosis and methods for their determination (review)[J]. Ceskoslovenska Fysiologie, 1999, 48(3): 107-118.

Sena da Silva I H, Gómez I, Pacheco S, et al. *Bacillus thuringiensis* Cry1Ab domain III β-16 is involved in binding to prohibitin, which correlates with toxicity against *Helicoverpa armigera* (Lepidoptera: Noctuidae)[J]. Applied and Environmental Microbiology, 2021, 87(2): e01930-20.

Sena J A D, Hernández-Rodríguez C S, Ferré J. Interaction of *Bacillus thuringiensis* Cry1 and Vip3A proteins with *Spodoptera frugiperda* midgut binding sites[J]. Applied and Environmental Microbiology, 2009, 75(7): 2236-2237.

Shao E, Zhang A, Yan Y, et al. Oligomer formation and insecticidal activity of *Bacillus thuringiensis* Vip3Aa toxin[J]. Toxins, 2020, 12(4): 274.

Shaw R L, Kohlmaier A, Polesello C, et al. The Hippo pathway regulates intestinal stem cell proliferation during *Drosophila* adult midgut regeneration[J]. Development, 2010, 137(24): 4147-4158.

Shen C, Jin J, Huang Z, et al. Screening and identification of anti-idiotypic nanobody capable of broad-spectrum recognition of the toxin binding region of Lepidopteran cadherins and mimicking domain II of Cry2Aa toxin[J]. Journal of Agricultural and Food Chemistry, 2024, 72(3): 1582-1591.

Shi J, Zhao Y, Wang K, et al. Cleavage of GSDMD by inflammatory caspases determines pyroptotic cell death[J]. Nature, 2015, 526(7575): 660-665.

Shylesha A N, Jalali S K, Gupta A, et al. Studies on new invasive pest *Spodoptera frugiperda* (JE Smith)(Lepidoptera: Noctuidae) and its natural enemies[J]. Journal of Biological control, 2018: 145-151.

Siegel J P. The mammalian safety of *Bacillus thuringiensis*-based insecticides[J]. Journal of invertebrate pathology, 2001, 77(1): 13-21.

Siegfried B D, Vaughn T T, Spencer T. Baseline susceptibility of western corn rootworm (Coleoptera: Crysomelidae) to Cry3Bb1 *Bacillus thuringiensis* toxin[J]. Journal of economic entomology, 2005, 98(4): 1320-1324.

Singh S R, Zeng X, Zhao J, et al. The lipolysis pathway sustains normal and transformed stem cells in adult *Drosophila*[J]. Nature, 2016, 538(7623): 109-113.

Song W, Veenstra J A, Perrimon N. Control of lipid metabolism by tachykinin in *Drosophila*[J]. Cell reports, 2014, 9(1): 40-47.

Spies A G, Spence K D. Effect of sublethal *Bacillus thuringiensi*s crystal endotoxin treatment on the larval midgut of a moth, *Manduca*: SEM study[J]. Tissue and Cell, 1985, 17(3): 379-394.

Subedi B, Poudel A, Aryal S. The impact of climate change on insect pest biology and ecology: Implications for pest management strategies, crop production, and food security[J]. Journal of Agriculture and Food Research, 2023, 14: 100733.

Suzuki A, Sekiya S, Gunshima E, et al. EGF signaling activates proliferation and blocks apoptosis of mouse and human intestinal stem/progenitor cells in long-term monolayer cell culture[J]. Laboratory investigation, 2010, 90(10): 1425-1436.

Syed T, Askari M, Meng Z, et al. Current insights on vegetative insecticidal proteins (Vip) as next generation pest killers[J]. Toxins, 2020, 12(8): 522.

Tabashnik B E, Carrière Y. Surge in insect resistance to transgenic crops and prospects for sustainability[J]. Nature biotechnology, 2017, 35(10): 926-935.

Tan S, Shang Z, Jia H, et al. Enhancing *Bacillus thuringiensis* Cry8Ea1 toxicity: Insights into protease sensitivity for the evolutionary adaptation of Cry toxins to insect hosts[J]. International Journal of Biological Macromolecules, 2025, 308: 142246.

Tanaka, Y. Yoshizawa, R. Sato, 2012. Response of midgut epithelial cells to Cry1Aa is toxin-dependent and depends on the interplay between toxin action and host apoptotic response. FEBS J., 279:1071 - 1079.

Terra W R, Ferreira C. Biochemistry and molecular biology of digestion[M]//Insect molecular biology and biochemistry. Academic Press, 2012: 365-418.

Tettamanti G, Grimaldi A, Casartelli M, et al. Programmed cell death and stem cell differentiation are responsible for midgut replacement in *Heliothis virescens* during prepupal instar[J]. Cell and tissue research, 2007, 330: 345-359.

Thammasittirong A, Thammasittirong S N R. Aromatic residues on the side surface of Cry4Ba-Domain II of *Bacillus thuringiensis* subsp. *israelensis* function in binding to their counterpart residues on the *Aedes aegypti* alkaline phosphatase receptor[J]. Toxins, 2023, 15(2): 114.

Thiery I, Frachon E. Identification, isolation, culture and preservation of entomopathogenic bacteria[M]//Manual of techniques in insect pathology. Academic Press, 1997: 55-IX.

Tian A, Benchabane H, Wang Z, et al. Regulation of stem cell proliferation and cell fate specification by Wingless/Wnt signaling gradients enriched at adult intestinal compartment boundaries[J]. PLoS genetics, 2016, 12(2): e1005822.

Tian A, Morejon V, Kohoutek S, et al. Damage-induced regeneration of the intestinal stem cell pool through enteroblast mitosis in the *Drosophila* midgut[J]. The EMBO Journal, 2022, 41(19): e110834.

Tian A, Shi Q, Jiang A, et al. Injury-stimulated Hedgehog signaling promotes regenerative proliferation of *Drosophila* intestinal stem cells[J]. Journal of Cell Biology, 2015, 208(6): 807-819.

Todd E L, Poole R W. Keys and illustrations for the armyworm moths of the noctuid genus *Spodoptera* Guenée from the Western Hemisphere[J]. Annals of the Entomological Society of America, 1980, 73(6): 722-738.

Toyam T, Yamagishi T, Sato R. The roles of enteroendocrine cell distribution and gustatory receptor expression in regulating peptide hormone secretion in the midgut of *Bombyx mori* larvae[J]. Archives of Insect Biochemistry and Physiology, 2023, 114(1): e22032.

Tracy Cai X, Li H, Safyan A, et al. AWD regulates timed activation of BMP signaling in intestinal stem cells to maintain tissue homeostasis[J]. Nature Communications, 2019, 10(1): 2988.

Valaitis A P. *Bacillus thuringiensis* pore-forming toxins trigger massive shedding of GPI-anchored aminopeptidase N from gypsy moth midgut epithelial cells[J]. Insect biochemistry and molecular biology, 2008, 38(6): 611-618.

Vega-Cabrera A, Cancino-Rodezno A, Porta H, et al. Aedes aegypti Mos20 cells internalizes cry toxins by endocytosis, and actin has a role in the defense against Cry11Aa toxin[J]. Toxins, 2014, 6(2): 464-487.

Vilas-Bôas G T, Peruca A P S, Arantes O M N. Biology and taxonomy of *Bacillus cereus*, *Bacillus anthracis*, and *Bacillus thuringiensis*[J]. Canadian journal of microbiology, 2007, 53(6): 673-687.

Visvikis O, Ihuegbu N, Labed S A, et al. Innate host defense requires TFEB-mediated transcription of cytoprotective and antimicrobial genes[J]. Immunity, 2014, 40(6): 896-909.

Wan Min, Tai Hongkun, Gu Rui, et al. Evaluation and control measures of economic loss of maize by Argyra herba in Dehong, Yunnan Province [J]. Plant Protection, 2022, 48(1): 220-226.

Wang K, Peng Y, Pu J, et al. Variation in RNAi efficacy among insect species is attributable to dsRNA degradation in vivo[J]. Insect biochemistry and molecular biology, 2016, 77: 1-9.

Wang Y, Li M, Ying J, et al. High-efficiency green management of potato late blight by a self-assembled multicomponent nano-bioprotectant[J]. Nature Communications, 2023, 14(1): 5622.

Wang Z, Fang L, Zhou Z, et al. Specific binding between *Bacillus thuringiensis* Cry9Aa and Vip3Aa toxins synergizes their toxicity against Asiatic rice borer (*Chilo suppressalis*)[J]. Journal of Biological Chemistry, 2018, 293(29): 11447-11458.

Wang Z, Wang K, Bravo A, et al. Coexistence of *cry9* with the *vip3a* gene in an identical plasmid of *Bacillus thuringiensis* indicates their synergistic insecticidal toxicity[J]. Journal of Agricultural and Food Chemistry, 2020, 68(47): 14081-14090.

Wang Z, Yang Y, Li S, et al. JAK/STAT signaling regulated intestinal regeneration defends insect pests against pore-forming toxins produced by *Bacillus thuringiensis*[J]. PLoS Pathogens, 2024, 20(1): e1011823.

Whitfield A E, Falk B W, Rotenberg D. Insect vector-mediated transmission of plant viruses[J]. Virology, 2015, 479: 278-289.

Wilson R, Goyal L, Ditzel M, et al. The DIAP1 RING finger mediates ubiquitination of Dronc and is indispensable for regulating apoptosis[J]. Nature cell biology, 2002, 4(6): 445-450.

Wu L, Chen J. Investigation on the occurrence regularity and detection method of rice Dicarborer in cold area [J]. China Plant Protection, 2009 (8): 19-20.

Wu S, Liu Y, Zheng Y, et al. The TEAD/TEF family protein Scalloped mediates transcriptional output of the Hippo growth-regulatory pathway[J]. Developmental cell, 2008, 14(3): 388-398.

Xiang J, Bandura J, Zhang P, et al. EGFR-dependent TOR-independent endocycles support *Drosophila* gut epithelial regeneration[J]. Nature communications, 2017, 8(1): 15125.

Xiang X, Liu S, Li H, et al. Defense strategies of rice in response to the attack of the herbivorous insect, *Chilo suppressalis*[J]. International Journal of Molecular Sciences, 2023, 24(18): 14361.

Xiao Y, Wu K. Recent progress on the interaction between insects and *Bacillus thuringiensis* crops[J]. Philosophical Transactions of the Royal Society B, 2019, 374(1767): 20180316.

Xu L, Abd El-Aty A M, Eun J B, et al. Recent advances in rapid detection techniques for pesticide residue: a review[J]. Journal of agricultural and food chemistry, 2022, 70(41): 13093-13117.

Yamanaka N, Roller L, Žitňan D, et al. *Bombyx* orcokinins are brain-gut peptides involved in the neuronal regulation of ecdysteroidogenesis[J]. Journal of Comparative Neurology, 2011, 519(2): 238-246.

Yan S, Qian J, Cai C, et al. Spray method application of transdermal dsRNA delivery system for efficient gene silencing and pest control on soybean aphid *Aphis glycines*[J]. Journal of Pest Science, 2020, 93: 449-459.

Yan S, Ren B Y, Shen J. Nanoparticle-mediated double-stranded RNA delivery system: a promising approach for sustainable pest management[J]. Insect Science, 2021, 28(1): 21-34.

Yang Y, Huang X, Yuan W, et al. *Bacillus thuringiensis* cry toxin triggers autophagy activity that may enhance cell death[J]. Pesticide Biochemistry and Physiology, 2021, 171: 104728.

Yu H, Zhang J, Huang D, et al. Characterization of *Bacillus thuringiensis* strain Bt185 toxic to the Asian cockchafer: *Holotrichia parallela*[J]. Current Microbiology, 2006, 53: 13-17.

Yu X, Zheng X, Xu H, et al. Burr behavior and its control in water stem stem [J]. Journal of Plant Protection, 2004, 31(1): 26-32.

Yuan J, Shaham S, Ledoux S, et al. The *C. elegans* cell death gene *ced-3* encodes a protein similar to mammalian interleukin-1β-converting enzyme[J]. Cell, 1993, 75(4): 641-652.

Zalucki M P, Clarke A R, Malcolm S B. Ecology and behavior of first instar larval Lepidoptera[J]. Annual review of entomology, 2002, 47(1): 361-393.

Zavascki A P, Barth A L, Gonçalves A L S, et al. The influence of metallo-β-lactamase production on mortality in nosocomial *Pseudomonas aeruginosa* infections[J]. Journal of Antimicrobial Chemotherapy, 2006, 58(2): 387-392.

Zeigler D R. *Bacillus* Genetic Stock Center Catalog of Strains, Volume 1: *Bacillus subtilis* 168[J]. 2000.

Zhai Z, Boquete J P, Lemaitre B. Cell-specific Imd-NF-κB responses enable simultaneous antibacterial immunity and intestinal epithelial cell shedding upon bacterial infection[J]. Immunity, 2018, 48(5): 897-910. e7.

Zhang L, Jin M, Zhang D, et al.. Molecular identification of invasive fall armyworm *Spodoptera frugiperda* in Yunnan province. Chin Plant Prot. 2019,45: 19–24.

Zhang L, Ren F, Zhang Q, et al. The TEAD/TEF family of transcription factor Scalloped mediates Hippo signaling in organ size control[J]. Developmental cell, 2008, 14(3): 377-387.

Zhang P, Edgar B A. Insect gut regeneration[J]. Cold Spring Harbor perspectives in biology, 2022, 14(2): a040915.

Zhang Q, Zhao L, He P, et al. Potential habitat area of *Argyria argyra* in Qujing City, Yunnan Province and its economic loss assessment [J]. Journal of Yunnan University (Natural Science Edition), 2020, 42(6): 1224-1229.

Zhang R, Hua G, Andacht T M, et al. A 106-kDa aminopeptidase is a putative receptor for *Bacillus thuringiensis* Cry11Ba toxin in the mosquito Anopheles gambiae[J]. Biochemistry, 2008, 47(43): 11263-11272.

Zhang X, Mysore K, Flannery E, et al. Chitosan/interfering RNA nanoparticle mediated gene silencing in disease vector mosquito larvae[J]. Journal of visualized experiments: JoVE, 2015 (97): 52523.

Zhang X, Zhang J, Zhu K Y. Chitosan/double-stranded RNA nanoparticle-mediated RNA interference to silence chitin synthase genes through larval feeding in the African malaria mosquito (*Anopheles gambiae*)[J]. Insect molecular biology, 2010, 19(5): 683-693.

Zheng X, Yu X, Lv Z, et al. Study on the occurrence and control of diallel moth in Rice stem fields [J]. Acta Agriculturae Zhejiangensis, 2003, 15(3): 0.

Zhuang M, Oltean D I, Gómez I, et al. *Heliothis virescens* and *Manduca sexta* lipid rafts are involved in Cry1A toxin binding to the midgut epithelium and subsequent pore formation[J]. Journal of Biological Chemistry, 2002, 277(16): 13863-13872.

Zotti M J, Smagghe G. RNAi technology for insect management and protection of beneficial insects from diseases: lessons, challenges and risk assessments[J]. Neotropical Entomology, 2015, 44: 197-213.

Appendices

List of publications

Accepted publications (peer reviewed)

1. Liang, J.,[#] Sun, Y.,[#] **Yang, Y.,[#]** Wang, Z.,[#] Wu, H., Gu, T., Zhang, R., Sun, X., Yao, B., Tu, T., Liu, X., Luo, H., Tong, G., Jiao, Y., Li, K.,* Zhang, J.,* Wu, K.* Agricultural biotechnology in China: product development, commercialization, and perspectives. *aBIOTECH*, 2025: 1-27.
2. Li, S, Wang, Z, **Yang, Y.**, Niu, X., Fang, Y., Soberón, M., Bravo, A., Wu, G., Zhang, J. Sequestosome 1 in autophagy regulates a defense response of the striped stem borer to the Cry9Aa protein[J]. *Journal of Agricultural and Food Chemistry*, 2025, 73(18): 11030−11040.
3. He, X., **Yang, Y.**, Soberón, M, Bravo, A., Zhang, L., Zhang, J., Wang, Z. *Bacillus thuringiensis* Cry9Aa insecticidal protein domain I helices α3 and α4 are two core regions involved in oligomerization and toxicity[J]. *Journal of Agricultural and Food Chemistry*, 2024, 72(2): 1321-1329
4. Wang, Z.,[#] **Yang, Y.,[#]** Li, S., Ma, W., Wang, K., Soberón, M., Yan, S., Shen, J., Francis, F., Bravo, A., Zhang, J. JAK/STAT signaling regulated intestinal regeneration defends insect pests against pore-forming toxins produced by *Bacillus thuringiensis*[J]. *PLoS Pathogens*, 2024, 20(1): e1011823.

Prepare to submit articles

1. **Yang, Y.,[#]** Wang, Z.,[#] Niu, X., Li, S., Francis, F., Shu, C., Ma, W., Zhang, J. Knockdown of *Egfr* and *Stmn4* by using an efficient oral feeding RNAi system increases the susceptibility of *Spodoptera frugiperda* larvae to Cry1Fa protein. Submitting.

Presentations at conferences (peer reviewed)

1. **Yang, Y**., Francis, F., Wang, Z., Zhang, J. Study on Caspase5-mediated midgut defense response of *Chilo suppressalis* larvae against Bt Cry9A protein. in **17th National Symposium for Young Researchers on *Bacillus***. 2022: Beijing, China. Oral presentation
2. **Yang, Y**., Wang, Z., Geng, L., Shu, C., Francis, F., Zhang, J. Knockdown of *Egfr* and *Stmn4* by using an efficient oral feeding RNAi system increases the susceptibility of *Spodoptera frugiperda* larvae to Cry1F protein. in **the Society for Invertebrate Pathology Annual Conference 2024**. 2024: Vienna, Austria. Oral presentation